Analysis of lifespan extending compounds using growth kinetics and replicative lifespan in *Saccharomyces cerevisiae*

Michael G. Kiflezghi

A dissertation

Submitted in partial fulfillment of the

requirements for the degree of

Doctor of Philosophy

University of Washington

2023

Reading Committee:

Matt Kaeberlein, Chair

Peter Rabinovitch

William Banks

Program Authorized to Offer Degree:

Molecular Medicine and Mechanisms of Disease

University of Washington

Abstract

Analysis of lifespan extending compounds using growth kinetics and replicative lifespan in *Saccharomyces cerevisae*

Michael G. Kiflezghi

Chair of the Supervisory Committee:

Matt Kaeberlein

Department of Laboratory Medicine and Pathology

Advances in modern medicine have facilitated stunning rises in life expectancy over the last two centuries. This longer life, however, is concomitant with a gradual decline in health and the onset of multiple age-associated pathologies including heart disease, neurodegeneration and cancer. Risk of developing and dying from these age-associated diseases increases dramatically with age suggesting a common underlying cause. Targeting the aging process itself with clinical intervention may allow for amelioration of the onset and progression of multiple age-associated pathologies simultaneously. The mechanistic Target of Rapamycin (mTOR) signaling pathway has emerged as an important clinical target in this regard with its dysregulation being observed in multiple pathologies including many cancers, autoimmune disorders, heart failure, neurodegeneration and type 2 diabetes. Importantly, genetic or pharmacological inhibition of mTOR signaling results in increased life-span across evolutionary distant organisms suggesting a conserved role for this signaling pathway in longevity regulation. A novel yeast-based system to identify putative mTOR inhibitors is described. Utilizing differential growth kinetics of WT and mutant strains sensitized to mTOR perturbations, this system successfully discriminates between allosteric (i.e. rapamycin) and ATP competitive mTOR inhibitors. A number of nutraceutical compounds were screened and of these, caffeine was confirmed to be an mTOR inhibitor (Chapter two). Next a screen of natural products and natural product mixtures were screened for effects on growth rate, mTOR-mediated growth inhibition, and replicative lifespan (RLS). No mTOR inhibitors were identified but two

treatments, berberine and green tea extract significantly reduced RLS. *Pterocarpus marsupium* extract (PME), a plant extract with a long history of use in Ayurvedic medicine, extended cellular lifespan (Chapter three). Constituents of this extract include several compounds with reported health span and life span extending properties: epicatechin, quercetin, berberine, and pterostilbene. Of these PME constituents, quercetin and epicatechin had no effect on cellular life span, while berberine decreased cellular life span. We describe the lifespan and outgrowth kinetics of pterostilbene-treated cells and report on dose-dependent effects on longevity, potent cytotoxicity, and a possible role for mitochondrial function in mediating these phenotypes (Chapter Four).

Table of Contents

Chapter 1: Introduction

An aging world

In 1800, estimated global life expectancy was about 30 years [1]. By the early 1900s, the global figure rose modestly to about 34 years. Over the last century, advances in medicine and public health have facilitated stunning increases in life expectancy, bringing the global average to 72 years in 2020 [2]. While the advent of modern medicine has enabled this increase in life expectancy, aging populations have a range of age-associated diseases to contend with that negatively impact the quality of life. Age is the major risk factor for multiple diseases affecting mortality, including cardiovascular disease, neurodegenerative diseases, and cancer [3]. Among other factors, increases in life expectancy and population size have altered the population structure of the United States. In 1900, 4.1% of the population was 65 and older. Nearly 120 years later in 2019, 65 and older individuals comprised 16% of the population. This figure is projected to rise to over 20% by 2050 [4, 5]. This growing population of aged individuals will require more significant investments in healthcare to protect health and quality of life. While modern medicine has facilitated increases in average lifespan, aging itself has not been a target for therapeutic intervention.

This increase in average lifespan is not necessarily concomitant with a prolongation of the quality of life, thus leaving many to suffer periods of illness and reduced quality of life as they age. There is a distinction between the measured lifespan of an individual and the amount of time they remain free of diseases or in good health. This period of time in good health is sometimes called health span, but is not rigorously defined [6]. Regardless, this concept remains useful in contextualizing an individual's lifespan.

Aging has primarily been viewed as an intractable and inevitable end state. However, nearly a century of research has shown that restricting the energy intake of an organism, also referred to as caloric restriction (CR) or dietary restriction (DR), can extend lifespan and delay the onset of age-associated pathologies in multiple animal models, including vertebrate and invertebrate species. Research into the molecular mechanisms of the CR response and the underlying biology of aging has

yielded several potential therapeutic targets, the controlled disruption of which extends lifespan in multiple, evolutionary distant model organisms.

The Biology of Aging

From the ambrosia of the Greek Gods to the ancient Egyptian Cup of Ankh and the age-old tale of the fountain of youth, antiquity is replete with references to extreme longevity conferred through food and drink, supernatural or otherwise. Humanity's fascination with extreme longevity has remained largely philosophical until relatively recently. In the early 20th century, nutrition experiments conducted in rats uncovered an unexpected phenomenon: restricting the food of laboratory animals would sometimes paradoxically extend their lifespan [7-9]. These works were the first published evidence that diet could influence longevity. These initial reports, however, had two common themes that complicated the interpretation of their results: to achieve growth inhibition, food restriction without regard for malnutrition was utilized, and animals were segregated on the basis of their growth rates. In their seminal 1935 publication McKay et al. addressed these issues, suggesting that prior work had not truly tested the hypothesis that inhibited growth results in extended lifespan because animals were segregated on the basis of their growth rates and, therefore, the slower-growing group would be biased towards individuals that die prematurely. McKay believed that food restriction in the context of malnutrition likely resulted in metabolic issues that extended beyond inhibiting growth [10]. They showed, for the first time, that CR extended the mean and maximal lifespan of rats compared to *ad libitum* fed animals [11]. Over the next several decades, the CR effect on longevity would be validated in multiple model organisms spanning a large evolutionary distance suggesting a conserved role for this effect.

Paralleling these experimental observations was the development of various theories of aging. In general, theories of aging can be segregated into two categories: programmed or damaged. Programmed theories of aging suggest that individuals age due to a deliberate or programmed deterioration. The disposable soma theory, which posits that an evolutionary trade-off between growth and reproduction drives organismal aging [12], is one such example. Theories of aging that fall into the damaged category generally suggest that aging results from the stochastic accumulation of damage intersecting with or causing the failure of repair mechanisms to repair this damage and that this inevitable damage

accumulation contributes to age-related declines in function. The free radical theory of aging [13] is a successful example with widespread experimental support and has even entered the general lexicon.

The first direct evidence that organismal longevity can be influenced genetically came from a screen for long-lived mutants in the nematode *Caenorhabditis elegans*. In 1983 Michael Klass published a method for isolating long-lived *C. elegans* mutants [14]. Klass had previously shown that CR could increase *C. elegans* lifespan [15] and was interested in identifying individual genes that influence aging. He was able to isolate eight long-lived mutants, none of which, he concluded, showed increased life spans as a primary effect: two of the mutants showed increased life span due to dauer formation, and the other six showed increased lifespan presumably due to CR caused by a pharyngeal pump defect. A few years later, Friedman and Johnson, working with Klass' mutants, were able to isolate one (hx564) that lacked the pharyngeal pump defect but retained a long lifespan finding that a mutation in the *age-1* gene increased mean lifespan by over 50% [16]. In another screen for long-lived mutants by Cynthia Kenyon, it was found that a mutation in *daf-2* could double *C. elegans* lifespan and that *daf-16* was required for this extension [17]. *daf-2* encodes the *C. elegans* homolog of human insulin and IGF-1 receptors [18], implicating the insulin/IGF-1 signaling (IIS) pathway in longevity regulation.

The unicellular eukaryote *Saccharomyces cerevisiae* has been successfully exploited to identify and characterize signaling pathways that may modulate biological aging. The mechanistic Target of Rapamycin (mTOR; TOR in budding yeast) signaling pathway is one such example [19]. The mTOR protein is a serine/threonine kinase and an atypical member of the phosphatidylinositol 3 kinase family that serves as a master regulator of cell growth and proliferation, allowing the cell to tie environmental nutrient status to cell fate. Budding yeasts are among the only eukaryotes to possess two mTOR genes: *TOR1* and *TOR2,* which arose from a genome duplication event. The yeast mTOR kinases comprise the catalytic subunit of two structurally and functionally distinct protein complexes: mTOR complex 1 (mTORC1; may contain *TOR1* or *TOR2*) and mTOR complex 2 (mTORC2; *TOR2* exclusive) [20]. Unlike yeast, multicellular eukaryotes possess a single mTOR-encoding gene, with its gene product comprising the catalytic subunit of both mTORC1 and mTORC2.

The macrolide antibiotic rapamycin is a specific and potent inhibitor of the mTOR kinase. Rapamycin inhibits mTORC1 activity by first complexing with the peptidyl-prolyl cis-trans isomerase FKBP12 (Fpr1 in yeast). The rapamycin-FKBP12 complex then forms a ternary complex with the mTOR kinase via the FKBP-rapamycin-binding (FRB) domain, likely resulting in both steric-occlusion of the kinase active site and inhibition of substrate recruitment [21-23]. Among its many functions, mTORC1 regulates protein synthesis and mRNA translation globally through two distinct and highly conserved substrates: ribosomal S6 kinase (S6K1) and eukaryotic translation initiation factor 4E-binding protein (4E-BP1).

mTORC2 is said to be “rapamycin insensitive” because it does not respond to direct inhibition by rapamycin or its analogs (rapalogs). This is perhaps due to steric occlusion of the FRB domain by mTORC2 component Rictor as was shown to be the case in budding yeast with the Rictor homolog Avo3 [24]. However, prolonged treatment with rapamycin has been shown to inhibit mTORC2 activity. This is thought to occur through sequestration of free mTOR kinases by the rapamycin-FKBP12 complex inhibiting the assembly of mTORC2 [25]. mTORC1 signaling has been characterized to a greater extent than mTORC2 signaling owing largely to the ability to interrogate mTORC1 function through genetic or pharmacological inhibition. While dual mTORC1/mTORC2 catalytic inhibitors have been developed, until recently, direct and specific pharmacological inhibition of mTORC2 had not yet been demonstrated. JR-AB2-011, a derivative of a compound (CID613034) from the NCI/DTP (National Cancer Institute Developmental Therapeutics Program) small molecule library was identified as a specific, sub-micromolar mTORC2 inhibitor. It was shown to be capable of binding to mTORC2 obligate regulatory subunit Rictor thereby preventing the association of mTOR with Rictor precluding the formation of functional mTORC2 [26].

mTOR signaling in aging

As a master regulator of cell growth and proliferation, the mTOR kinase plays a role in a diverse set of cellular functions. While mTOR inhibition has been shown to increase lifespan in multiple model organisms, the specific mechanism by which this occurs is not well understood. The role of the mTOR pathway in regulating life span has been attributed, in part, to its function as a nutrient sensor. Nutrient

sensing pathways are thought to act as major determinants of longevity. This is consistent with evidence that inhibition of both the mTOR signaling pathway and IIS pathway increase longevity in multiple model organisms. Suppression of these signaling pathways is also thought to be one of the mechanisms by which CR mediates its beneficial effects. Consistent with this notion are the observations that CR does not further increase life span in: genetically modified *S. cerevisiae* lacking TOR1 [27]; RNAi of TOR in *C. elegans* [28]; or overexpression of the negative upstream mTOR regulator dTsc2 in *D. melanogaster* [29].

mTOR was first implicated in the regulation of longevity when it was found that a mutation or deletion of *SCH9*, a yeast functional homolog of mammalian S6K1 and mTORC1 substrate, increased the chronological lifespan of yeast cells [30]. This was soon followed with studies in multiple models establishing a direct role for mTOR in aging: RNA interference (RNAi) knockdown of mTOR (*let-363*) [31] or mutation of mTORC1 component Raptor (daf-15) [32] extended lifespan in *Caenorhabditis elegans*; overexpression of upstream negative mTORC1 regulators tuberous sclerosis complex genes 1 and 2 (TSC1, TSC2) as well as dominant negative forms of mTOR or S6K1 increased lifespan in *Drosophila melanogaster [29]*; deletion of either *SCH9* or *TOR1* increased lifespan in *Saccharomyces cerevisiae* [27]. Building on this paradigm, rapamycin has been used to effect pharmacological inhibition of mTOR resulting in lifespan extension in yeast [33, 34], nematodes [35], fruit flies [36], and mice [37-39]. These data demonstrate a clear and important role for mTOR in the regulation of longevity across evolutionarily distant species.

In 2013 the “Hallmarks of Aging” was published [40]. In an attempt to consolidate knowledge in the field à la the “Hallmarks of Cancer,” this seminal work proposed 9 “hallmarks” as common denominators of aging: genomic instability, telomere attrition, epigenetic alterations, loss of proteostasis, deregulated nutrient-sensing, mitochondrial dysfunction, cellular senescence, stem cell exhaustion, and intracellular communication [40]. In keeping with the observations implicating mTOR in longevity regulation, a number of these “hallmarks” are known to be affected by mTOR.

Alterations in protein homeostasis or proteostasis are linked to aging [41]. The maintenance of proteostasis occurs via a complex interplay of protein synthesis, protein clearance, and quality control mechanisms such as the unfolded protein response (UPR). Deletion of different components of the

translational machinery resulting in a decrease in protein biosynthesis has been shown to increase lifespan in *S. cerevisiae, C. elegans, and D. melanogaster* [42]. mTORC1 stimulates protein synthesis through its evolutionary conserved substrates S6K and 4E-BPs [43] and suppresses autophagy. mTORC1 may also suppress protein degradation by controlling proteasomal activity: mTORC1 inhibition enhances ubiquitination, thereby increasing protein degradation by the proteasome [44].

Mitochondrial dysfunction is a distinct characteristic of aging cells characterized by: elevated ROS production and mitochondrial DNA mutations; decreased electron transport function, membrane potential, and ATP production; altered mitochondrial dynamics or dysregulated mitophagy [40, 45]. mTORC1 stimulates transcription and subsequent translation of nuclear-encoded mitochondrial genes such as components of the electron transport chain and mitochondrial ribosomal proteins [46]. In addition to its established role as an inhibitor of autophagy [47], mTORC1 has been shown to be involved in the regulation of mitophagy [48].

Cellular senescence is characterized by a permanent exit from the cell cycle [49]. Senescent cells display an increase in cell size and mitochondrial mass as well as mitochondrial dysfunction and the development of the senescence-associated secretory phenotype (SASP) [50]. mTOR plays a role in the promotion of the secretory phenotype of senescent cells, while its inhibition has been shown to prevent stem cell senescence [51-53].

mTOR is truly a master regulator of cell fate. Its impact on many functions speaks to an incredibly complex cross-talk with multiple signaling pathways influencing diverse cellular processes. Its pharmacological or genetic inhibition can extend lifespan in multiple model organisms. It has been implicated in the CR response and multiple age-associated pathologies. As such, there is growing interest in identifying novel mTOR inhibitors.

Chapter 2: A System to Identify Inhibitors of mTOR Signaling Using High-resolution Growth Analysis in *Saccharomyces cerevisiae*

This chapter is lightly modified from Lee, et al. Published in *Geroscience* 39(4):419-428. 2017. doi: 10.1007/s11357-017-9988-4.

Abstract

The mechanistic target of rapamycin (mTOR) is a central regulator of growth and proliferation. mTOR inhibition is a promising therapy for a variety of diseases and disorders. Inhibition of mTOR complex I (mTORC1) with rapamycin delays aging, increases healthy longevity in laboratory animals, is used clinically at high doses to prevent organ transplant rejection and as a treatment of some cancers. Clinical use of rapamycin is associated with several unwanted side effects, however, and several strategies are being taken to identify mTORC1 inhibitors with fewer side effects. We describe here a yeast-based growth assay that can be used to screen for novel inhibitors of mTORC1. By testing compounds using a wild-type strain and isogenic cells lacking either TOR1 or FPR1, we can resolve not only whether a compound is an inhibitor of mTORC1 but also whether the inhibitor acts through a mechanism similar to rapamycin by binding Fpr1. Using this assay, we show that rapamycin derivatives behave similarly to rapamycin, while caffeine and the ATP competitive inhibitors Torin 1 and GSK2126458 are mTORC1 inhibitors in yeast that act independently of Fpr1. Some mTOR inhibitors in mammalian cells do not inhibit mTORC1 in yeast, and several nutraceutical compounds were not found to specifically inhibit mTOR but resulted in a general inhibition of yeast growth. Our screening method holds promise as a means of effectively assaying drug libraries for mTOR-inhibitory molecules in vivo that may be adapted as novel treatments to fight diseases and extend healthy longevity.

Introduction

The budding yeast, *Saccharomyces cerevisiae*, is a premier model system for identifying conserved genetic and pharmacological interventions that extend lifespan [54, 55]. A particularly good example of this is the mechanistic target of rapamycin (mTOR) pathway that was first genetically implicated in aging in yeast [56] and has since emerged as an important target for delaying aging in multicellular invertebrates and mice [57, 58]. Likewise, the small molecule mTOR inhibitor, rapamycin, was first shown to extend lifespan in yeast [59] and has since been shown to have similar pro-longevity effects in nematodes [60], fruit flies [61], and mice [37].

In addition to increased lifespan, rapamycin maintains organismal health during aging in mice, evidenced by decreased occurrence of multiple age-related diseases [62]. Rapamycin treatment in aging mice reduces cancer [63, 64], prevents cognitive dysfunction [65, 66], attenuates declining renal and hepatic function [67], improves muscle and visual performance [67], and reverses cardiac [68, 69] and immune decline [70]. Improved cardiac function from rapamycin treatment has recently been similarly observed in middle-aged companion dogs [71], while improved immune function has been observed in healthy elderly people treated with the rapamycin derivative everolimus (RAD001) [72]. Transient rapamycin treatment regimens lasting as few as twelve weeks and initiated late in life are also effective at increasing lifespan and healthspan in mice [73]. These findings place rapamycin and other mTOR inhibitors among the leading candidates for translational interventions to promote healthy aging in people and companion animals [74-76].

The mechanistic target of rapamycin (mTOR) is a nutrient and growth factor responsive kinase that functions in two distinct protein complexes: mTOR complex 1 (mTORC1) and mTOR complex 2 (mTORC2) [77, 78]. Rapamycin binds to the FK506 binding protein FKPB12 (Fpr1 in yeast), and the FKBP12-rapamycin complex inhibits the activity of mTORC1 by disrupting the physical interaction between the mTOR protein and a second mTORC1 component, raptor (Kog1 in yeast) [79, 80]. Deletion of *FPR1* confers resistance to rapamycin in yeast [79, 81]. The mTORC1 complex regulates a variety of downstream cellular processes including mRNA translation, autophagy, and mitochondrial metabolism, all of which are affected

by rapamycin treatment [82]. Unlike mTORC1, mTORC2 activity is not directly inhibited by rapamycin [83]. The mTORC2 complex is less well characterized than mTORC1, but is similarly involved in regulating a variety of cellular processes including cytoskeleton organization and regulation of metabolism. Long-term treatment with rapamycin in mammals is reported to cause indirect inhibition of mTORC2, which is implicated in metabolic defects including insulin resistance and glucose intolerance [84]. Both mTOR complexes are essential for viability in yeast and multicellular eukaryotes.

Budding yeast contain two genes that encode the mTOR kinase: *TOR1* and *TOR2*. Tor1 functions exclusively in mTORC1, while Tor2 functions in both complexes [85]. Consistent with this, deletion of *TOR2* leads to inviability due to lack of functional mTORC2 activity [86], while deletion of *TOR1* results in viable cells that are long-lived and sensitive to rapamycin, due to reduced mTORC1 activity [19, 79]. Despite their sensitivity to rapamycin, *tor1Δ* yeast cells do not show a substantial reduction in mRNA translation or doubling time [87, 88], indicating that Tor2 provides sufficient mTORC1 activity for normal growth in rich medium.

Multiple pharmaceutical mTORC1 and general mTOR inhibitors are used as chemotherapeutic agents [89-93]. Additionally, several natural products and natural product mixtures are reported to inhibit mTOR signaling in cell culture and rodent models, including: curcumin [94, 95], green tea extract [96], epigallocatechin-3-gallate [96, 97], caffeine [98, 99], genistein [100], lycopene and eicosapentaenoic acid (EPA) [93], sulforaphane [101], alpha-lipoic acid [102, 103], glucosamine [104], quercetin [105, 106], berberine [107] and resveratrol [108]. In most cases, the mechanistic basis for inhibition of mTOR via these natural products is unknown, and it remains unclear whether these compounds act via direct inhibition of mTOR, mTORC1, or through indirect effects on components of the mTOR/nutrient response network.

To facilitate identification of new small molecule mTOR inhibitors *in vivo*, we have developed a simple yeast-based assay that quantifies differential growth inhibition in rapamycin-sensitized and rapamycin-resistant genetic backgrounds using a Bioscreen C MBR plate reader/shaker/incubator. We have previously optimized the Bioscreen C MBR machine to obtain high-resolution growth curves of budding yeast cells for chronological lifespan analysis [109, 110] and assessing differential sensitivities of yeast strains to different chemical and environmental stressors [111]. Here we extend this method by

assessing the impact of rapamycin and several other small molecules on doubling time and outgrowth in rich media for wild type BY4742 cells and isogenic *tor1Δ* and *fpr1Δ* cells. Our method relies on the fact that deletion of *TOR1* confers sensitivity to rapamycin due to diminished mTORC1 activity, while deletion of *FPR1* confers resistance to rapamycin due to the necessary role of Fpr1 in rapamycin-mediated mTORC1 inhibition. Given this, we predict that mTORC1 inhibitors with mechanisms similar to rapamycin will display similar differential growth inhibition across the three genotypes, while compounds that inhibit mTORC1 by a mechanism distinct from rapamycin will have a greater inhibitory effect on growth of *tor1Δ* cells relative to WT or *fpr1Δ* cells, but that WT and *fpr1Δ* cells will show similar inhibition of growth at a given drug concentration. Drugs that do not inhibit mTORC1 will either have no effect on growth in any of the genotypes or will similarly inhibit growth across all three genotypes. We report the validation of this assay using rapamycin, rapamycin derivatives, and mTOR catalytic inhibitors. We also report the effect of several natural product compounds on mTORC1 inhibition and outgrowth, finding that among the natural products tested, only caffeine displays the outgrowth profile expected for an *in vivo* inhibitor of mTORC1 in yeast.

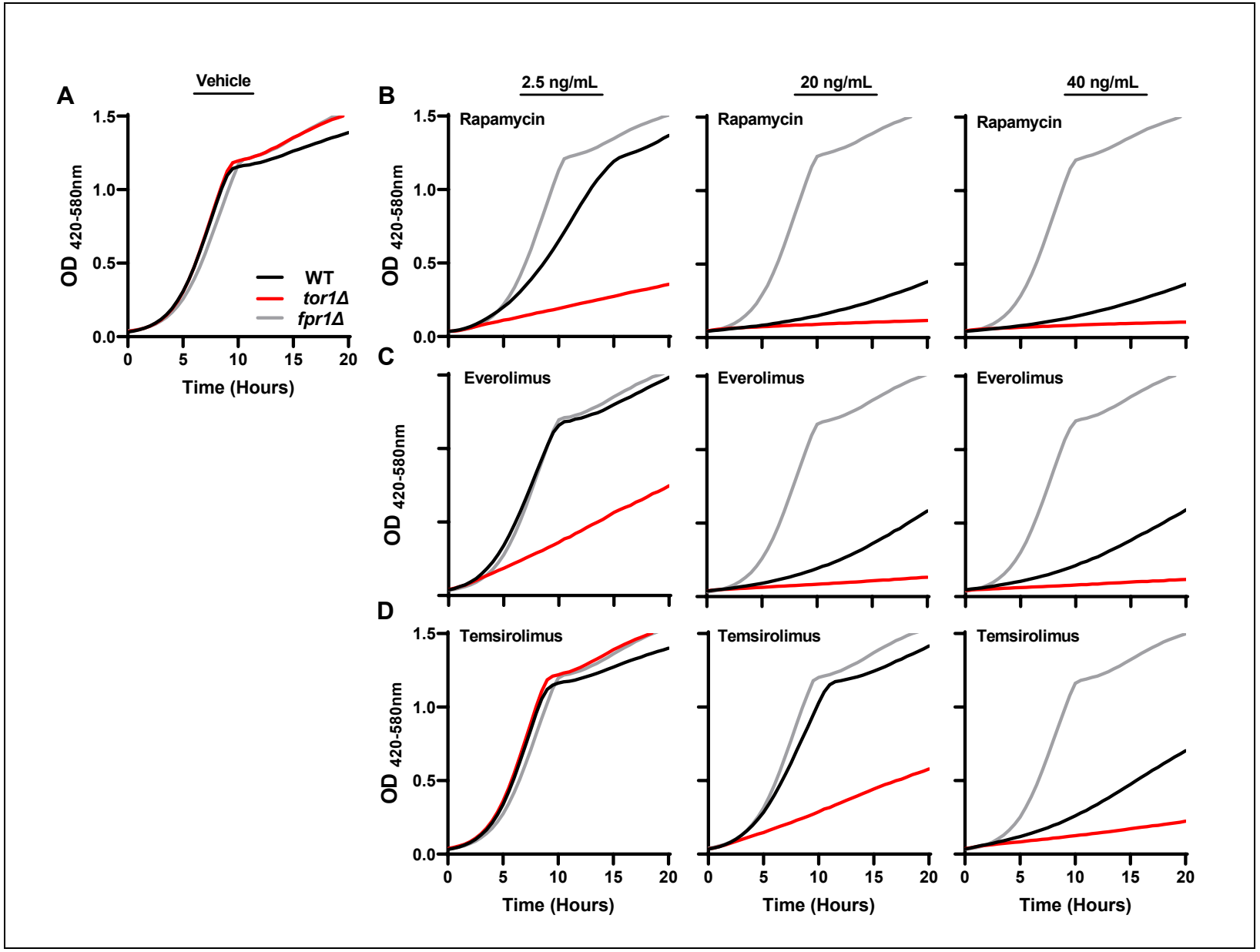
A
Vehicle
OD 420-580nm
1.5
1.0
0.5
0.0
0
5
10
15
20
Time (Hours)
WT
tor1Δ
fpr1Δ
B
2.5 ng/mL
20 ng/mL
40 ng/mL
Rapamycin
C
Everolimus
D
Temsirolimus

Figure 1. *tor1Δ* mutants are hypersensitive and *fpr1Δ* mutants are resistant to rapamycin and rapalogs. Representative growth curves of WT (black), *tor1*Δ (red), and *fpr1*Δ (gray) yeast grown in YPD with A) 1.5% DMSO (vehicle) or 2.5-40 ng/mL (left to right) B) rapamycin (R), C) everolimus (E), or D) temsirolimus (T).

Results

TOR1 mutants are hypersensitive and FPR1 mutants are resistant to rapamycin and rapalogs

We tested the effect of known mTORC1 inhibitors on growth kinetics in three haploid yeast strains: wild type (WT) BY4742 and isogenic *tor1Δ*, and *fpr1Δ* single-gene deletion mutants. We began by analyzing dose responses for rapamycin and two rapalogs, everolimus and temsirolimus. As expected, all concentrations of rapamycin tested reduced *tor1Δ* outgrowth to a greater extent than WT cells, while *fpr1Δ* cells were resistant to growth inhibition (**Figures 1 and 2**). Everolimus and rapamycin produced remarkably similar growth inhibitory responses, while higher concentrations of temsirolimus were necessary to achieve growth inhibition comparable to the other two drugs.

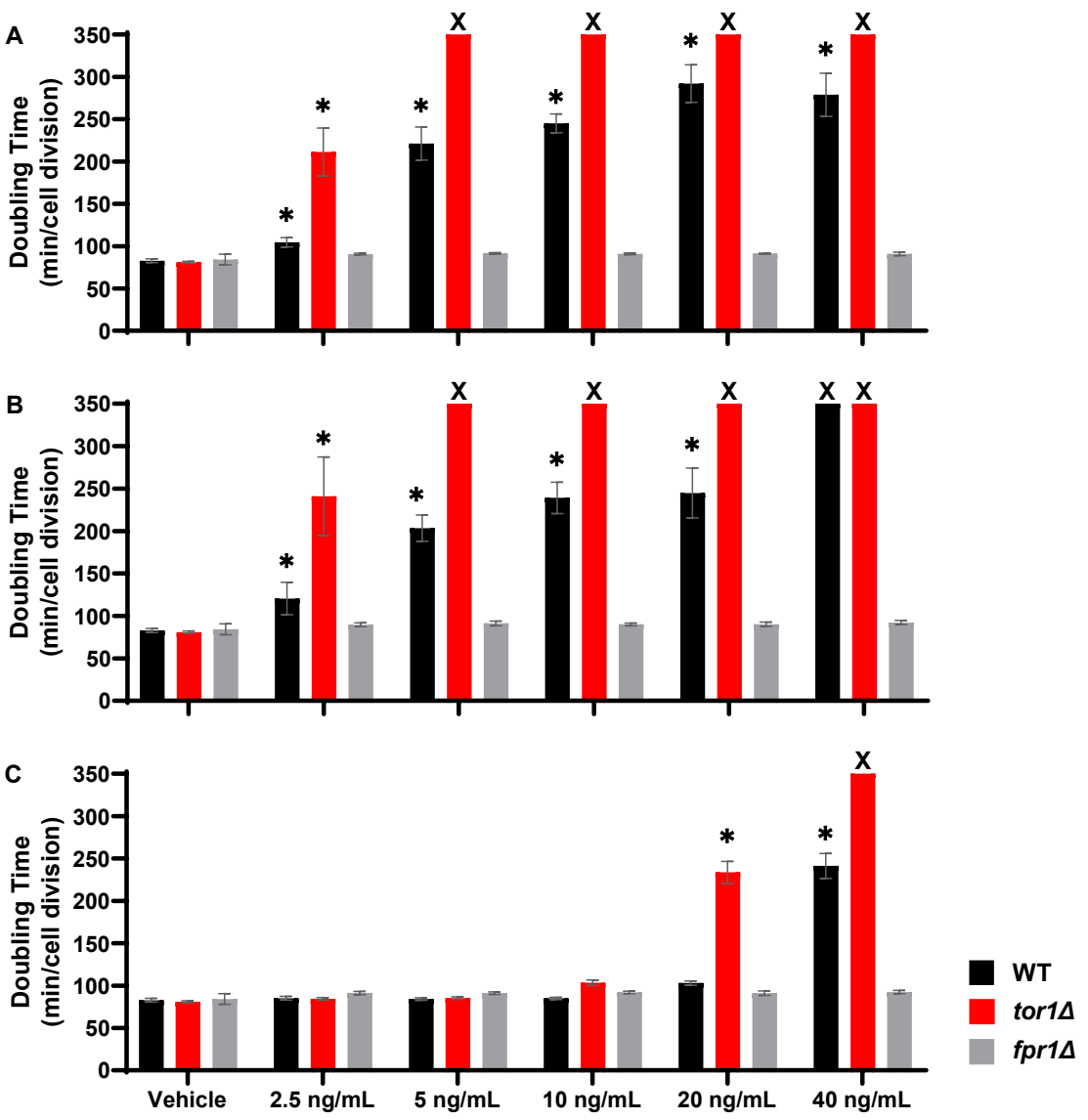

Figure 2. Peak doubling times (DT) (minutes/cell division) of WT (black), *tor1*Δ (red), and *fpr1*Δ (gray) in vehicle and 2.5-40 ng/mL A) rapamycin (R), B) everolimus (E), or C) temsirolimus (T) (n=3-5 for each treatment). Error bars = SEM. * = significantly different from 1.5% DMSO control ($p < 0.05$, Welch's t-test). x = doubling time could not be calculated due to no growth, indicated by OD ≤ 0.3 after 20 hours.

Sensitivity of the *tor1Δ* strain to mTORC1 inhibitors can been seen at 2.5 ng/mL rapamycin or everolimus and at 20 ng/mL temsirolimus, where deletion of *TOR1* results in a significantly greater increase

in doubling time relative to WT (**Figure 2 and Supplemental table 1**). Resistance of the *fpr1Δ* strain is most evident at the highest concentration of each drug tested, where both WT and *tor1Δ* strains have doubling times exceeding 200 minutes, while the *fpr1Δ* cells are still growing as rapidly as in the vehicle control (doubling time 80-90 minutes).

One consequence of diminished mTORC1 signaling is diminished protein translation [112, 113]. To determine if diminished protein translation is sufficient to recapitulate rapamycin-like patterns of growth inhibition, we tested concentrations of the general protein translation inhibitor cycloheximide (CHX) ranging from 1-500 ng/mL. Cycloheximide treatment potently and similarly inhibits growth of all three strains at concentrations of 50 ng/mL and greater (**Supplemental figure 1**).

ATP competitive inhibitors of mTORC1 produce a distinct growth inhibitory profile compared to rapamycin treatment

In addition to rapamycin-like compounds that inhibit mTORC1 signaling via interaction with Fpr1, several drugs have been developed that act as ATP-competitive inhibitors of mTOR in mammalian cells. To understand how these compounds differentially impact growth in our yeast strains, we tested dose responses for Torin 1, GSK2126458, GDC-0941, and AZD8055 (**Figure 3**, **Supplemental figure 2**, and **Supplemental table 2**). All of the ATP-competitive inhibitors required micromolar concentrations to inhibit growth, compared to nanomolar concentrations when using rapamycin and rapalogs. At 10 μM Torin 1, *tor1Δ* cells were strongly growth inhibited (87% increase in doubling time relative to vehicle, $p < 0.01$, Welch's t-test), while WT (42% increase, $p < 0.01$, Welch's t-test) or *fpr1Δ* (30% increase, $p < 0.05$, Welch's t-test) were less effected (**Figure 3** and **Supplemental table 2**). At 25 μM Torin 1, growth of all three strains was severely impacted, with WT and *fpr1Δ* cells showing similar reductions in growth rate, as expected for a catalytic inhibitor of mTOR that does not act through Fpr1.

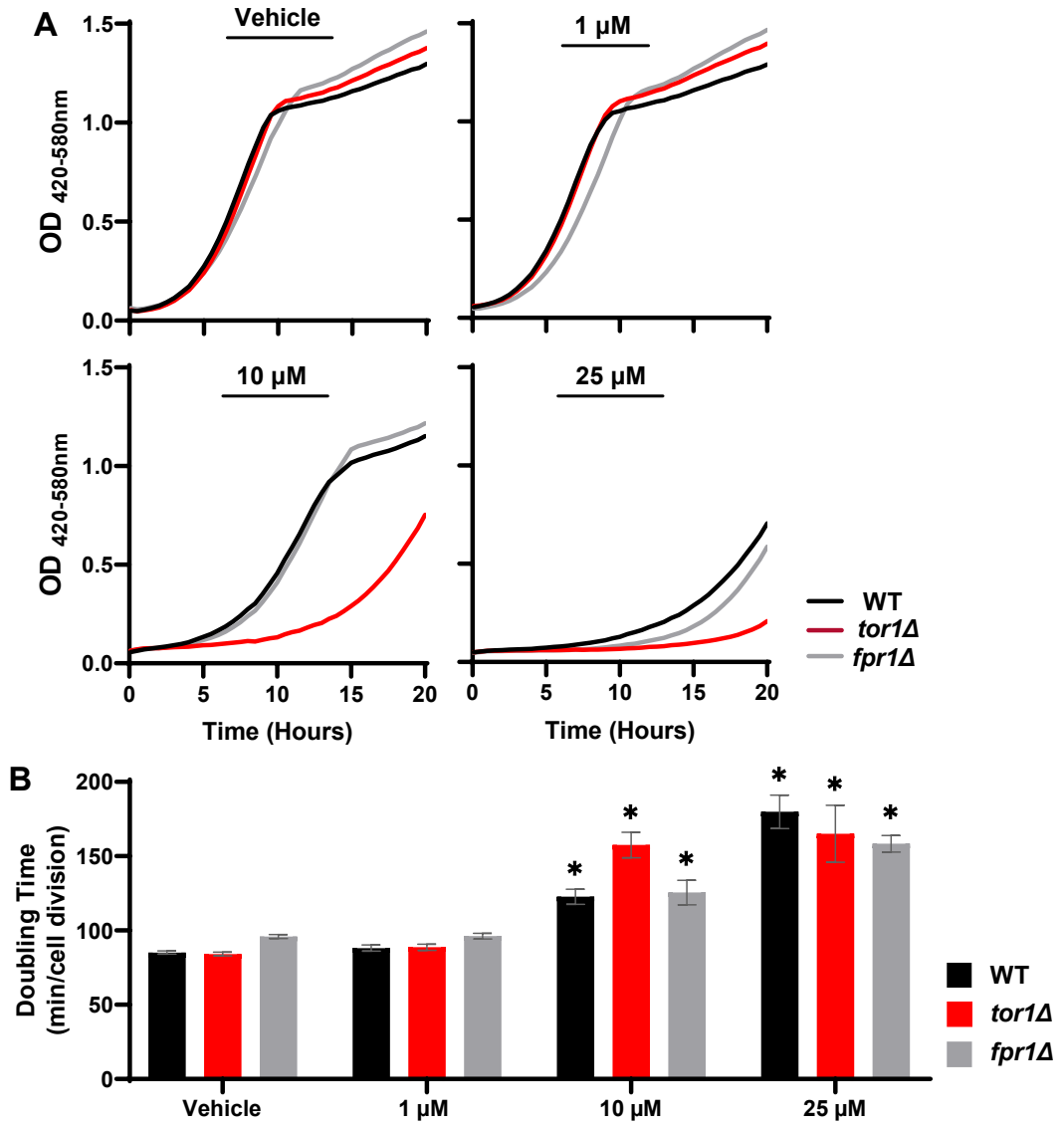

Figure 3. Torin 1 (a catalytic inhibitor of mTOR) produces a distinct growth inhibitory profile relative to rapamycin. *tor1Δ* mutants are hypersensitive to Torin 1 and *fpr1Δ* mutants are not resistant. A) Representative growth curves of WT, *tor1Δ*, and *fpr1Δ* outgrown in the presence of 2.5% DMSO (vehicle control) (top left), 1µM Torin 1 (top right), 10µM Torin 1 (bottom left), or 25µM Torin 1 (bottom right). B) Doubling time (minutes/cell division) for WT, *tor1Δ*, and *fpr1Δ* strains grown in either 2.5% DMSO (vehicle control) (n=9 for WT and *fpr1Δ*, and n=10 for *tor1Δ*) or 1-25µM Torin 1 (n=4 for each strain in 1µM Torin

1 and n=5 for each strain in 10 and 25μM Torin 1). * = significantly different from 1.5% DMSO control ($p < 0.05$, Welch's t-test).

GSK2126458, another catalytic inhibitor of mTOR, only weakly impacted yeast growth (**Supplemental figure 2** and **Supplemental table 2**). Doubling time was modestly increased by 100 μM GSK2126458 in all three strains, while growth of only the *tor1Δ* cells was impacted by lower concentrations. Interestingly, neither GDC-0941 nor AZD8055 produced a measurable change in growth in any yeast strains (**Supplemental figure 2** and **Supplemental table 2**).

Among several putative mTORC1 inhibitory nutraceuticals, only caffeine shows specificity for mTORC1 in yeast

Many nutraceutical compounds are described as having an mTORC1 modulatory effect, particularly in the context of human cancer cell culture models. To identify and validate mTORC1-modulating nutraceuticals in yeast, we tested a subset of these compounds in our Bioscreen C MBR assay (**Table 1**). Most of the tested nutraceuticals produced no effect on growth at concentrations up to 100 μg/mL (**Table 1**). Quercetin significantly inhibited WT and *tor1Δ* doubling time by 23% and 25%, respectively, at the highest concentration tested ($p < 0.01$, Welch's t-test), but did not produce a significant difference in *fpr1Δ* doubling time ($p = 0.24$, Welch's t-test) even though a trend toward increased doubling time is seen in the strain. Two compounds tested, berberine and lycopene, inhibited growth in a genotype-independent manner. Lycopene only modestly impacted growth, while berberine strongly inhibited growth at 100 μg/mL.

Among the nutraceuticals tested, caffeine was the only compound that showed growth inhibition consistent with an mTOR inhibitory effect, increasing doubling time specifically in the *tor1Δ* mutant cells at 100 μg/mL (**Figure 4**). Caffeine also increased WT and *fpr1Δ* doubling times at concentrations greater than 750 μg/mL. To assess epistatic relationships between Fpr1 and mTORC1, we constructed a *tor1Δ fpr1Δ* double mutant. Growth inhibitory profiles in *tor1Δ fpr1Δ* were identical to those of *tor1Δ* in our caffeine

dose response (Figure 4C), confirming that Fpr1 is not required for caffeine-mediated growth inhibition in yeast.

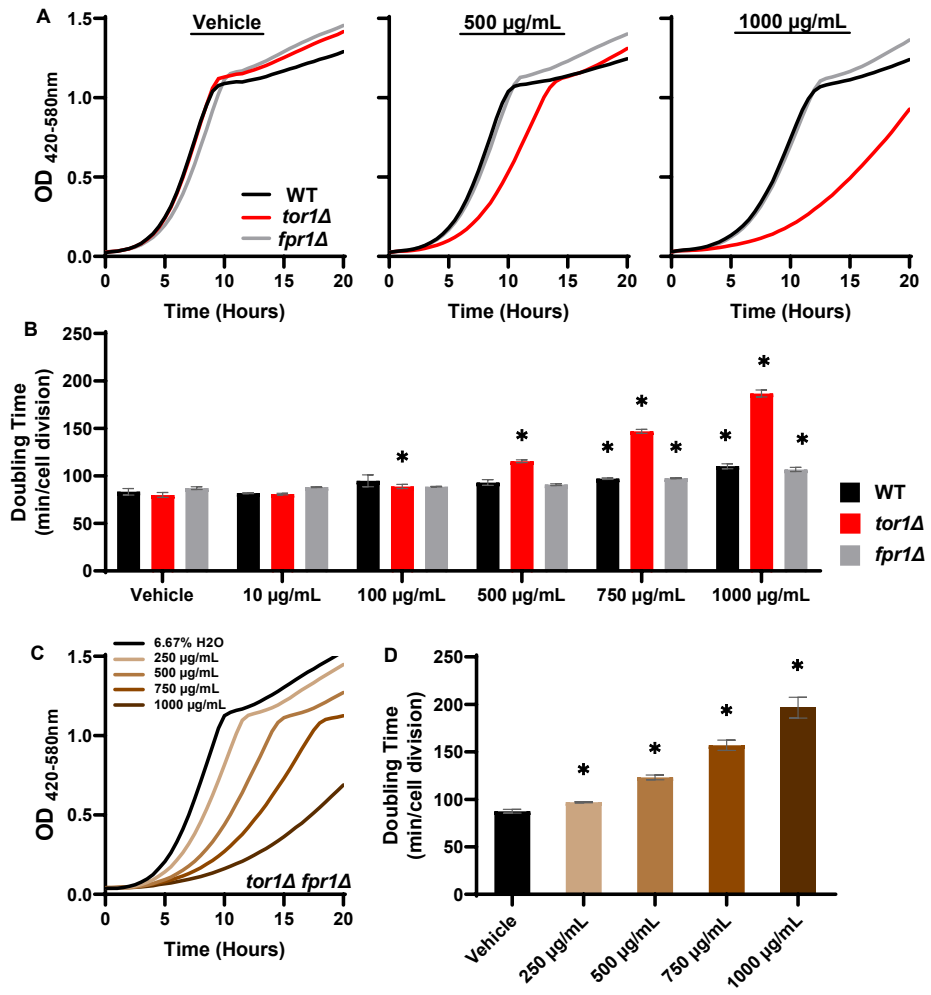

Figure 4. Caffeine inhibits yeast growth in *tor1Δ* cells independently of Fpr1.

A) Representative growth curves of 6.67% H_2O (vehicle) (top left), 500µg/mL (middle), and 1000µg/mL (right). B) Peak doubling time (minutes/cell division) for WT, *tor1Δ*, and *fpr1Δ* yeast grown in H_2O or 10-1000µg/mL caffeine (n=3-5 independent cultures for each strain*treatment tested). * = significantly different from 1.5% DMSO control ($p < 0.05$, Welch's t-test). C) *tor1Δ fpr1Δ* are sensitive to caffeine, indicating that caffeine-mediated growth inhibition in *tor1Δ* cells is independent of Fpr1. D) Peak doubling times for *tor1Δ fpr1Δ* grown in H_2O or 250-1000µg/mL caffeine (n=6 independent cultures for each strain*treatment tested).

Discussion

Rapamycin and other mTOR inhibitors have emerged as one of the most promising classes of molecules for treating a variety of diseases and promoting healthy longevity [114]. The largest barrier to clinical utilization of these compounds for such purposes is the risk of adverse side effects. While it remains unclear how significant an issue this is in relatively healthy people at lower doses, the perception that mTOR inhibitors are risky drugs remains a significant challenge. Thus, there is a need to develop novel mTOR inhibitors that are effective *in vivo* and which may have fewer side effects. Of particular interest are natural product "nutraceutical" mTOR inhibitors.

By utilizing yeast strains with differential sensitivity to mTORC1 inhibition, we developed an *in vivo* screening platform that allows us to preliminarily categorize compounds as growth inhibitory, mTOR inhibitory, and/or rapamycin mimetics. Compounds that inhibit WT, *tor1Δ*, and *fpr1Δ* cells similarly are general growth inhibitors but are unlikely to be either direct or indirect mTOR inhibitors, at least in yeast. Compounds that induce growth inhibition preferentially or specifically in *tor1Δ* cells are candidate mTOR inhibitors, and if *fpr1Δ* cells are resistant to these compounds, then they are likely inhibiting mTOR by a mechanism similar to rapamycin. The assay system performed as expected here for rapamycin, the rapalogs everolimus and temsirolimus, the catalytic mTOR inhibitors Torin 1 and GSK2126458, and the natural product mTOR inhibitor caffeine. Therefore, we conclude that this assay system is likely to be suitable for identification of novel, unknown pharmaceutical and natural product mTOR inhibitors.

Our analyses also confirmed previously observed cases of differential sensitivity between yeast and mammals with regard to the catalytic mTOR inhibitors AZD8055 and GDC-0941, which may be due to sequence differences between the mammalian and yeast proteins [115]. It is also possible that some compounds will be more or less able to get into yeast cells relative to mammalian cells and that yeast may be able to clear or otherwise detoxify certain compounds more or less effectively. Thus, it is important to recognize that any hits identified in the yeast-based screening system described here will need to be validated in mammalian cells to confirm similar mTOR-inhibitory effects, and that failure to detect mTOR inhibition in this system for a given compound does not rule out the possibility that the compound could

inhibit mTOR in mammalian cells. Nonetheless, given the biochemical and mechanistic similarities between yeast and mammalian mTORC1 and mTORC2, we anticipate that many compounds will behave similarly in both systems, as is the case for several examples reported here.

It is of particular interest that, among the nutraceutical compounds tested, only caffeine demonstrated growth kinetics consistent with mTORC1 inhibition in our yeast assay. This supports prior studies of caffeine on mTOR activity in budding yeast [99, 116] and fission yeast [117], and is of interest in light of numerous reports that caffeine can extend lifespan in invertebrate models [118, 119] and that coffee consumption is associated with reduced mortality in people [120, 121]. It is intriguing to speculate that these effects could be related to caffeine's mTOR inhibitory activities.

The absence of effects from the other nutraceutical compounds tested suggests that they may not be true mTOR inhibitors. One potential explanation is that some of these compounds, which were generally reported to inhibit mTOR in cancer cell culture models, act via indirect mechanisms through targets that are not present or not similarly affected in yeast. Another possibility is that some of these compounds inhibit mammalian cell growth or nutrient uptake, perhaps specifically in the context of cancer cell culture models, which could have indirect effects on mTOR signaling in response. One interesting example is resveratrol, which is reported to have numerous targets in mammalian cells and to inhibit mTOR through both direct and indirect mechanisms. In one study, resveratrol was found to enhance the physical interaction between mTOR and its inhibitor DEPTOR [122], which has no obvious yeast ortholog. Resveratrol has also been suggested to inhibit mTOR by indirect mechanisms including regulation of phosphoinositide 3-kinase (PI3K), Akt [123], and AMP-activated protein kinase (AMPK) [124]. We found no evidence here to support an mTOR-inhibitory role for resveratrol in yeast, nor any effect on growth at all, consistent with prior work showing that resveratrol does not impact yeast replicative lifespan [125].

Overall, the system described here represents a sensitive, high-throughput, and inexpensive approach to identify growth inhibitory molecules with specificity for mTOR *in vivo*. It may be possible to further optimize this system, for example by screening compounds in a drug sensitized background or by humanizing the system through expression of human proteins in the mTOR signaling pathway in yeast. Additionally, this method is easily adapted for testing drug interactions by adding a mixture of two or more

compounds, as well as for investigating the impact of genetic diversity on mTORC1 inhibition through use of large-scale genetic libraries or wild isolate yeast strains [126, 127]. The identification of new mTOR inhibitors and genetic variants that impact sensitivity to mTOR inhibition will facilitate the development of new therapies and personalized approaches for a breadth of conditions where mTOR signaling is perturbed.

Materials and Methods

Yeast strains and culture conditions.

All yeast strains used were in the BY4742 genetic background (*MATα his3Δ1 leu2Δ0 lys2Δ0 ura3Δ0*). BW1121 (BY4742) was purchased from Thermo Fisher Scientific (Waltham, MA). GS668 (*fpr1Δ::kanMX4*) and GS983 (*tor1Δ::kanMX4*) were obtained from the haploid *MATα* yeast deletion collection [128]. PCR was used to confirm knockout identity. For GS983, 5'-TTGAATCCTAATTTCTTGCTCAATC-3' and 5'-AAGGCATATATTGATGCTCAAAAAG-3' primers were used to confirm knockout. For GS668, 5'-GTTACTTGATGATATTAAGCACGGG-3' and 5'-ACAAAAATGAACCATTAGCAAAGAG-3' primers were used to confirm knockout. The *tor1Δ fpr1Δ* double deletion strain was constructed by mating *tor1Δ::URA3* (gift of Lindsay Fox) and *fpr1Δ::kanMX4* and selecting for Ura^+ $G418^r$ haploid spores after sporulation and tetrad dissection. PCR was used to verify presence of gene deletions. For overnight culture and growth analysis, YPD (1% w/v Bacto™ yeast extract (BD), 2% w/v Bacto™ peptone (BD), 2% w/v dextrose) media was used. Yeast were cultured at 30°C for all experiments.

Growth analysis using Bioscreen C MBR

Growth analysis of yeast strains was performed using a Bioscreen C CMB (Growth curves USA, Piscataway NJ, USA) as previously described [109]. Briefly, colonies outgrown from frozen stocks were inoculated into 5 mL YPD and incubated at 30°C in a roller drum for 12-16 hours. Two µL of outgrown culture was used to inoculate 148 µL YPD into 100-well honeycomb plates for growth analysis. At least three colonies per strain were analyzed in triplicate for each drug treatment. Doubling times were

calculated identifying the slope of the inflection point along growth curves using the online web tool Yeast Outgrowth Data Analyzer (YODA) [129]. Welch's (unequal variance) t-test was used to assess statistical significance.

Drug preparation and suppliers

All drugs except caffeine and cycloheximide were suspended in DMSO (these drugs suspended in H_2O). Rapamycin, everolimus, and temsirolimus, were purchased from LC Laboratories (Woburn MA, USA). Cycloheximide and berberine were purchased from Sigma-Aldrich (St. Louis MO, USA). Torin 1 was purchased from Cayman Chemical (Ann Arbor MI, USA). AZD8055, GDC-0941, and GSK2126458 were kind gifts from Jason Pitt. Caffeine was purchased from MP Biomedicals (Santa Ana CA, USA). Resveratrol was purchased from AstaTech Inc. (Bristol PA, USA). Alpha-lipoic acid, broccoli concentrate, glucosamine, lycopene, and quercetin were provided by USANA Health Sciences, Inc. (Salt Lake City UT, USA).

Supplemental Figures

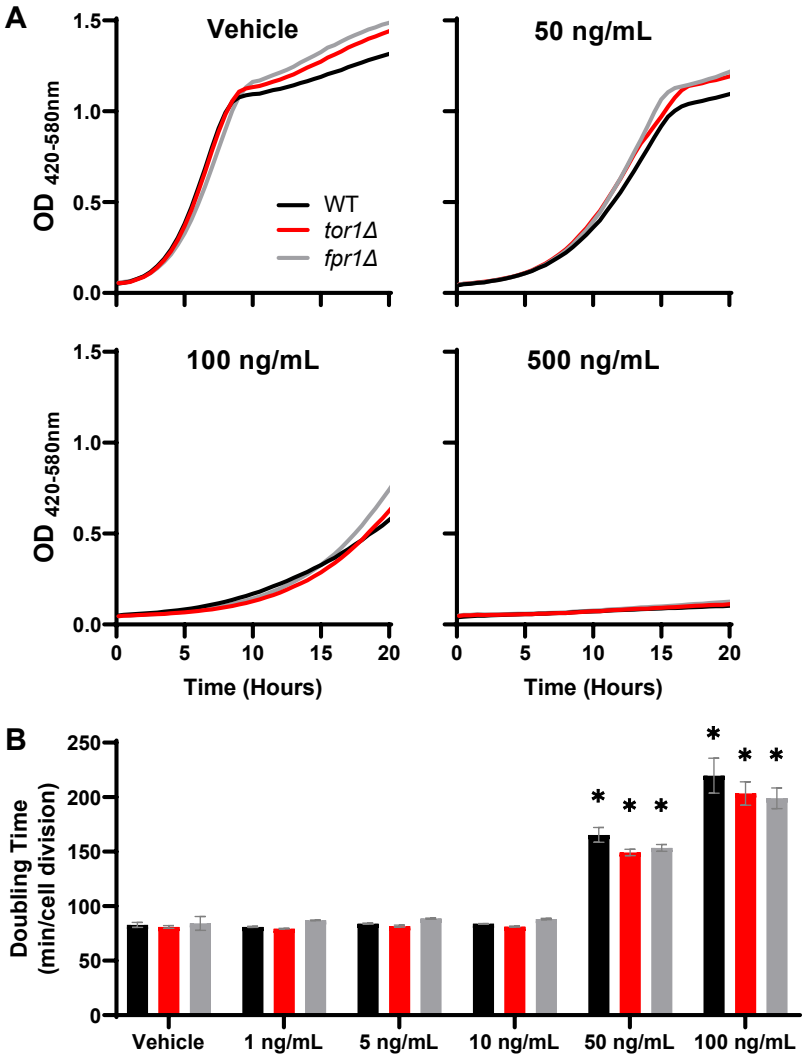

Supplemental figure 1. Cycloheximide (CHX) is a general growth inhibitor in yeast. A) WT (black), *tor1Δ* (red), and *fpr1Δ* (gray) grown in YPD with vehicle (top left), 50ng/mL (top right), 100ng/mL (bottom left), and 500ng/mL (bottom right) CHX. B) Peak doubling time (DT) (minutes/cell division) of WT, *tor1Δ*, *fpr1Δ* cells outgrown in the presence of 1-100ng/mL CHX (n=3-5 biological replicate cultures tested for each strain and treatment). *significantly different from 1.5% DMSO control ($p < 0.05$, Welch's t-test). Error bars = SEM. 500ng/mL CHX treatment could not be calculated because outgrowing cultures failed to reach OD = 0.3 after 20 hours.

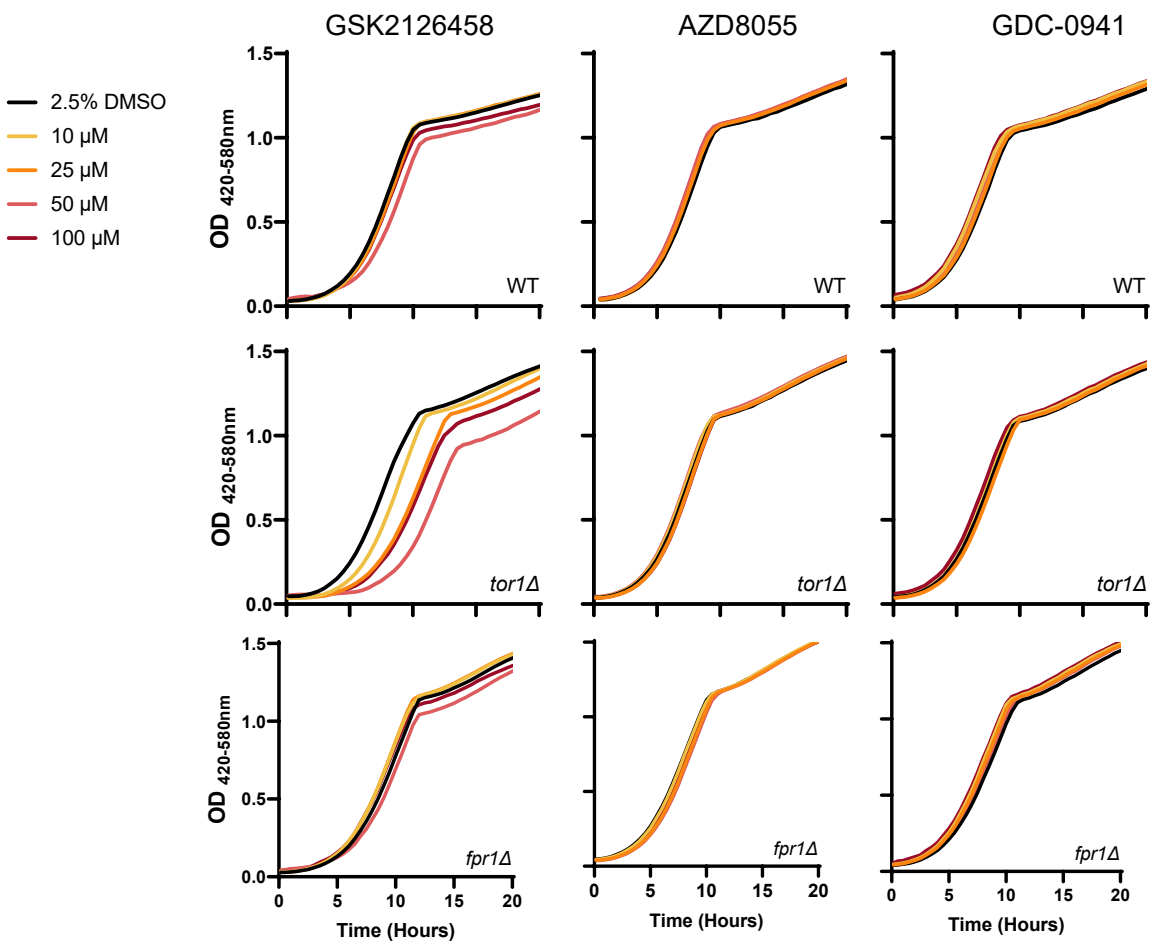

Supplemental figure 2. Many mTOR catalytic inhibitors have limited or no effect on yeast growth. GSK2126458, but not AZD8055 or GDC-0941, impacts growth of *tor1Δ* mutant yeast. Outgrowth of WT (A), *tor1Δ* (B), and *fpr1Δ* (C) in 2.5% DMSO (vehicle control) or 10-100μM GSK2126458 (left), AZD8055 (middle), or GDC-0941 (right). n=3-5 biological replicate cultures tested for each strain and treatment.

Table 1. Doubling time (DT) (minutes/cell division), standard error of the mean (SEM), percent change, and number of cultures tested (n) for putative mTOR-inhibitory neutraceutical compounds.

Treatment	WT			*tor1Δ*			*fpr1Δ*		
	DT (SEM)	% change	n	DT (SEM)	% change	n	DT (SEM)	% change	n
1% DMSO	83.3 (0.9)	-	13	82.8 (0.9)	-	13	90.8 (1.0)	-	13
100µg/mL alpha lipoic acid	85.4 (2.3)	2.6	3	85.2 (1.2)	2.9	3	91.7 (2.1)	-6.2	3
100µg/mL Broccoli concentrate	83.3 (1.1)	0.0	3	82.7 (2.8)	-0.2	3	89.2 (1.9)	-1.8	3
100µg/mL Glucosamine	81.0 (2.5)	-2.8	4	81.2 (2.1)	-2.0	4	87.5 (2.6)	-3.6	4
100µg/mL Lycopene	95.8 (0.3)	15.0*	3	101.1 (2.8)	22.2*	3	107.7 (0.7)	18.6*	3
100µg/mL Quercetin	104.1 (3.1)	25.0*	4	102.0 (6.0)	23.2*	4	105.4 (10.2)	16.1	4
100µg/mL Resveratrol	82.7 (0.8)	-0.7	3	82.4 (0.5)	-0.5	3	87.0 (1.5)	-4.2	3
1µg/mL Berberine	80.2 (2.4)	-3.7	3	79.7 (2.6)	-3.7	3	87.0 (4.2)	-4.2	3
10µg/mL Berberine	102.2 (1.9)	22.7*	3	95.2 (1.8)	14.9*	3	101.8 (2.3)	12.1*	3
100µg/mL Berberine	227.1 (6.7)	172.6*	3	228.6 (2.9)	176.1*	3	238.1 (2.5)	162.3*	3

*= $p < 0.05$, compared to 1% DMSO, Welch's (unequal variance) t-test.

Supplemental Table 1. Doubling time (DT) (minutes/cell division), standard error of the mean (SEM), percent change, and number of cultures tested (n) for rapamycin and rapalogs.

	WT			*tor1Δ*			*fpr1Δ*		
Treatment	DT (SEM)	% change	n	DT (SEM)	% change	n	DT (SEM)	% change	n
1.5% DMSO	82.8 (2.2)	-	5	80.9 (1.2)	-	5	84.3 (6.4)	-	5
2.5ng/mL Rapamycin	104.6 (5.6)	26.3*	4	211.4 (28.3)	161.3*	4	90.6 (1.0)	7.5	4
5ng/mL Rapamycin	221.3 (19.5)	167.2*	4	NG	-	4	91.5 (0.8)	8.5	4
10ng/mL Rapamycin	245.1 (11.0)	196.1*	4	NG	-	4	91.0 (0.9)	7.9	4
20ng/mL Rapamycin	292.0 (22.2)	252.7*	4	NG	-	4	91.1 (0.6)	8.1	4
40ng/mL Rapamycin	278.9 (25.5)	236.9*	4	NG	-	4	90.9 (2.2)	7.8	4
2.5ng/mL Everolimus	120.5 (2.2)	45.5*	4	241.0 (46.3)	198.0*	4	89.7 (2.2)	6.4	4
5ng/mL Everolimus	203.4 (19.1)	145.7*	3	NG	-	3	91.2 (2.7)	8.2	3
10ng/mL Everolimus	239.1 (18.4)	188.7*	3	NG	-	3	90.0 (1.7)	6.7	3
20ng/mL Everolimus	244.8 (29.2)	195.7*	3	NG	-	3	90.3 (2.4)	7.1	3
40ng/mL Everolimus	NG	-	3	NG	-	3	92.2 (2.4)	9.4	3
2.5ng/mL Temsirolimus	85.1 (2.2)	2.8	3	84.4 (1.5)	4.3	3	91.3 (1.8)	8.3	3
5ng/mL Temsirolimus	84.2 (1.4)	1.7	3	85.2 (1.5)	5.3	3	91.2 (1.4)	8.2	3
10ng/mL Temsirolimus	84.9 (1.3)	2.5	3	103.4 (3.2)	27.8*	3	92.1 (1.5)	9.2	3
20ng/mL Temsirolimus	103.0 (2.5)	24.4*	3	233.6 (13.1)	188.8*	3	91.2 (2.6)	8.2	3
40ng/mL Temsirolimus	241.3 (14.7)	191.4*	3	NG	-	3	92.4 (1.9)	9.6	3

* = $p < 0.05$, compared to 2.5% DMSO, Welch's (unequal variance) t-test.

NG = DT could not be calculated due to no growth, indicated by OD ≤ 0.3 after 20 hours.

Supplemental Table 2. Doubling time (DT) (minutes/cell division), standard error of the mean (SEM), percent change, and number of cultures tested (n) for catalytic mTOR inhibitors.

	WT			*tor1Δ*			*fpr1Δ*		
Treatment	DT (SEM)	% change	n	DT (SEM)	% change	n	DT (SEM)	% change	n
2.5% DMSO	85.9 (0.9)	-	12	84.6 (1.0)	-	13	96.9 (1.1)	-	12
10μM AZD8055	92.4 (8.4)	7.5	4	93.0 (7.5)	9.9	4	104.4 (10.8)	7.7	4
25μM AZD8055	86.2 (1.4)	0.3	3	87.3 (2.2)	3.1	3	95.7 (1.1)	-1.2	3
50μM AZD8055	87.6 (2.6)	1.9	3	89.5 (2.6)	5.8	3	96.9 (3.2)	0.0	3
100μM AZD8055	87.7 (3.3)	2.1	3	89.6 (2.3)	5.9	3	98.6 (2.8)	1.8	3
10μM GDC-0941	85.7 (2.0)	-0.3	3	84.2 (2.1)	-0.5	3	95.9 (2.4)	-1.0	3
25μM GDC-0941	84.6 (1.6)	-1.6	3	82.5 (1.0)	-2.6	3	95.2 (1.2)	-1.7	3
50μM GDC-0941	86.8 (2.8)	1.0	3	85.8 (2.1)	1.4	3	96.8 (2.9)	-0.1	3
100μM GDC-0941	94.3 (3.3)	9.7	3	93.1 (2.6)	10.0	3	102.5 (4.4)	5.8	3
10μM GSK2126458	85.4 (1.5)	-0.6	6	92.5 (1.6)	9.3*	6	97.8 (2.9)	1.0	6
25μM GSK2126458	89.9 (2.5)	4.6	7	105.7 (2.6)	24.9*	7	96.7 (2.3)	-0.1	7
50μM GSK2126458	80.6 (6.3)	-6.2	6	93.2 (4.1)	10.1	6	95.6 (1.6)	-1.3	6
100μM GSK2126458	103.8 (5.4)	20.8*	6	117.3 (6.8)	38.6*	6	112.4 (5.3)	16.0*	6
1μM Torin 1	88.1 (2.0)	2.6	4	88.7 (2.1)	4.9	4	96.2 (2.0)	-0.7	4
10μM Torin 1	122.7 (5.0)	42.8*	5	157.5 (8.6)	86.2*	5	125.5 (8.3)	29.6*	5
25μM Torin 1	179.9 (11.2)	109.4*	5	165.1 (19.1)	95.1*	5	158.4 (5.6)	63.5*	5

*= $p < 0.05$, compared to 2.5% DMSO, Welch's (unequal variance) t-test.

Chapter 3: Pterocarpus marsupium extract extends replicative lifespan in budding yeast

This chapter is lightly modified from Lee, et al. Published in *Geroscience* 2021 Oct; 43(5):2595-2609. doi: 10.1007/s11357-021-00418-x

Abstract

As the molecular mechanisms of biological aging become better understood, there is growing interest in identifying interventions that target those mechanisms to promote extended health and longevity. The budding yeast *Saccharomyces cerevisiae* has served as a premier model organism for identifying genetic and molecular factors that modulate cellular aging and is a powerful system in which to evaluate candidate longevity interventions. Here we screened a collection of natural products and natural product mixtures for effects on growth rate, mTOR-mediated growth inhibition, and replicative lifespan. No mTOR inhibitory activity was detected, but several of the treatments affected growth rate and lifespan. The strongest lifespan shortening effects were observed for green tea extract and berberine. The most robust lifespan extension was detected from an extract of *Pterocarpus marsupium* and another mixture containing *Pterocarpus marsupium* extract. These findings illustrate the utility of the yeast system for longevity intervention discovery and identify *Pterocarpus marsupium* extract as a potentially fruitful longevity intervention for testing in higher eukaryotes.

Introduction

The field of geroscience has yielded important mechanistic insights into biological aging processes and their connection to disease [130], with invertebrate model organisms at the forefront of these discoveries [131]. Several evolutionarily conserved molecular “hallmarks” or “pillars” of aging appear to play a causal role in the cellular, tissue, and functional declines that accompany old age [132, 133]. As our understanding of aging biology evolves, a growing emphasis is now being placed on identifying interventions that target these hallmarks of aging. Such interventions have the potential to delay the onset and progression of multiple age-related diseases simultaneously, with the goal of significantly extending both lifespan and healthspan.

The budding yeast *Saccharomyces cerevisiae* has been used extensively to characterize genetic and molecular mechanisms of cellular aging [54, 55]. Replicative lifespan (RLS) in yeast is defined as the number of daughter cells produced by a mother cell prior to irreversible cell cycle arrest [134]. Numerous studies over the past two decades indicate that many of the genetic and environmental determinants of aging in multicellular eukaryotes are shared with yeast during replicative aging. For example, studies in budding yeast contributed substantially to our understanding of the mechanisms by which caloric restriction [135, 136], sirtuins [137, 138], and mechanistic target of rapamycin (mTOR) [19, 56] signaling impact aging, and how conserved molecular processes including mitochondrial function [111, 139-143], pH homeostasis [144-148], proteasome activity [149, 150], autophagy [151, 152], and genome instability [153, 154] all play important roles during yeast replicative aging.

Identifying pharmacological interventions that directly target the molecular mechanisms of biological aging and thereby increase healthspan and lifespan is a rapidly growing area of research [155]. The nematode *Caenorhabditis elegans* is used effectively in this regard, as evidenced by the fact that more than 50% of the experiments contained in the DrugAge database are performed in this organism [156, 157]. Budding yeast is the fourth most utilized model system (3.5%) in DrugAge, behind both fruit flies (26.2%) and mice (6%). While this frequency does not specify magnitude or direction of effect on lifespan, it does

provide an indication of the relative use of each model system for intervention studies within the field. Despite the fact that lifespan studies in yeast are less expensive and less time consuming than studies in mice, or even fruit flies, the utility of this system as a discovery platform for pro-longevity interventions has lagged.

We recently described a system for identifying candidate pro-longevity compounds in yeast through analysis of high-resolution growth kinetics [158]. This system specifically detects compounds with either direct or indirect mTOR-inhibitory effects by quantifying differential effects on growth rate in different genetic backgrounds. This system also successfully discriminates between allosteric rapamycin-like inhibitors and ATP-competitive catalytic inhibitors. From a small unbiased natural product screen [158], we identified caffeine as an mTOR inhibitor. This may explain its lifespan-extending properties in yeast [116] and worms [118, 119]. Here we describe lifespan and outgrowth analyses of additional natural products from a collection of natural product compounds, extracts, and mixtures. While no new mTOR-inhibitory compounds were identified, we did observe significant lifespan extension from an extract of *Pterocarpus marsupium*, a tree found in southeast Asia with a long history of use in Ayurvedic medicine.

Results

A screen of 42 natural product compounds, extracts, (**Table 1**) and mixtures (**Table 2**) was conducted to understand their impact on growth, mTOR inhibition, and lifespan in yeast. Several of the tested compounds or mixture components were previously reported to impact lifespan in different organisms (**Table 1**). All compounds and mixtures were initially tested at a concentration of 100 ug/mL in rich growth medium (YPD) (see **Materials and Methods**). The results of the growth analyses are summarized in **Table 3** with outgrowth curves and doubling time analysis provided in **Supplemental Figure 1**. None of the compounds or mixtures tested showed evidence for particular mTOR inhibitory activity in the initial screen, which is determined by greater growth inhibition in a *tor1D* strain relative to wild type and *fpr1D* [158]. Several compounds, extracts, and mixtures significantly inhibited growth in at least one strain, including grape seed (Indena), lutein, mixture 2, mixture 6, *Polygonum cuspidatum* root, *Pterocarpus*

marsupium, turmeric, and withaferin A (Figure 1). While not every strain reached statistically significant growth inhibition with these treatments, all strains showed a trend toward increased doubling time. Two compounds, ellipticine and isoliquiritigenin, had particularly pronounced effects on growth at 100 ug/mL. All of the cultures treated with ellipticine failed to achieve OD of 0.3 after 20 hours of growth and therefore fell below our threshold for doubling time quantitation (see Methods). For isoliquiritigenin, all strains were also severely growth inhibited at this concentration, with most cultures falling below our

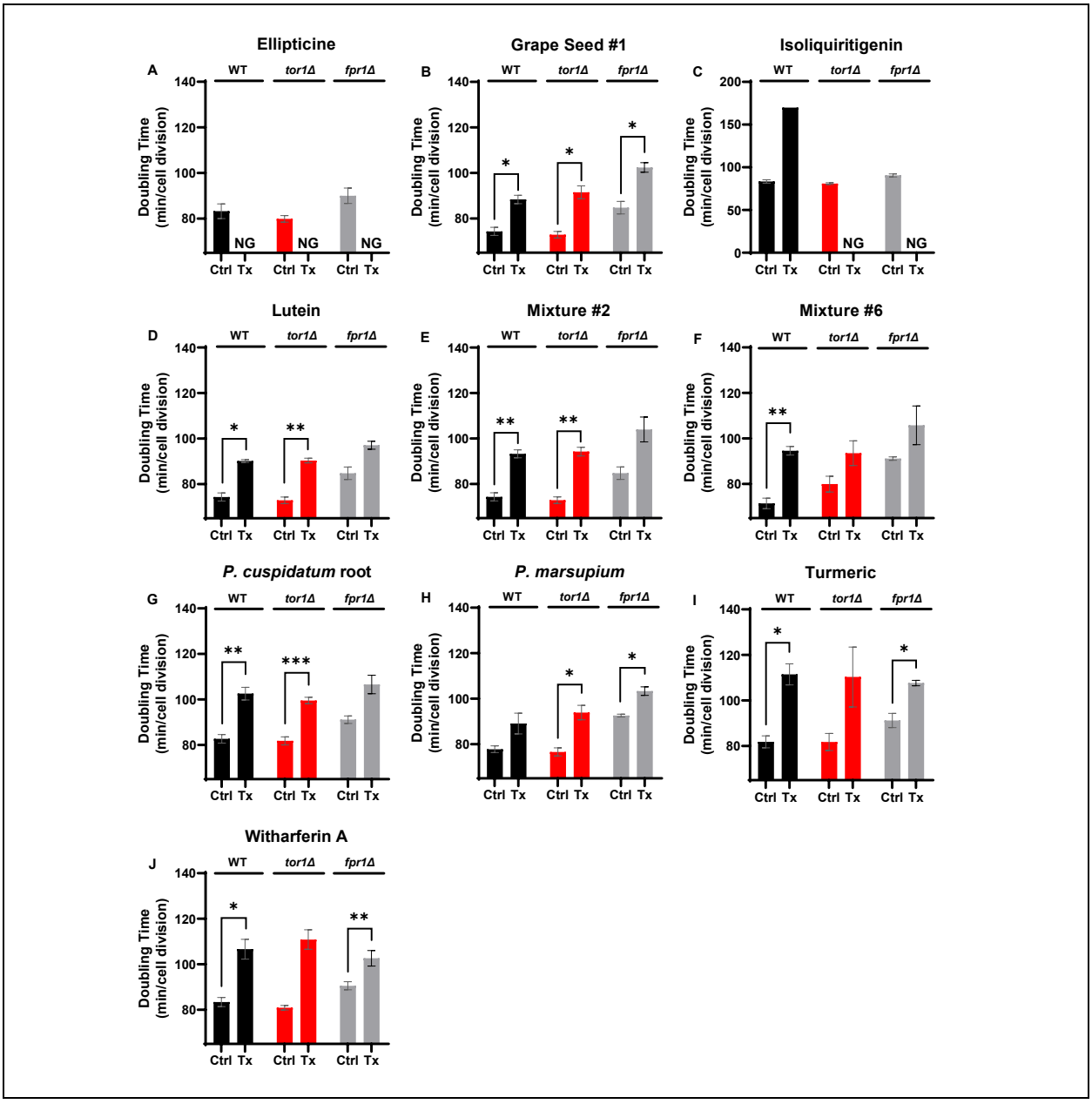

Figure 1. Doubling times for compounds, extracts, and mixtures that significantly inhibit growth. Inflection doubling time (DT) of WT, *tor1Δ* and *fpr1Δ* microcultures. Number of replicates n = 3 for panels A, B, D-F, H and I. Number of replicates n = 6 for panels C, G, and J. Welch's T-test with Bonferroni-correction used to compare treatment (Tx) to vehicle (Ctrl) (* p<0.05, ** p<0.01, *** p<0.001). NG denotes no growth (see methods for more details).

threshold for quantitative doubling time calculation and those that did grow to OD > 0.3 barely achieving this threshold, indicating severe inhibition (**Figure 1**). To better understand the growth inhibitory effect of isoliquiritigenin, we performed a follow-up dose response (**Table 4**). Gradual growth inhibition was observed with increasing concentration of isoliquiritigenin from 1 to 50 µg/mL without evidence for mTOR-inhibitory effects (**Supplemental Figure 1**).

Twenty-four compounds and mixtures were selected from our initial screen and a prior study [158] for RLS analysis in wild type cells (**Supplemental Figure 1 and Table 5**). Across all of the compounds and mixtures tested, no significant correlation was observed between doubling time and lifespan (**Figure 2A**, Standard major axis regression; adjusted R-squared = 0.06, p-value = 0.24). Most substances had no significant effect on lifespan, including alpha-lipoic acid, glucosamine, quercetin, and *Polygonum cuspidatum* root extract, which is 50% resveratrol (w/w) (**Supplemental Figure 1**). Significant shortening of lifespan was observed for green tea extract (p-value < 0.001, Wilcoxon rank sum test, Bonferroni-corrected) (**Figure 2B**). Turmeric extract (raw p-value = 0.009, Bonferroni-corrected p-value = 0.208, Wilcoxon rank sum test) and mixture 5 (raw p-value = 0.042, Bonferroni-corrected p-value = 0.997, Wilcoxon rank sum test) significantly shortened lifespan when p-values were uncorrected, but these did not reach significance after Bonferroni-correction (**Supplemental Figure 1**). Mixture 5 is 13.9% w/w turmeric and one of only two mixtures tested that contains turmeric (the other, mixture 4, contains only 3.4% turmeric w/w) (**Table 2**).

Berberine, in particular, has been described as a potential geroprotective compound with mTOR inhibitory properties [159]. In a previous growth screen, we failed to detect an mTOR inhibitory effect in cells treated with 100 ug/mL berberine [158]. However, the severe growth inhibition at 100 ug/mL

suggested that this concentration is above the toxic threshold for this compound. We therefore performed a dose-response RLS experiment and follow-up mTOR activity screen for concentrations of berberine ranging from 1-50 ug/mL **(Figure 2C-D and Tables 4 and 6)**. We also performed dose response mTOR activity and RLS experiments for 5-100 μM celastrol, an activator of the heat shock response and putative healthspan intervention [160-162]. We resolved no significant RLS effects with any celastrol dose, but concentrations ≥10 μM weakly inhibited growth in all strains (**Tables 4 and 6 and Supplemental Figures 1 and 2**). The significant growth inhibitory effect of berberine seen at 100 ug/mL was also observed in all strains at 50 ug/mL (p-value ≤ 0.01, Welch's t-test, Bonferroni-corrected) with less pronounced effects on growth at lower concentrations (**Figure 2C and Table 4**)**.** RLS was significantly shortened at 50 ug/mL berberine (p-value < 0.001, Wilcoxon rank sum test), but no difference was detected at either 10 ug/mL or 1 ug/mL compared to YPD control (berberine suspended in sterile H_2O instead of DMSO for RLS) (**Figure 2D and Table 6**).

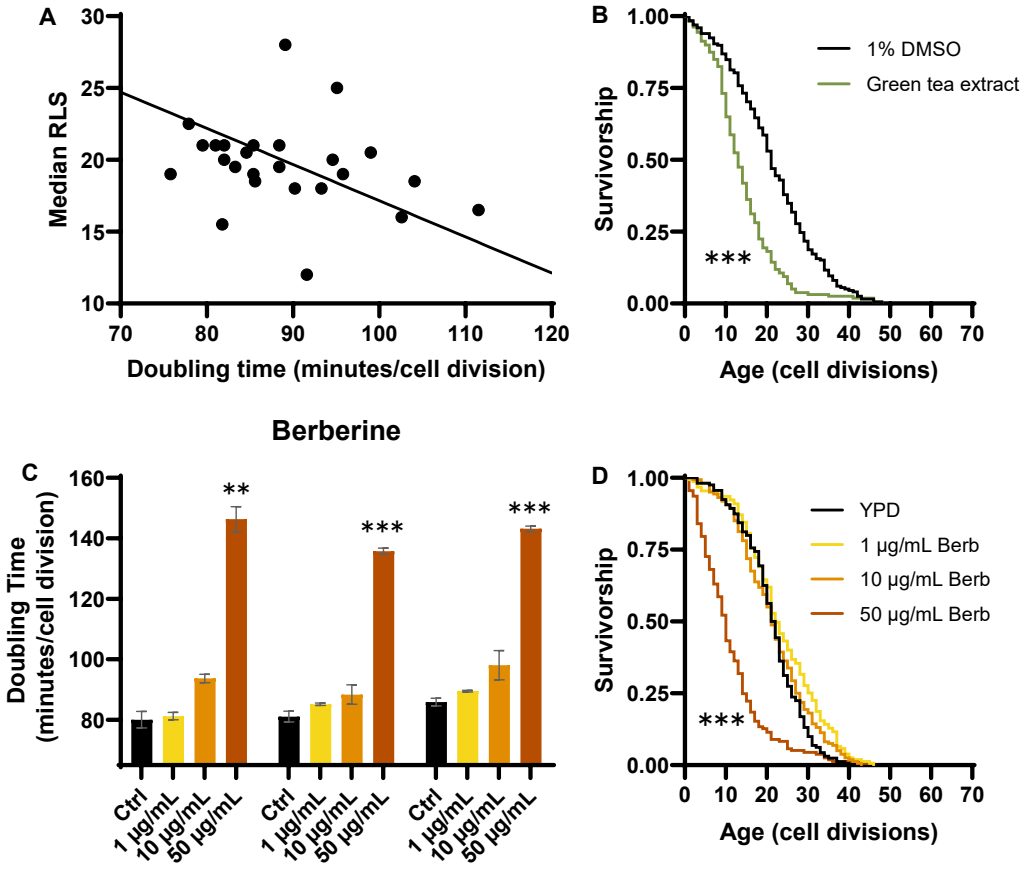

Figure 2. Doubling time and lifespan of natural product treated yeast with outgrowth kinetics and Kaplan-Meier curves for lifespan decreasing treatments. A) Relationship between doubling time (minutes/cell division) and median RLS for natural product-treated yeast (Standard major axis regression, adjusted R-squared = 0.06, p-value = 0.24). B) Green tea extract (GTE) decreases RLS (Wilcoxon rank sum test, Bonferroni-corrected (* $p<0.05$, ** $p<0.01$, *** $p<0.001$)). C) Berberine is a general inhibitor of yeast growth (Welch's T-test, Bonferroni-corrected). D) Berberine RLS dose response (Wilcoxon rank sum test, Bonferroni-corrected). For number of cells or cultures tested and p-values, see Tables 5 and 6.

Only one treatment, *Pterocarpus marsupium* extract (PME), significantly extended lifespan (p-value < 0.001, Wilcoxon rank sum test, Bonferroni-corrected) (**Table 5 and Figure 3**). Mixture 1 significantly

extended lifespan when p-values were uncorrected but did not reach significance after Bonferroni-correction (raw p-value = 0.009, Bonferroni-corrected p-value = 0.219, Wilcoxon rank sum test) (**Table 5 and Supplemental Figure 1**). Interestingly, mixture 1 is the only mixture to contain PME as its primary constituent, along with lesser amounts of alpha-lipoic acid, quercetin, and olive fruit extract (**Table 2**). This suggests that the lifespan extension from mixture 1 may be related to the presence of PME in the mixture.

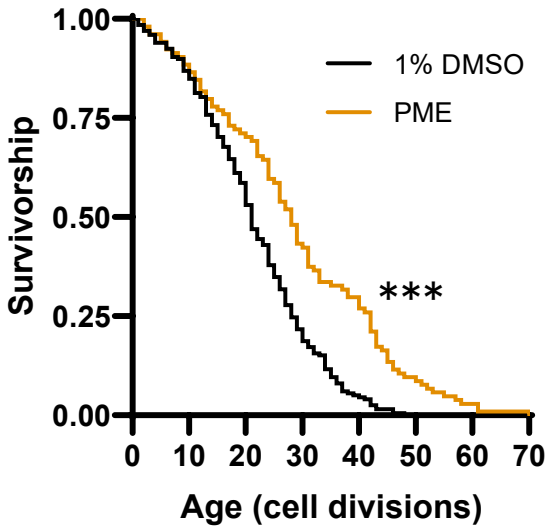

Figure 3. *Pterocarpus marsupium* extract (PME) extends replicative lifespan. 100 µg/mL PME (n = 104) extends lifespan compared to 1% DMSO vehicle control (n = 198) ($p < 0.001$, Wilcoxon rank sum test, Bonferroni-corrected).

Discussion

From a screen of 42 natural products and natural product mixtures, we identified PME as a novel pro-longevity intervention in yeast. PME is an extract from the plant *Pterocarpus marsupium* with well-known antidiabetic properties [163-165]. PME contains several components, presumably one or more of which contributes to its positive effects on RLS. Common components of PME include pterostilbene, epicatechin, pterosupin, marsupin, liquiritigenin, along with a variety of other molecules present in lower abundance [166-168].

Two of the most abundant PME constituents, pterostilbene and epicatechin, are suggested to promote longevity [169, 170], although we could find no published data supporting lifespan extension from pterostilbene. Epicatechin, on the other hand, has been reported to increase lifespan in fruit flies [171]; however, other studies failed to detect significant lifespan extension from epicatechin in worms or flies [172-174]. It will be of interest in future studies to determine which of the various components of PME contribute to the RLS extension observed here, as well as their mechanisms of action.

It is unexpected that none of the compounds or mixtures tested showed consistent evidence for mTOR inhibitory activity, as several have previously been reported to inhibit mTOR signaling. These include both resveratrol [122, 175] and berberine [176-178]. While the Bioscreen C MBR assay is extremely sensitive, there are several potential explanations for the lack of mTOR inhibition observed from the compounds and mixtures in this study. For example, some pharmaceutical compounds that act as ATP-competitive mTOR inhibitors are less effective in yeast relative to mammalian cells [158, 179]. Likewise, compounds that affect mTOR signaling indirectly in mammalian cells, via upstream regulators of mTOR or through other components of the mTOR signaling network such as AMP kinase, may not have identical effects in yeast. For example, the tuberous sclerosis complex proteins TSC1 and TSC2 act as key upstream regulators of mTOR in mammals but do not have clear orthologs in either *S. cerevisiae or C. elegans* [180-182]. Thus, compounds affecting mTOR activity via interactions with TSC1/2 in mammalian cells would not be predicted to have these effects in budding yeast.

Some compounds previously reported to extend lifespan in various model systems did not show lifespan extending effects in our screen and, in some cases, shortened lifespan. There are many potential explanations for this, including the possibility that lifespan extension would have been observed at concentrations other than those tested here. Resveratrol was initially reported to extend RLS in yeast by more than 70% in another strain background [183]. However, we failed to observe any effect on lifespan in the BY4742 strain background with a *Polygonum cuspidatum* root extract containing 50% w/w resveratrol, which is consistent with prior data using a >95% pure resveratrol preparation [125]. Importantly, while

resveratrol has continued to be widely studied for a variety of health effects in both mice and people, it does not appear to extend mouse lifespan [184]. Interestingly, in our mTOR inhibitor screen, *Polygonum cuspidatum* root extract behaved as a general growth inhibitor. A previous study by our group showed no effect of pure resveratrol on yeast growth [158], suggesting that the growth inhibitory effects of *Polygonum cuspidatum* root extract are independent of, or at least not solely mediated by, resveratrol.

Berberine was recently reported to attenuate senescence in fibroblasts, as well as extend lifespan in middle-aged mice and in yeast [185]. However, using similar doses of berberine, we failed to resolve a lifespan extending effect and instead observed significant growth inhibition and shortening of RLS. A key difference between the two studies is RLS assay method; manual dissection of yeast on solid media was used in our study as opposed to a microfluidics-based approach where yeast are submerged in liquid media. While it could be argued that effects in human cells and mice are likely to be more translationally relevant, the strong dose-dependent toxicity of berberine seen in our study suggests that caution is warranted when considering its untested and unregulated use by people, especially over months or years.

Green tea has long been touted as a health and longevity-promoting beverage [186-188]. In yeast, however, it shortens lifespan, at least at the concentrations tested here. One reported mechanism for green tea's health benefits is by altering the gut and oral microbiomes [189, 190], and *S. cerevisiae* and related fungal species are present in the human microbiome [191]. For interventions that improve human health by modifying the microbiome, it is not obvious what effects to expect on individual microbes from among the impacted community. It could be that the set of interventions that negatively impact yeast lifespan are enriched for interventions that could improve human health by remodeling the microbiome. More broadly, novel antifungal compounds identified as part of screening for lifespan-extending interventions may have clinical utility outside of geroscience.

Using combined growth and lifespan analysis in yeast, we identified a lifespan-extending natural product, *Pterocarpus marsupium* extract. Our approach sets the foundation for future genetic and biochemical studies to characterize the mechanistic basis for lifespan extension from PME and provides

incentive to test PME in invertebrate and mammalian model systems. Overall, our study demonstrates the utility of using yeast as a rapid and inexpensive screening tool to identify interventions of interest for geroscience and medicine.

Materials and Methods

Yeast strains and culture conditions

All yeast strains used were in the BY4742 genetic background (*MATα his3Δ1 leu2Δ0 lys2Δ0 ura3Δ0*) and have been previously described [158] except for the celastrol RLS dose response which used the BY4741 genetic background (*MATa his3Δ1 leu2Δ0 met15Δ0 ura3Δ0*) [192]. For overnight culture and growth analysis, YPD (1% w/v Bacto™ yeast extract (BD), 2% w/v Bacto™ peptone (BD), 2% w/v dextrose) media was used. Yeast were cultured at 30°C for all experiments.

Outgrowth analysis

All compounds and mixtures were initially screened at a concentration of 100 µg/mL in DMSO, except for hesperidin which was suspended in 0.027 N NaOH. Analysis of maximal growth rate in yeast strains was performed to identify growth inhibiting interventions using a Bioscreen C MBR (Growth curves USA, Piscataway NJ, USA) as previously described [109, 158, 193, 194]. Raw optical density data were smoothed using the R package “smooth.spline”. Doubling times were calculated using the inflection method - identifying the maximum semi-log slope along growth curves within the optical density range linearly correlated with number of yeast cells - with the online web tool Yeast Outgrowth Data Analyzer (YODA) [129]. All experiments were repeated with at least three biological replicates. The number of biological replicates is indicated in each figure caption. Doubling time was calculated for all cultures where OD ≥ 0.3 after 20 hours growth. Otherwise, culture was listed as no growth (NG). In one case (isoliquirtiginin), growth was below this threshold in most cultures and near the threshold in the remaining cultures and is also reported as NG. Interventions were classified as mTOR-inhibitors based on preferential growth inhibition in the *tor1Δ* strain, relative to WT and *fpr1Δ* strains, as previously described [195]. Welch’s (unequal variance) t-test with Bonferroni multiple testing correction was used to assess differences relative

to experiment-matched vehicle control cultures using R. We applied multiple testing correction using the p.adjust function.

Replicative lifespan analysis

A modified RLS protocol for treatments was developed based on previously described methods [196, 197]. Briefly, cells were grown on freshly prepared YPD plates at 30°C until single colonies were visible. Cells were selected from a single colony and lightly patched onto YPD plates supplemented with the designated treatment or vehicle overnight. In the morning, founder cells were aligned and selected as newborn daughter cells using a micromanipulator. Cells were monitored for cell divisions every 90-120 minutes, and subsequent budded daughter cells were separated and removed as they formed. The process continued until cells stopped dividing. Replicative lifespan was calculated as the number of times each mother cell divided before it underwent permanent cell cycle arrest. Plates were kept in the refrigerator at 4°C overnight. Plates were kept wrapped in tinfoil except while being dissected to avoid potential light sensitivity of any compounds. All experimenters were blinded to the identity of any of the treatments at the time of dissection. Cells were dissected in groups of 20 and 39-198 cells dissected for each intervention tested. Linear model comparing doubling time and median RLS of treated yeast constructed using the standard major axis regression (SMA) option in the lmodel2 package in R.

Intervention preparation and suppliers

All compounds and mixtures were suspended in DMSO, except hesperidin which was suspended in 0.027 N NaOH. Berberine was purchased from Sigma-Aldrich (St. Louis MO, USA). Celastrol was purchased from Cayman Chemical (Ann Arbor MI, USA). All other compounds and mixtures were provided by USANA Health Sciences, Inc. (Salt Lake City UT, USA). The composition of the mixtures tested is provided in **Table 2**.

Tables

Table 1. Natural product compounds and extracts used in this study along with reported lifespan extension. For compound source information, see methods.

Compound/extract	Lifespan extension
Allantoin	Worms [198]
Alpha-lipoic acid	Worms [199, 200], flies [201]
Ashwagandha root	Worms [202]
Berberine	Mice [185], flies [203]
Broccoli concentrate	-
Cardamonin	-
Celastrol	Worms [204]
Choline bitartrate	-
Coumaric Acid	-
Curcumin phytosome complex	-
Dong Quai	-
Ellipticine	
Ginseng	-
Ginsenoside Rc	Worms [205]
Glucosamine	Mice and worms [206]
Grape seed #1	-
Grape seed #2	-
Green tea	Worms [207], flies [208, 209], mice – midlife effect in females [210]
Hesperidin	Yeast [211]
Hydroxytyrosol	-
Isoliquiritigenin	-
Licorice root	Worms [212]
Lutein	Flies [213]
Lycopene	-
Milk thistle	Worms [214]
N-acetyl L-cysteine	Worms [215], flies [216, 217], mice [218]
Olive fruit	-
Polygonum cuspidatum root	-
Pterocarpus marsupium	-
Quercetin	Worms [219, 220], flies [172]
Rutin	Flies [221], mice [222]
Turmeric	Flies [223]
Tyrosol	Worms [224]
Umbelliferone	-
Verbascoside	-
Withaferin A	Mice [225], flies [226]

Table 2. Natural product mixtures used in this study. Composition of mixtures are shown by weight. All mixtures provided by USANA Health Science Inc.

Mixture	Description
1	40.4% *Pterocarpus marsupium* extract, 34.6% alpha lipoic acid, 23.1% quercetin, 1.9% olive fruit extract
2	22.7% alpha lipoic acid, 19.2% hesperdin, 14.1% resveratrol, 12.1% curcumin phytosome complex, 11.7% green tea extract, 10.6% quercetin, 7.1% rutin, 2.5% olive fruit extract
3	87.8% choline bitartrate, 4.5% coenzyme Q10, 4.2% lutein, 3.5% lycopene
4	30.1 % choline bitartrate, 19.0% milk thistle extract, 17.8% N-acetyl L-cysteine, 16.8% alpha lipoic acid, 5.7% broccoli concentrate, 3.6% green tea extract, 3.4% turmeric extract, 1.9% biotine, 1.7% olive fruit extract
5	86.1% glucosamine, 13.9% turmeric extract
6	60% grape seed extract #1, 40% grape seed extract #2

Table 3. Growth and mTOR inhibitor screen of natural product compounds, extracts, and mixtures. Doubling time (DT) (minutes/cell division), standard error of the mean (SEM), percent change compared to experiment-matched vehicle control, and number of biological replicate cultures tested (n) for wild type (WT), *tor1Δ*, and *fpr1Δ* cells. Interventions tested at 100 µg/mL.

	WT			*tor1Δ*			*fpr1Δ*		
Treatment	DT (SEM)	% change	n	DT (SEM)	% change	n	DT (SEM)	% change	n
1% DMSO	79.5 (1.0)	-	29	79.6 (0.8)	-	29	89.8 (0.7)	-	29
2% DMSO	85.4 (1.6)	-	6	84.2 (2.2)	-	6	92.3 (3.1)	-	6
0.27 N NaOH	74.5 (0.04)	-	3	77.4 (0.2)	-	3	85.8 (1.7)	-	3
Compounds and extracts									
Allantoin	81.7 (1.2)	-2.0	6	80.0 (1.0)	-1.1	6	87.7 (2.2)	-3.1	6
Ashwagandha root	82.5 (1.1)	-0.9	3	80.4 (1.1)	0.6	3	87.9 (1.6)	-2.4	3
Cardamonin†	78.7 (2.0)	-7.9	6	84.4 (1.1)	0.3	6	96.4 (1.1)	4.4	6
Choline bitartrate	82.0 (2.5)	14.8	3	81.2 (1.8)	1.6	3	89.4 (1.6)	-1.9	3
Coumaric acid	82.2 (1.3)	-1.4	6	81.0 (1.3)	0.1	6	89.3 (2.5)	-1.4	6
Curcumin phytosome complex	75.8 (0.9)	2.0	3	71.0 (1.5)	-2.6	3	89.8 (0.7)	6.0	3
Dong Quai	79.9 (1.6)	-4.2	6	81.0 (1.2)	0.1	6	87.7 (2.3)	-3.2	6
Ellipticine	NG**	-	3	NG**	-	3	NG**	-	3
Ginseng	83.4 (2.6)	0.04	6	81.9 (1.7)	1.2	6	89.3 (3.0)	-1.4	6
Ginsenoside Rc	83.4 (3.7)	0.2	3	80.1 (2.3)	0.2	3	90.5 (2.4)	0.5	3
Grape seed #1	88.4 (1.8)	18.9*	3	91.6 (2.8)	25.6*	3	102.4 (2.1)	20.8*	3

Grape seed #2	99.0 (5.6)	38.5	3	77.3 (2.6)	-3.3	3	88.2 (2.0)	-3.2	3
Green tea	91.6 (0.2)	11.9	3	92.9 (1.8)	13.5	3	103.3 (1.6)	13.2	3
Hesperidin[#]	76.5 (0.9)	2.7	3	76.6 (0.2)	-1.0	3	80.7 (1.2)	-6.0	3
Hydroxytyrosol	83.3 (2.3)	-0.1	6	82.5 (1.8)	2.0	6	90.9 (2.7)	0.4	6
Isoliquiritigenin[††]	169.9 (26.2)	103.7	2	NG**	-	6	NG**	-	6
Licorice root	83.8 (2.2)	1.4	6	83.6 (2.9)	2.2	6	89.9 (3.0)	-1.4	6
Lutein	90.2 (0.6)	21.3*	3	90.4 (1.0)	23.9*	3	97.1 (1.8)	14.5	3
Milk thistle	85.4 (1.5)	3.3	6	85.8 (2.9)	4.8	6	94.7 (3.0)	3.9	6
N-acetyl L-cysteine	82.0 (1.2)	-0.9	6	81.0 (1.3)	-1.0	6	89.0 (2.3)	-2.3	6
Olive fruit	84.6 (1.4)	2.3	6	84.4 (2.0)	3.1	6	92.1 (3.1)	1.1	6
Polygonum cuspidatum root	102.6 (2.8)	24.0*	6	99.6 (1.4)	21.7*	6	106.6 (4.1)	17.0	6
Pterocarpus marsupium	89.1 (4.6)	14.5	3	93.9 (3.2)	22.6*	3	103.3 (1.9)	11.6*	3
Rutin	85.6 (1.2)	3.5	6	83.7 (1.5)	2.3	6	92.8 (2.8)	1.8	6
Turmeric	111.5 (4.6)	36.1*	3	110 (13.2)	34.9	3	107.7 (1.2)	18.0*	3
Tyrosol	82.0 (2.0)	-1.5	3	79.5 (0.3)	-0.5	3	88.3 (0.8)	-1.9	3
Umbelliferone	86.5 (1.3)	3.7	6	83.7 (0.5)	3.5	6	91.9 (2.8)	1.5	6
Verbascoside	84.2 (2.2)	1.2	3	82.6 (1.1)	3.3	3	91.2 (3.7)	1.3	3
Withaferin A	106.6 (4.4)	27.9*	6	110.9 (4.3)	37.0*	6	102.6 (3.4)	13.3	6
Mixtures									
1	95.1 (4.8)	22.2	3	103.9 (8.7)	35.6	3	110.2 (13.4)	19.0	3
2	93.3 (1.7)	25.4*	3	94.3 (1.9)	29.3*	3	104 (5.5)	22.7	3

3	88.4 (0.7)	23.8	3	88.2 (1.2)	10.4	3	94.2 (0.8)	3.3	3
4	77.9 (7.5)	9.0	3	91.2 (2.9)	14.1	3	83.1 (4.1)	-8.9	3
5	81.8 (1.7)	10.0	3	76.5 (1.7)	4.9	3	81.3 (1.0)	-4.1	3
6	94.6 (1.9)	32.4*	3	93.5 (5.4)	17.0	3	105.8 (8.5)	16.0	3

* = $p < 0.05$, compared to vehicle, Welch's (unequal variance) t-test

** = Doubling time not calculated due to minimal growth over the time-course of the experiment. See Methods.

= 0.27N NaOH vehicle

† = 2% DMSO vehicle

†† = Doubling time for four of six tested WT cultures could not be calculated.

Table 4. Dose response for selected natural product compounds. Doubling time (DT) (minutes/cell division), standard error of the mean (SEM), percent change, and number of biological replicate cultures tested (n) for wild type (WT), *tor1Δ*, and *fpr1Δ* cells.

	WT			*tor1Δ*			*fpr1Δ*		
Treatment	DT (SEM)	% change	n	DT (SEM)	% change	n	DT (SEM)	% change	n
1% DMSO	80.0 (2.8)	-	3	81.1 (1.8)	-	3	85.9 (1.3)	-	3
Berberine 1 µg/mL	81.2 (1.2)	1.5	3	85.2 (0.4)	5.1	3	89.5 (0.3)	4.2	3
Berberine 10 µg/mL	93.7 (1.4)	17.0	3	88.3 (3.2)	9.0	3	98.1 (4.8)	14.2	3
Berberine 50 µg/mL	146.3 (4.2)	82.8*	3	135.7 (1.0)	67.4*	3	143.1 (0.9)	66.7*	3
1% DMSO	83.1 (1.6)	-	3	82.3 (0.7)	-	3	92.0 (1.4)	-	3
Celastrol 5 µM	86.0 (0.8)	3.4	3	85.8 (1.1)	4.3	3	92.4 (0.7)	0.4	3
Celastrol 10 µM	92.7 (2.1)	11.5	3	92.4 (1.2)	12.3*	3	102.0 (0.8)	10.9*	3
Celastrol 100 µM	94.2 (2.8)	13.4	3	92.5 (4.2)	12.4	3	100.8 (2.4)	9.5	3
1% DMSO	81.6 (0.8)	-	3	79.1 (1.4)	-	3	90.7 (1.6)	-	3
Isoliquiritigenin 1 µg/mL	79.3 (1.2)	-2.8	3	77.7 (1.2)	-1.8	3	87.1 (1.1)	-4.0	3
Isoliquiritigenin 10 µg/mL	82.4 (2.1)	1.0	3	81.3 (1.1)	2.8	3	92.4 (2.5)	2.0	3
Isoliquiritigenin 50 µg/mL	98.7 (2.9)	21.0	3	99.0 (1.7)	25.2*	3	113.6 (2.5)	25.3*	3

*= $p < 0.05$, compared to 1% DMSO, Welch's (unequal variance) t-test

Table 5. Median RLS (95% confidence intervals), number of cells dissected (n), percent change, and p-value (Wilcoxon rank sum test, Bonferroni-corrected p-value for multiple testing and uncorrected p-value in parentheses) of natural product compounds, extracts, and mixtures compared to vehicle (1% DMSO) control. All interventions tested at 100 µg/mL.

Treatment	n	Median RLS (95% CI)	% change	Bonferroni-corrected p-value (uncorrected)
1% DMSO (vehicle control)	198	21 (20-24)	0.0	-
Compounds and extracts				
Alpha-lipoic acid	40	21 (19-26)	0.0	1 (0.859)
Broccoli concentrate	80	19.5 (16-24)	-7.2	1 (0.342)
Choline bitartrate	160	21 (19-23)	0.0	1 (0.820)
Curcumin phytosome complex	40	19 (17-24)	-9.5	1 (0.480)
Glucosamine HCl	116	21 (19-25)	0.0	1 (0.815)
Grape seed #1	118	19.5 (18-24)	-7.2	1 (0.913)
Grape seed #2	80	20.5 (19-24)	-2.4	1 (0.945)
Green tea	160	12 (11-14)	-42.9	< 0.001 (< 0.001)
Lutein	39	18 (16-28)	-14.3	1 (0.984)
Lycopene	118	19 (17-22)	-9.5	1 (0.096)
Milk thistle	40	19 (15-26)	-9.5	1 (0.540)
N-actetyl L-cysteine	39	20 (17-27)	-4.8	1 (0.664)
Olive fruit	80	20.5 (19-26)	-2.4	1 (0.722)
Polygonum cuspidatum root	40	16 (13-22)	-23.8	1 (0.073)
Pterocarpus marsupium	104	28 (25-31)	33.3	0.001 (< 0.001)
Quercetin	40	18.5 (16-27)	-11.9	1 (0.836)
Rutin	40	18.5 (15-26)	-11.9	1 (0.309)
Turmeric	40	16.5 (14-22)	-21.4	0.208 (0.009)
Mixtures				
1	80	25 (22-27)	19.0	0.219 (0.009)
2	40	18 (14-21)	-14.3	1 (0.056)
3	80	21 (18-23)	0.0	1 (0.609)
4	40	22.5 (20-26)	7.1	1 (0.883)
5	40	15.5 (13-21)	-26.2	0.997 (0.042)
6	40	20 (16-24)	-4.8	1 (0.377)

Table 6. Median RLS (95% confidence intervals), number of cells dissected (n), percent change, and p-value (Wilcoxon rank sum test, Bonferroni-corrected for multiple testing within each dose response) of natural products compared to vehicle control. Note: separate control used for each compound. Berberine suspended in H_2O and thus compared to YPD.

Treatment	Concentration	n	Median RLS (95% CI)	% change	Bonferroni-corrected p-value
YPD	NA	160	21.5 (20-23)	-	-
Berberine	1 µg/mL	155	22 (21-25)	2.3	0.173
Berberine	10 µg/mL	160	21 (20-23)	-2.3	1
Berberine	50 µg/mL	157	10 (9-11)	-53.5	< 0.001
DMSO	1%	60	23.5 (21-30)	-	-
Celastrol	5 µM	60	24.5 (22-29)	4.3	1
Celastrol	10 µM	60	25 (23-29)	6.4	1
Celastrol	100 µM	60	23 (18-28)	-2.1	0.841

Supplemental Figures

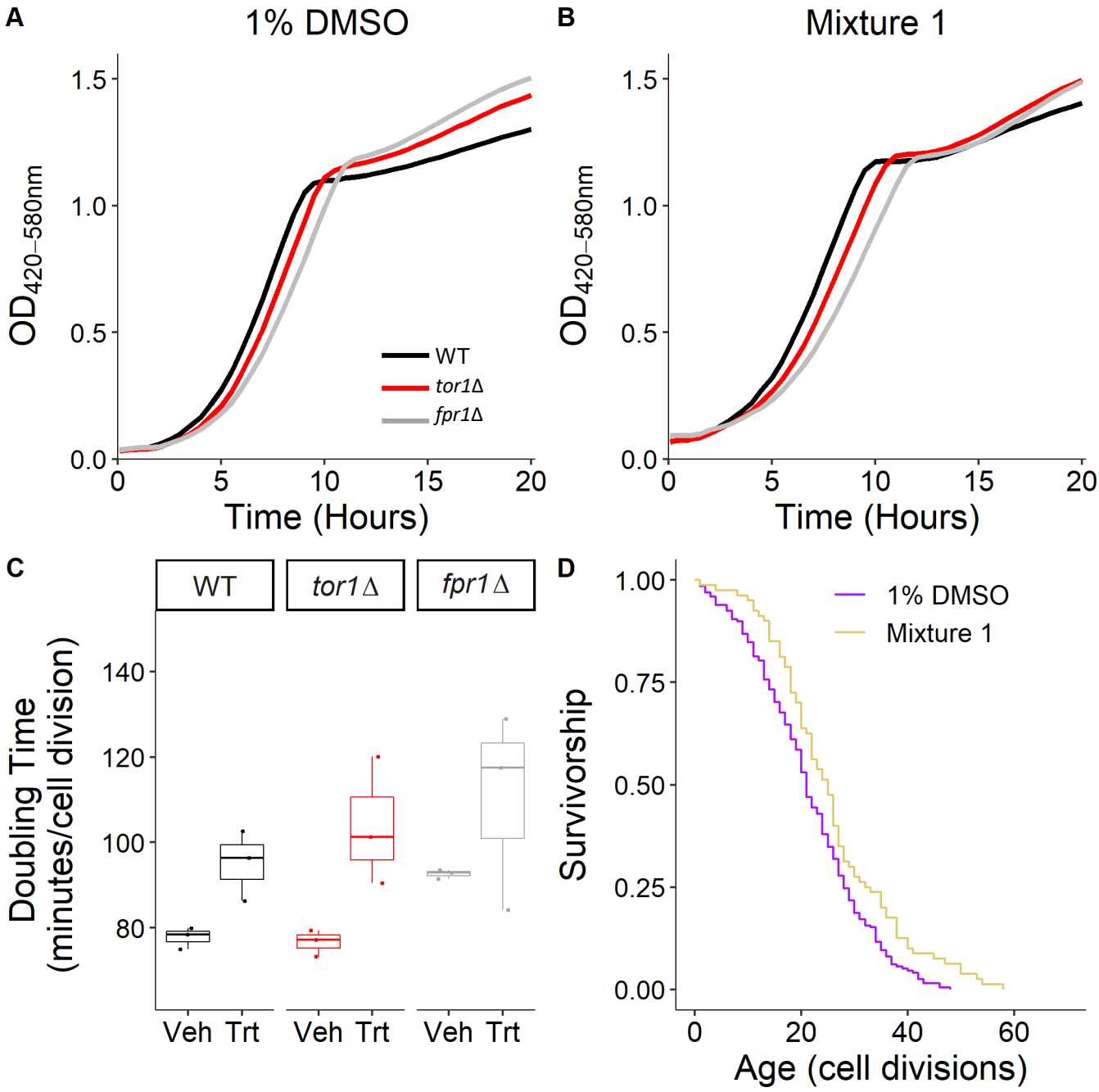

Figure S1-1. **Representative growth curves, doubling times, and replicative lifespan for mixture 1.** Representative growth kinetics of WT, *tor1Δ*, and *fpr1Δ* microcultures at **A)** 1% DMSO and **B)** 100 µg/mL mixture 1. **C)** Inflection doubling time (DT) of WT, *tor1Δ*, and *fpr1Δ* microcultures. Mixture 1 does not significantly increase DT (control n = 3, treated n = 3). Treatment compared to vehicle control using Welch's T-test; * p<0.05, ** p<0.01, *** p<0.001. **D)** Mixture 1 replicative lifespan (RLS) survival curve. For number of cells tested in RLS and Wilcoxon rank sum p-values, see Table 4.

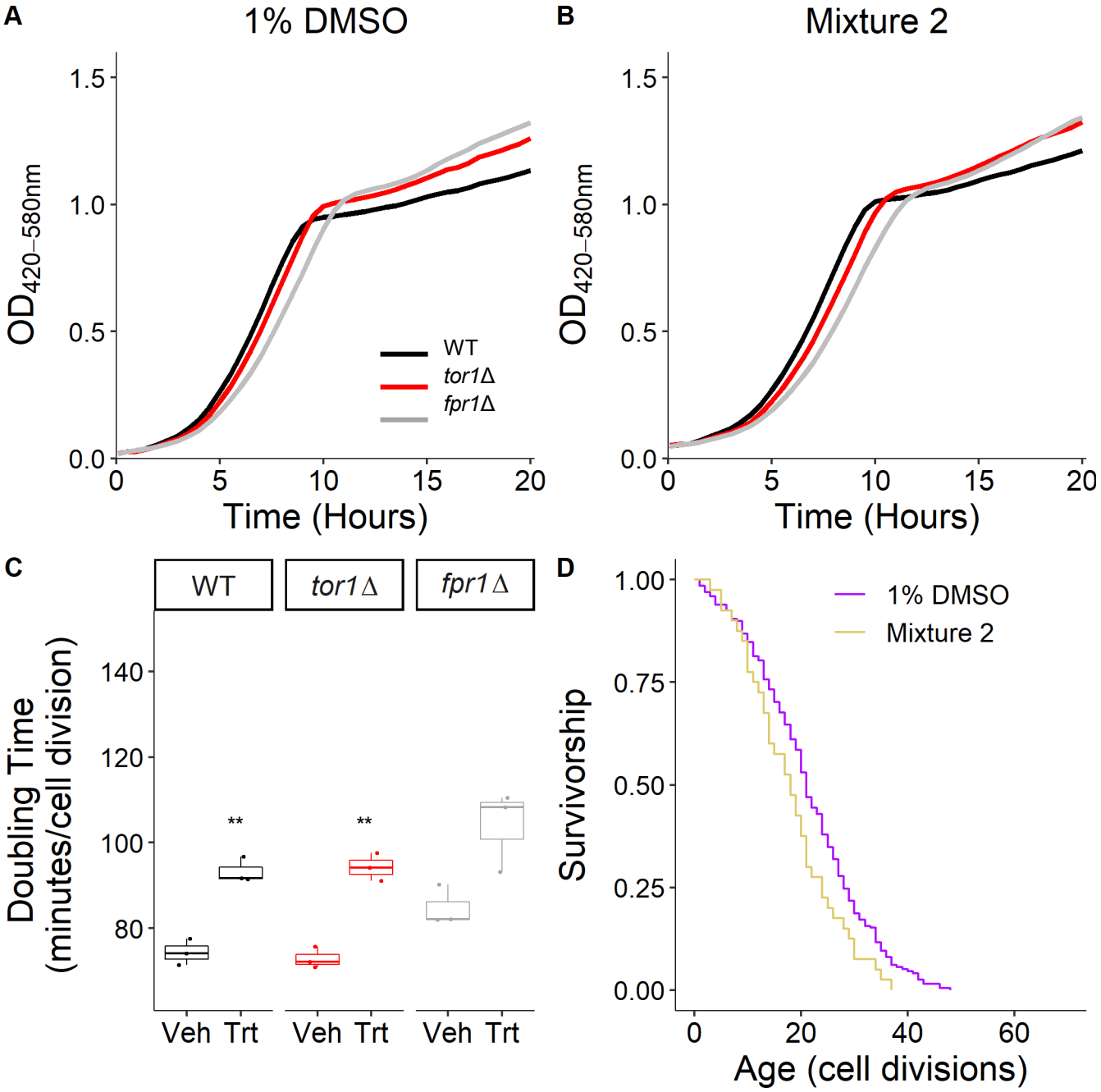

Figure S1-2. **Representative growth curves, doubling times, and replicative lifespan for mixture 2.** Representative growth kinetics of WT, *tor1Δ*, and *fpr1Δ* microcultures at **A)** 1% DMSO and **B)** 100 µg/mL mixture 2. **C)** Inflection doubling time (DT) of WT, *tor1Δ*, and *fpr1Δ* microcultures. Mixture 2 significantly increases WT and *tor1Δ* DT (control n = 3, treated n = 3). Treatment compared to vehicle control using Welch's T-test; * p<0.05, ** p<0.01, *** p<0.001. **D)** Mixture 2 replicative lifespan (RLS) survival curve. For number of cells tested in RLS and Wilcoxon rank sum p-values, see Table 4.

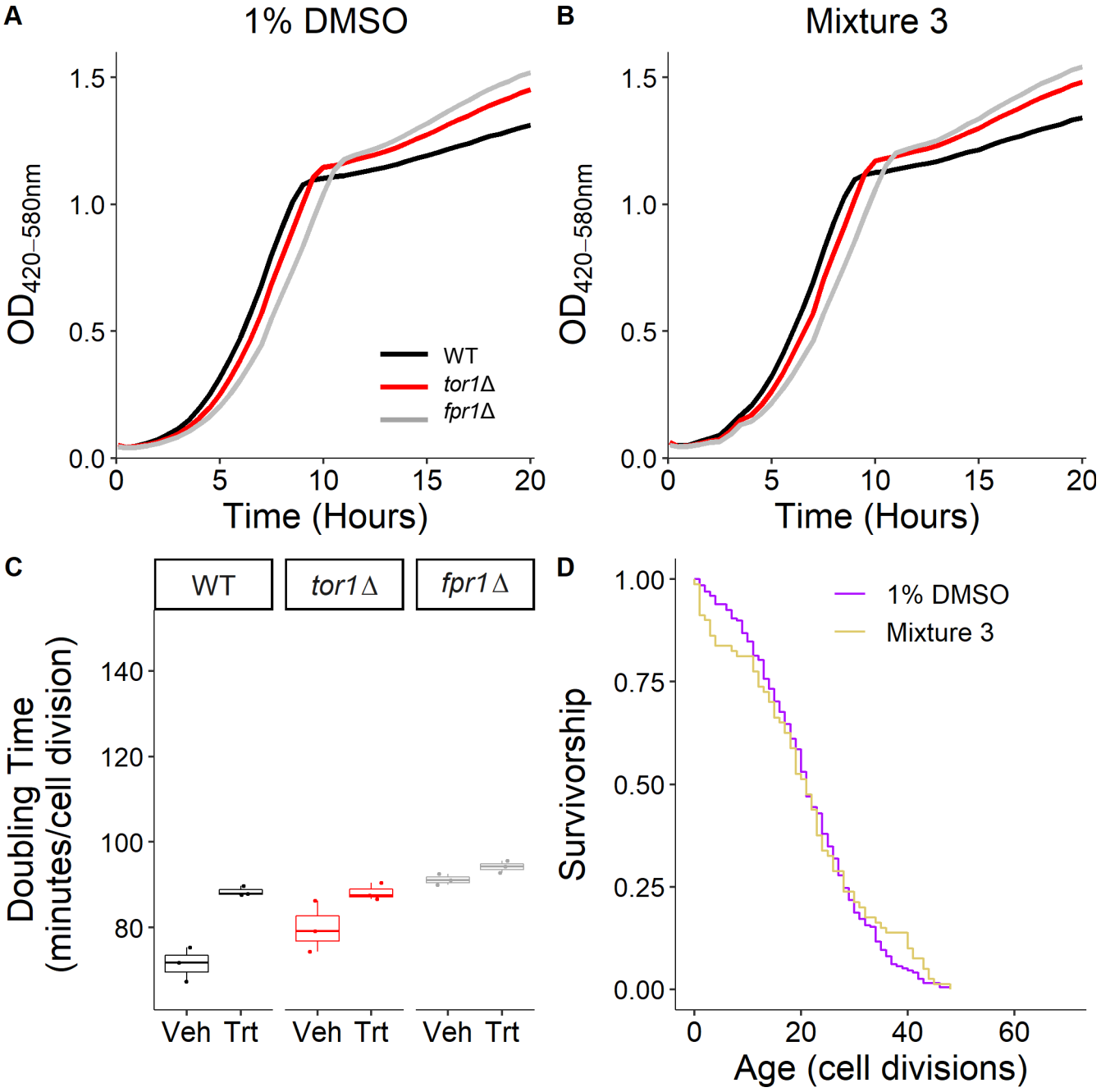

Figure S1-3. **Representative growth curves, doubling times, and replicative lifespan for mixture 3.** Representative growth kinetics of WT, *tor1Δ*, and *fpr1Δ* microcultures at **A)** 1% DMSO and **B)** 100 µg/mL mixture 3. **C)** Inflection doubling time (DT) of WT, *tor1Δ*, and *fpr1Δ* microcultures. Mixture 3 does not significantly increase DT (control n = 3, treated n = 3). Treatment compared to vehicle control using Welch's T-test; * p<0.05, ** p<0.01, *** p<0.001. **D)** Mixture 3 replicative lifespan (RLS) survival curve. For number of cells tested in RLS and Wilcoxon rank sum p-values, see Table 4.

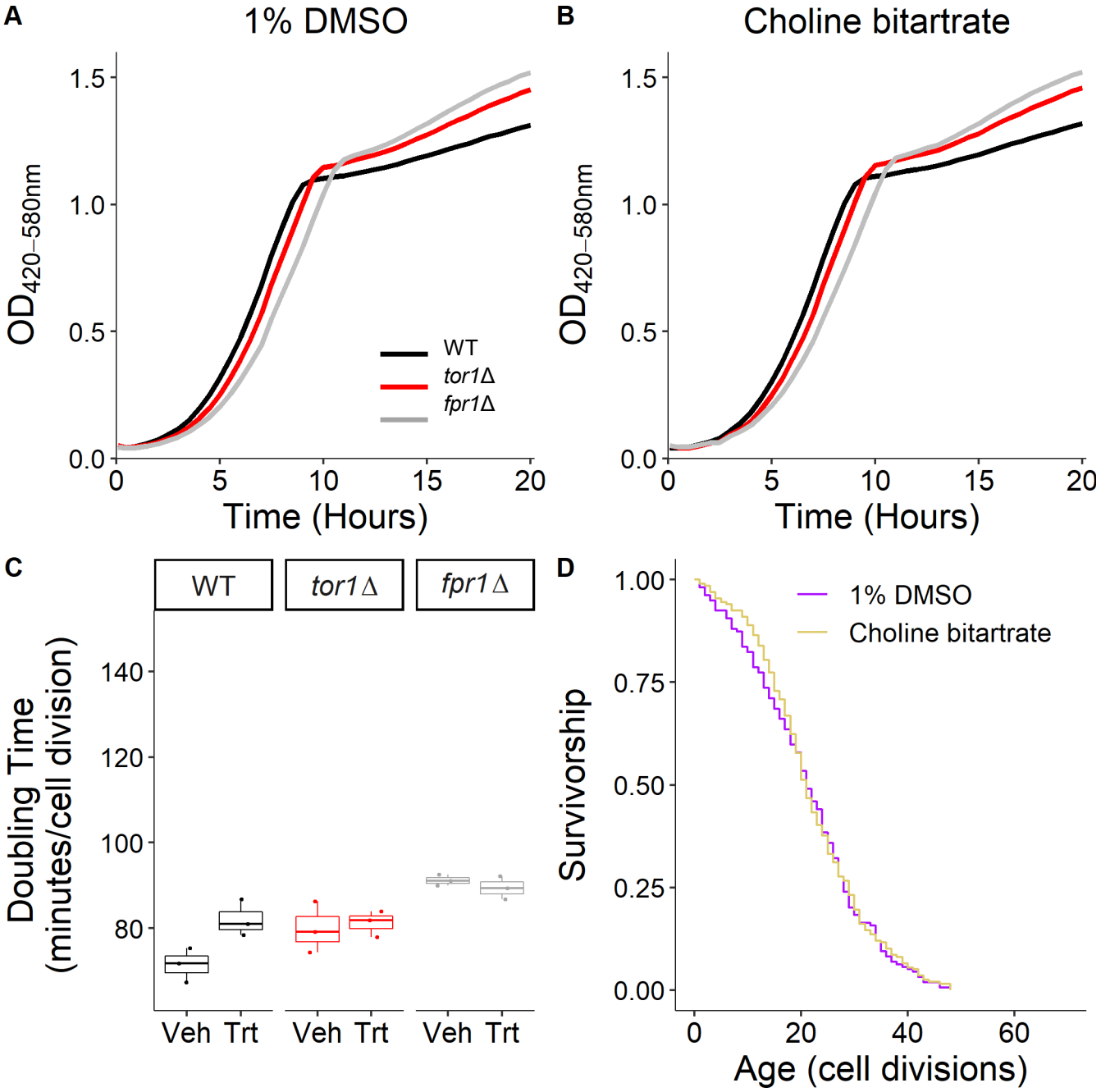

Figure S1-4. **Representative growth curves, doubling times, and replicative lifespan for choline bitartrate.** Representative growth kinetics of WT, *tor1Δ*, and *fpr1Δ* microcultures at **A)** 1% DMSO and **B)** 100 µg/mL choline bitartrate. **C)** Inflection doubling time (DT) of WT, *tor1Δ*, and *fpr1Δ* microcultures. Choline bitartrate does not significantly increase DT (control n = 3, treated n = 3). Treatment compared to vehicle control using Welch's T-test; * p<0.05, ** p<0.01, *** p<0.001. **D)** Choline bitartrate replicative lifespan (RLS) survival curve. For number of cells tested in RLS and Wilcoxon rank sum p- values, see Table 4.

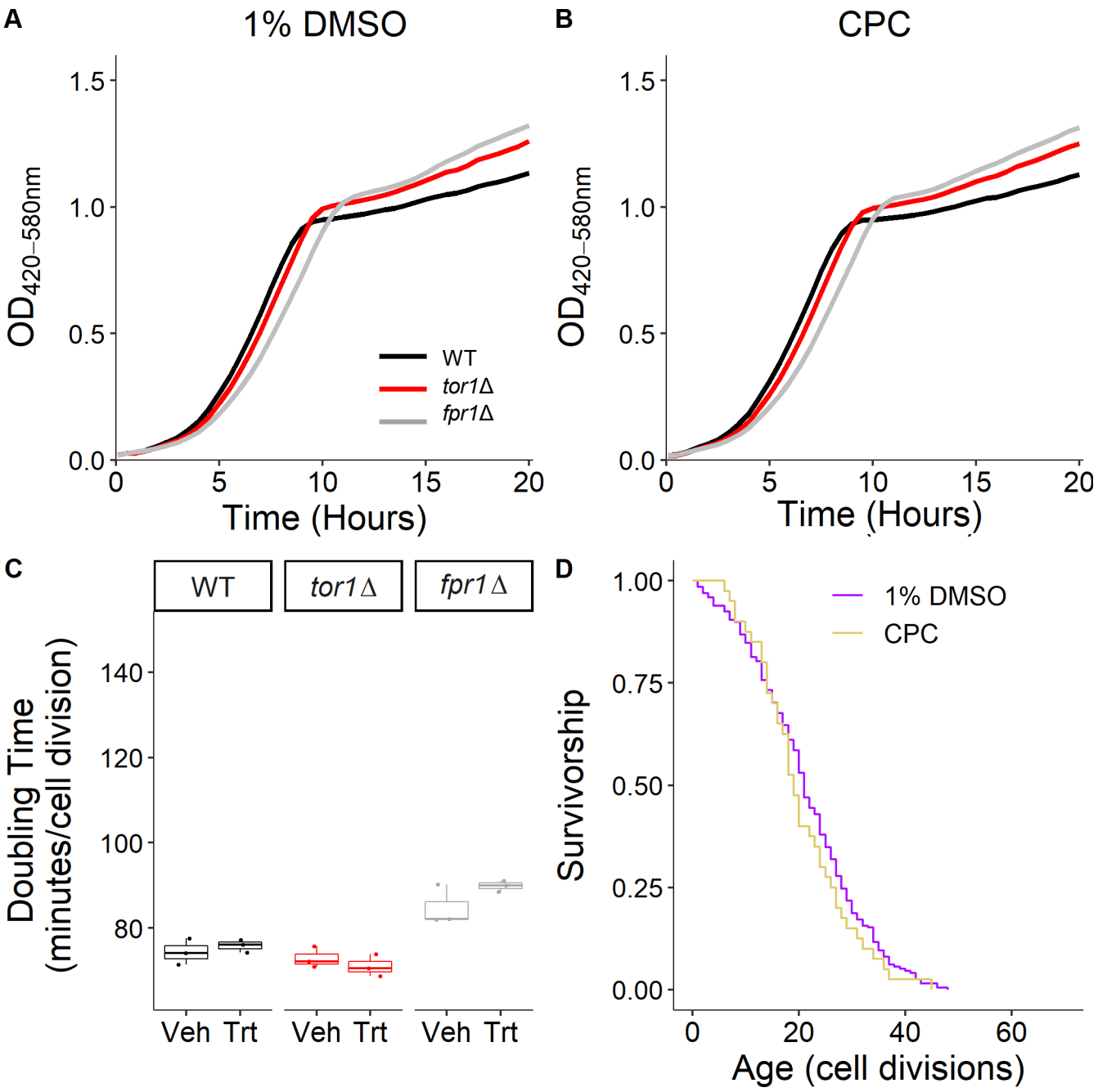

Figure S1-5. **Representative growth curves, doubling times, and replicative lifespan for curcumin phytosome complex (CPC).**

Representative growth kinetics of WT, *tor1Δ*, and *fpr1Δ* microcultures at **A)** 1% DMSO and **B)** 100 µg/mL curcumin phytosome complex. **C)** Inflection doubling time (DT) of WT, *tor1Δ*, and *fpr1Δ* microcultures. Curcumin phytosome complex does not significantly increase DT (control n = 3, treated n = 3).Treatment compared to vehicle control using Welch's T-test; * p<0.05, ** p<0.01, *** p<0.001. **D)** Curcumin phytosome complex replicative lifespan (RLS) survival curve. For number of cells tested in RLS and Wilcoxon rank sum p-values, see Table 4.

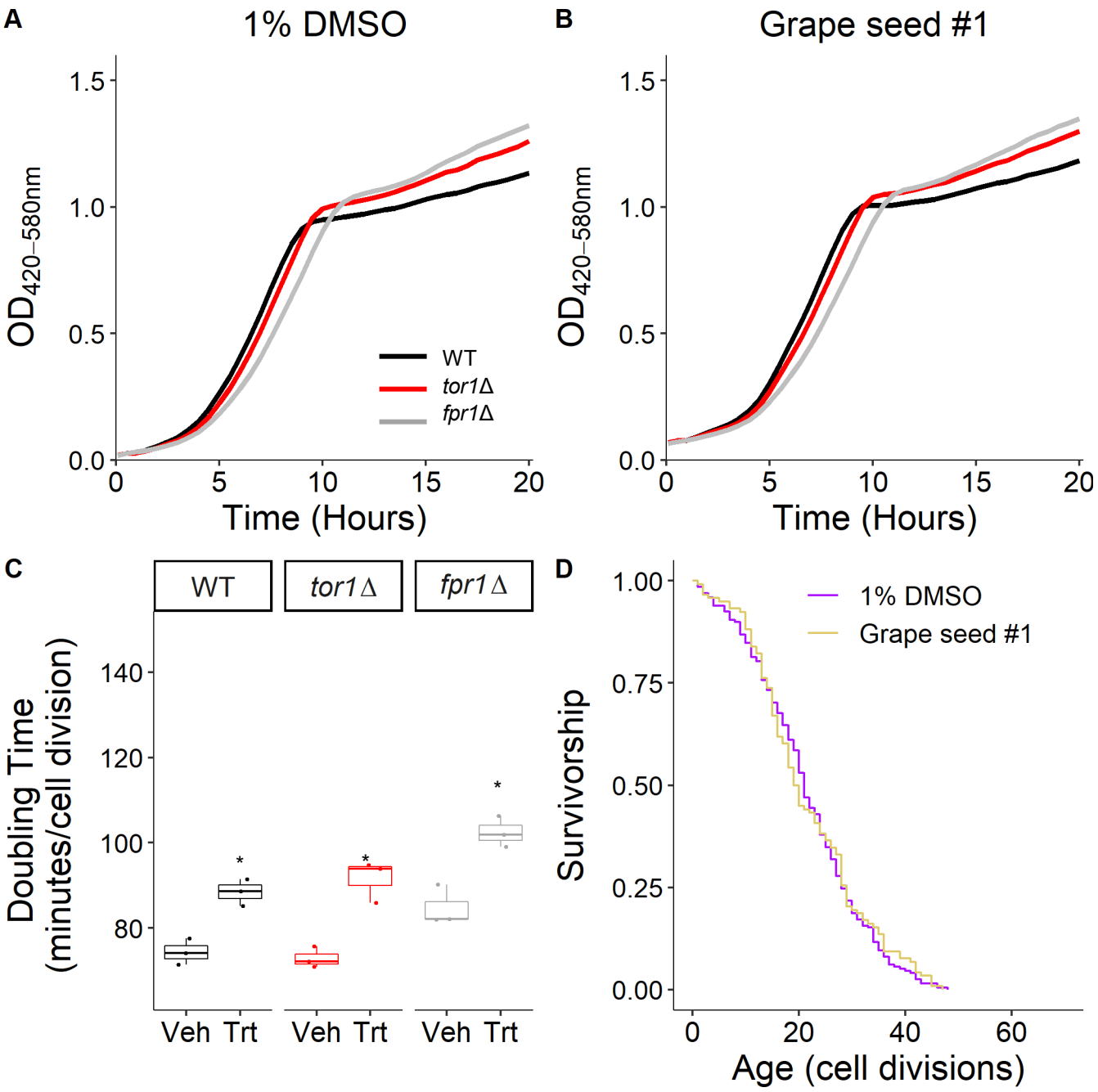

Figure S1-6. **Representative growth curves, doubling times, and replicative lifespan for grape seed extract #1.** Representative growth kinetics of WT, *tor1Δ*, and *fpr1Δ* microcultures at **A)** 1% DMSO and **B)** 100 µg/mL grape seed extract #1. **C)** Inflection doubling time (DT) of WT, *tor1Δ*, and *fpr1Δ* microcultures. Grape seed extract #1 significantly increases WT, *tor1Δ* and *fpr1Δ* DT (control n = 3, treated n = 3). Treatment compared to vehicle control using Welch's T-test; * p<0.05, ** p<0.01, *** p<0.001. **D)** Grape seed extract #1 replicative lifespan (RLS) survival curve. For number of cells tested in RLS and Wilcoxon rank sum p-values, see Table 4.

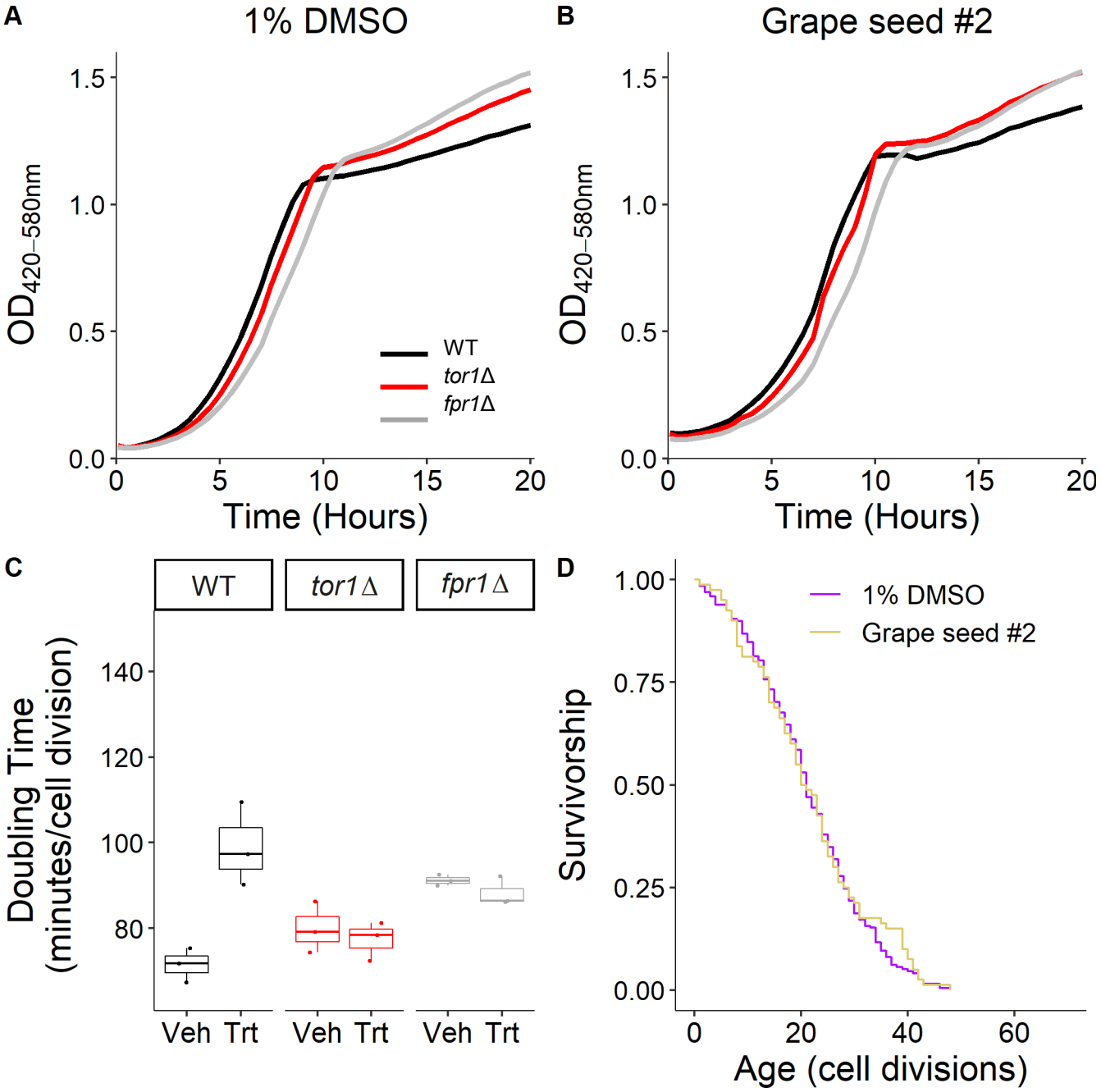

Figure S1-7. **Representative growth curves, doubling times, and replicative lifespan for grape seed extract #2.** Representative growth kinetics of WT, *tor1Δ*, and *fpr1Δ* microcultures at **A)** 1% DMSO and **B)** 100 µg/mL grape seed extract #2. **C)** Inflection doubling time (DT) of WT, *tor1Δ*, and *fpr1Δ* microcultures. Grape seed extract #2 does not significantly increase DT (control n = 3, treated n = 3). Treatment compared to vehicle control using Welch's T-test; * p<0.05, ** p<0.01, *** p<0.001. **D)** Grape seed extract #2 replicative lifespan (RLS) survival curve. For number of cells tested in RLS and Wilcoxon rank sum p-values, see Table 4.

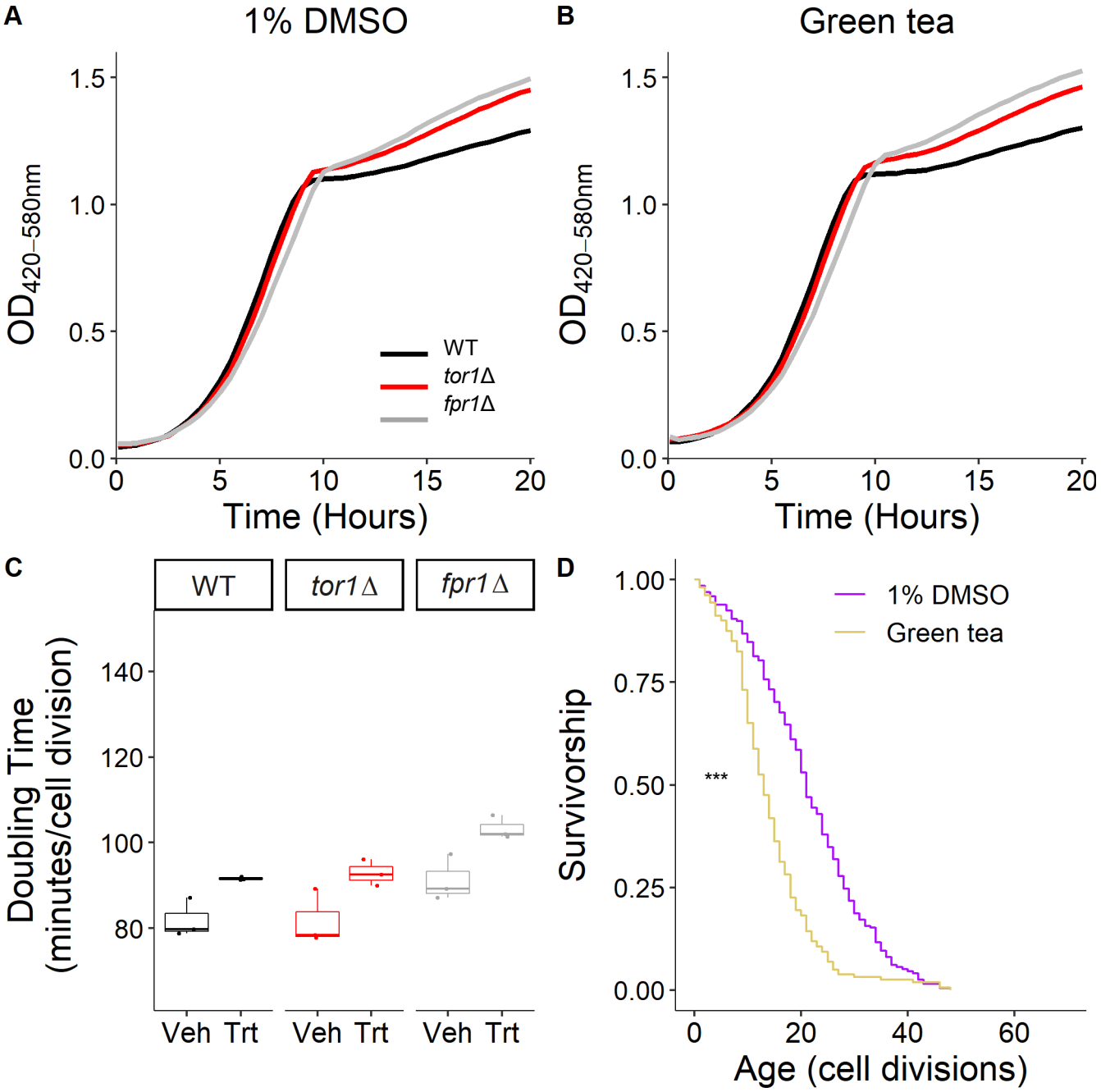

Figure S1-8. **Representative growth curves, doubling times, and replicative lifespan for green tea extract.** Representative growth kinetics of WT, *tor1Δ*, and *fpr1Δ* microcultures at **A)** 1% DMSO and **B)** 100 µg/mL green tea extract. **C)** Inflection doubling time (DT) of WT, *tor1Δ*, and *fpr1Δ* microcultures. Green tea extract does not significantly increase DT (control n = 3, treated n = 3). Treatment compared to vehicle control using Welch's T-test; * p<0.05, ** p<0.01, *** p<0.001. **D)** Green tea extract replicative lifespan (RLS) survival curve. For number of cells tested in RLS and Wilcoxon rank sum p- values, see Table 4.

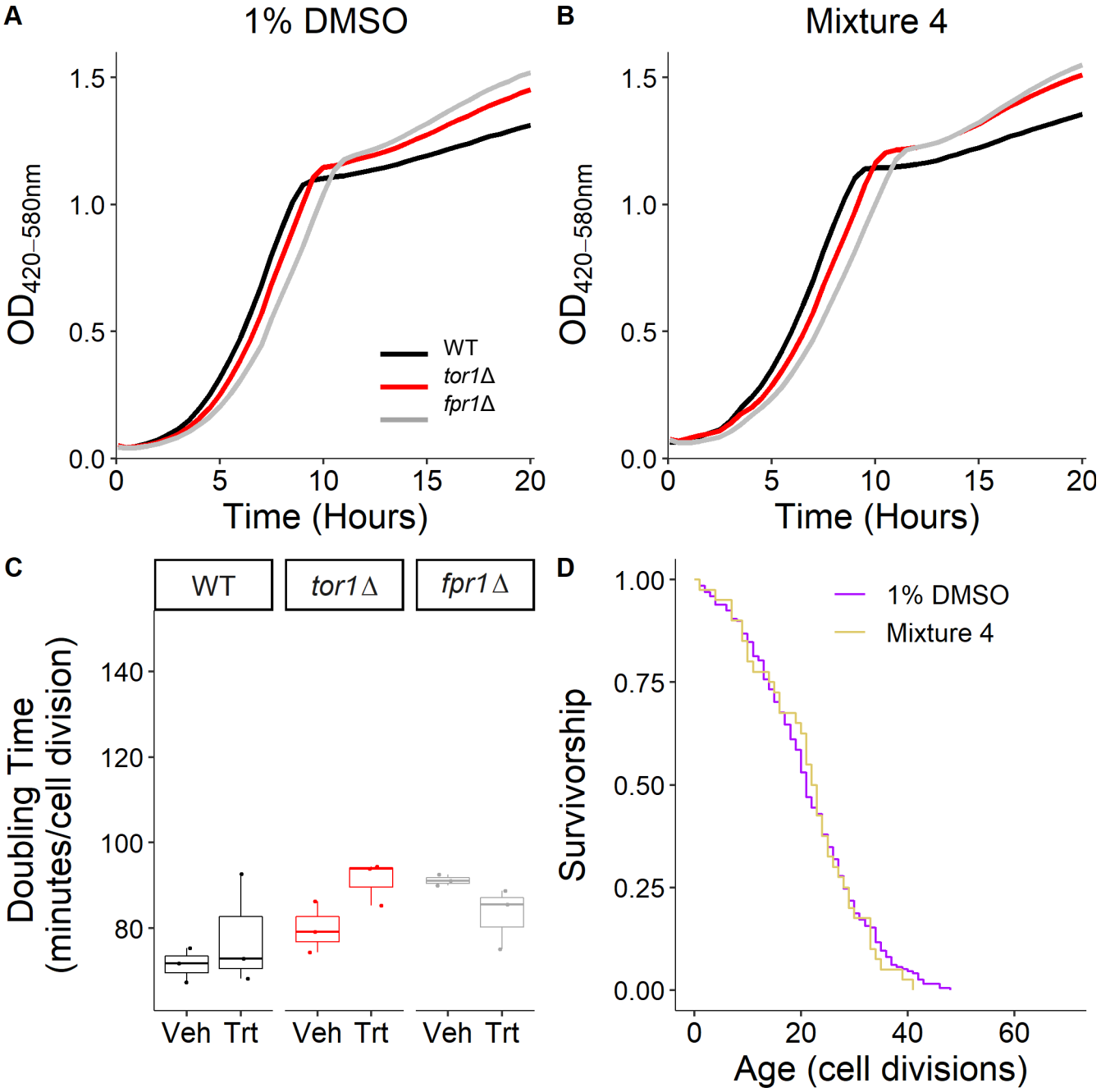

Figure S1-9. **Representative growth curves, doubling times, and replicative lifespan for mixture 4.** Representative growth kinetics of WT, *tor1Δ*, and *fpr1Δ* microcultures at **A)** 1% DMSO and **B)** 100 µg/mL mixture 4. **C)** Inflection doubling time (DT) of WT, *tor1Δ*, and *fpr1Δ* microcultures. Mixture 4 does not significantly increase DT (control n = 3, treated n = 3). Treatment compared to vehicle control using Welch's T-test; * p<0.05, ** p<0.01, *** p<0.001. **D)** Mixture 4 replicative lifespan (RLS) survival curve. For number of cells tested in RLS and Wilcoxon rank sum p-values, see Table 4.

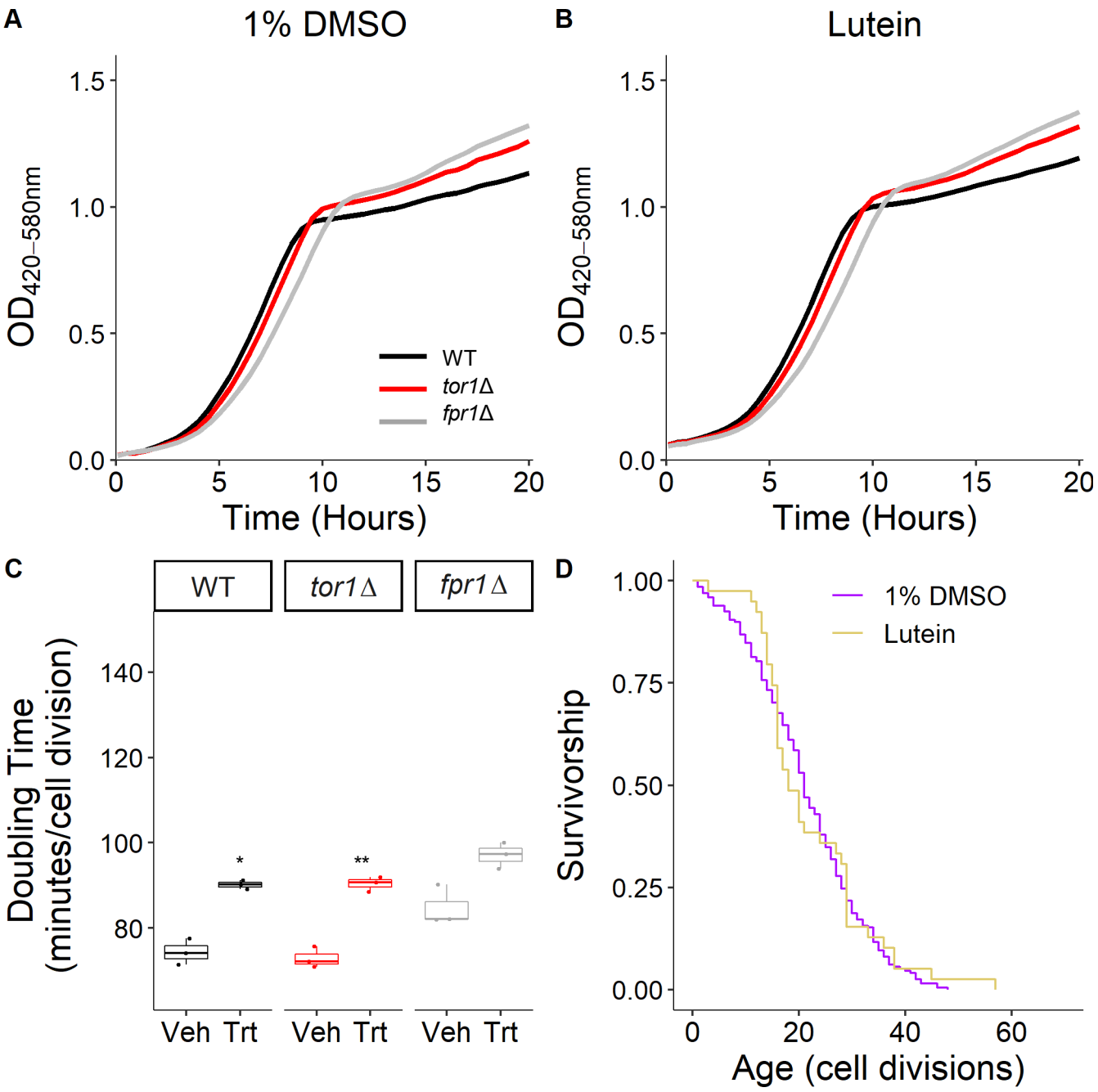

Figure S1-10. **Representative growth curves, doubling times, and replicative lifespan for lutein.** Representative growth kinetics of WT, *tor1Δ*, and *fpr1Δ* microcultures at **A)** 1% DMSO and **B)** 100 µg/mL lutein. **C)** Inflection doubling time (DT) of WT, *tor1Δ*, and *fpr1Δ* microcultures. Lutein significantly increases WT and *tor1Δ* DT (control n = 3, treated n = 3). Treatment compared to vehicle control using Welch's T-test; * p<0.05, ** p<0.01, *** p<0.001. **D)** Lutein replicative lifespan (RLS) survival curve. For number of cells tested in RLS and Wilcoxon rank sum p-values, see Table 4.

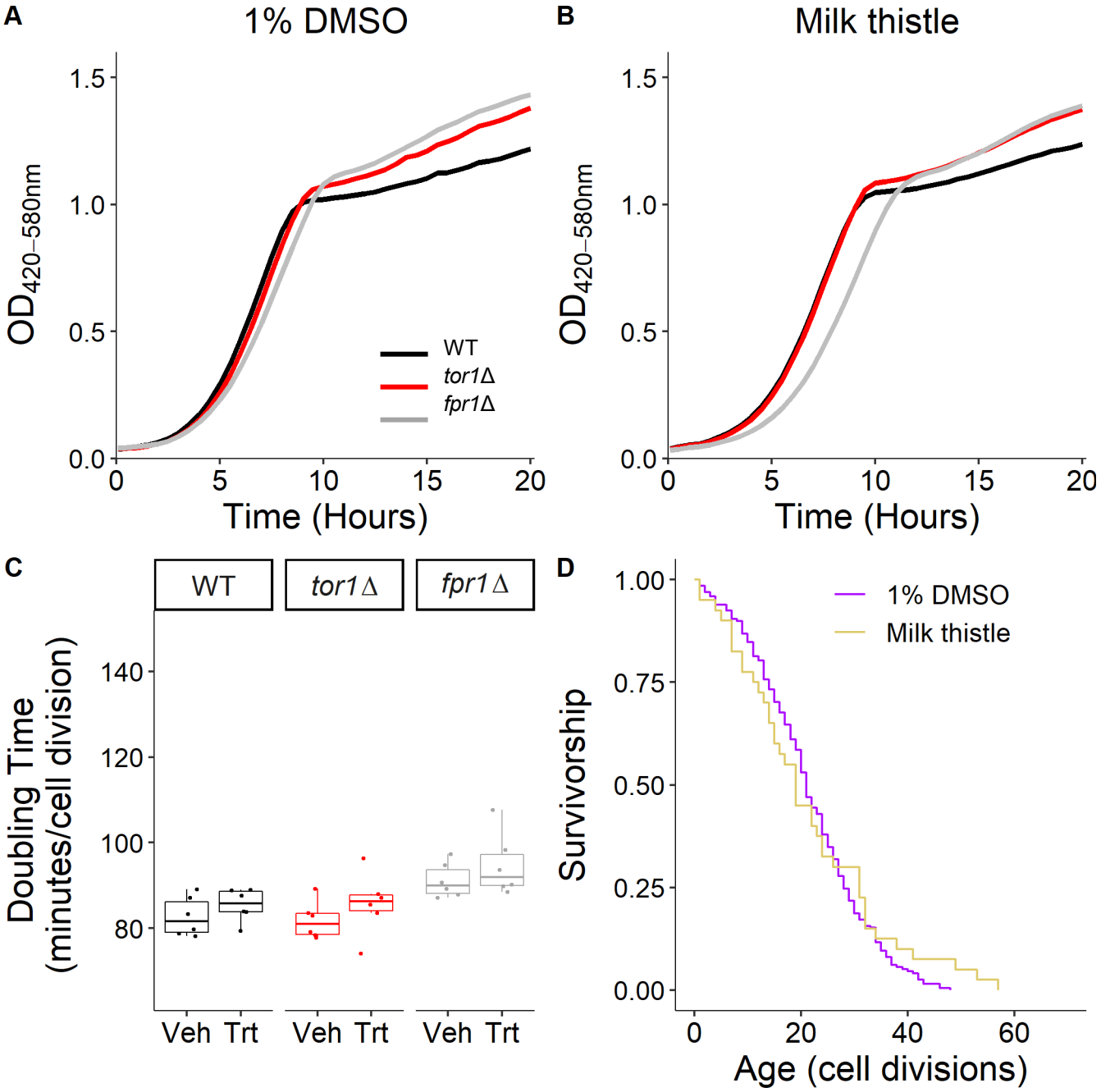

Figure S1-11. **Representative growth curves, doubling times, and replicative lifespan for milk thistle extract.** Representative growth kinetics of WT, *tor1Δ*, and *fpr1Δ* microcultures at **A)** 1% DMSO and **B)** 100 µg/mL milk thistle extract. **C)** Inflection doubling time (DT) of WT, *tor1Δ*, and *fpr1Δ* microcultures. Milk thistle extract does not significantly increase DT (control n = 6, treated n = 6). Treatment compared to vehicle control using Welch's T- test; * p<0.05, ** p<0.01, *** p<0.001. **D)** Milk thistle extract replicative lifespan (RLS) survival curve. For number of cells tested in RLS and Wilcoxon rank sum p-values, see Table 4.

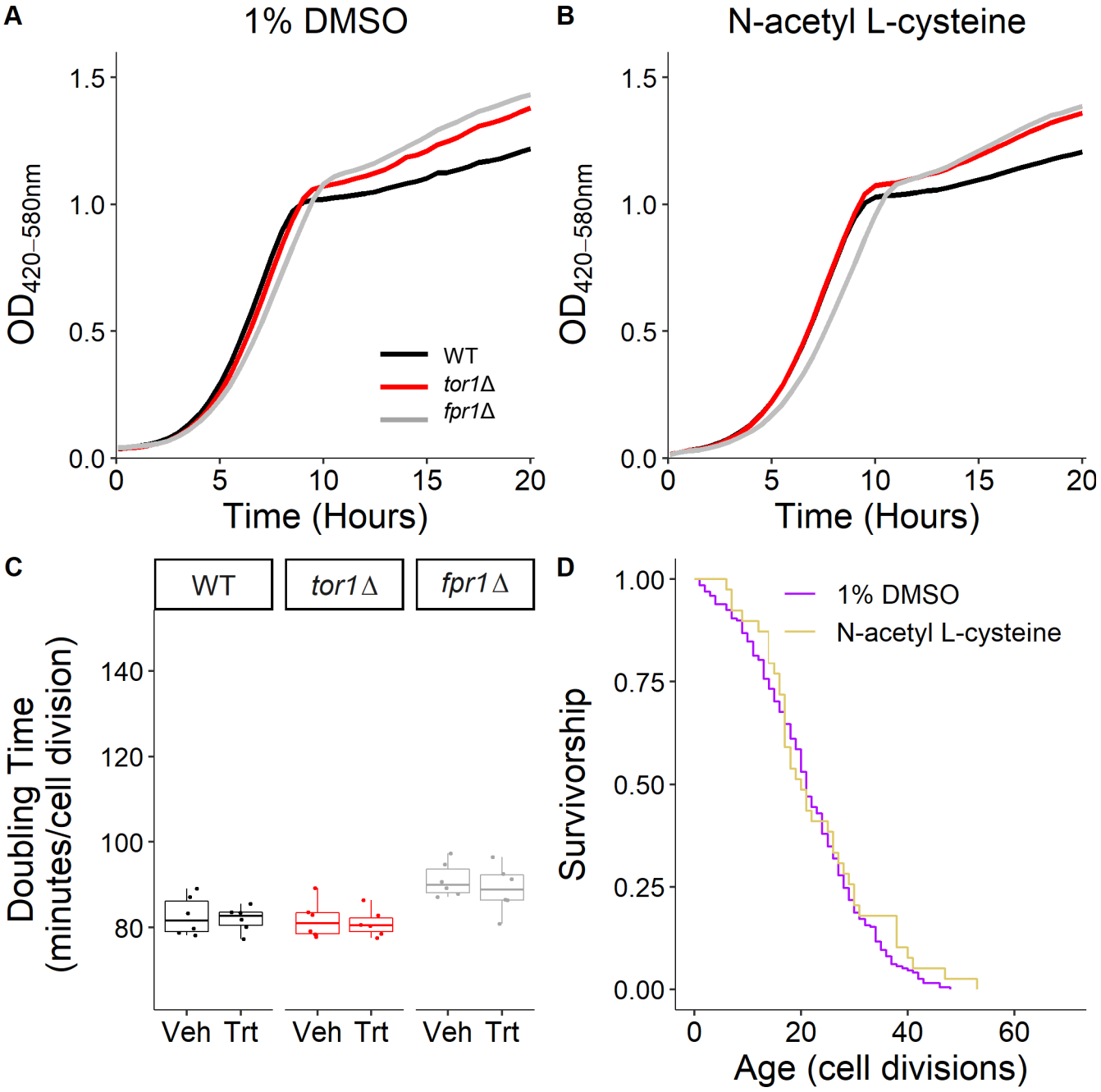

Figure S1-12. **Representative growth curves, doubling times, and replicative lifespan for N-acetyl L-cysteine.** Representative growth kinetics of WT, *tor1Δ*, and *fpr1Δ* microcultures at **A)** 1% DMSO and **B)** 100 µg/mL N- acetyl L-cysteine. **C)** Inflection doubling time (DT) of WT, *tor1Δ*, and *fpr1Δ* microcultures. N-acetyl L-cysteine does not significantly increase DT (control n = 6, treated n = 6). Treatment compared to vehicle control using Welch's T- test; * p<0.05, ** p<0.01, *** p<0.001. **D)** N-acetyl L-cysteine replicative lifespan (RLS) survival curve. For number of cells tested in RLS and Wilcoxon rank sum p-values, see Table 4.

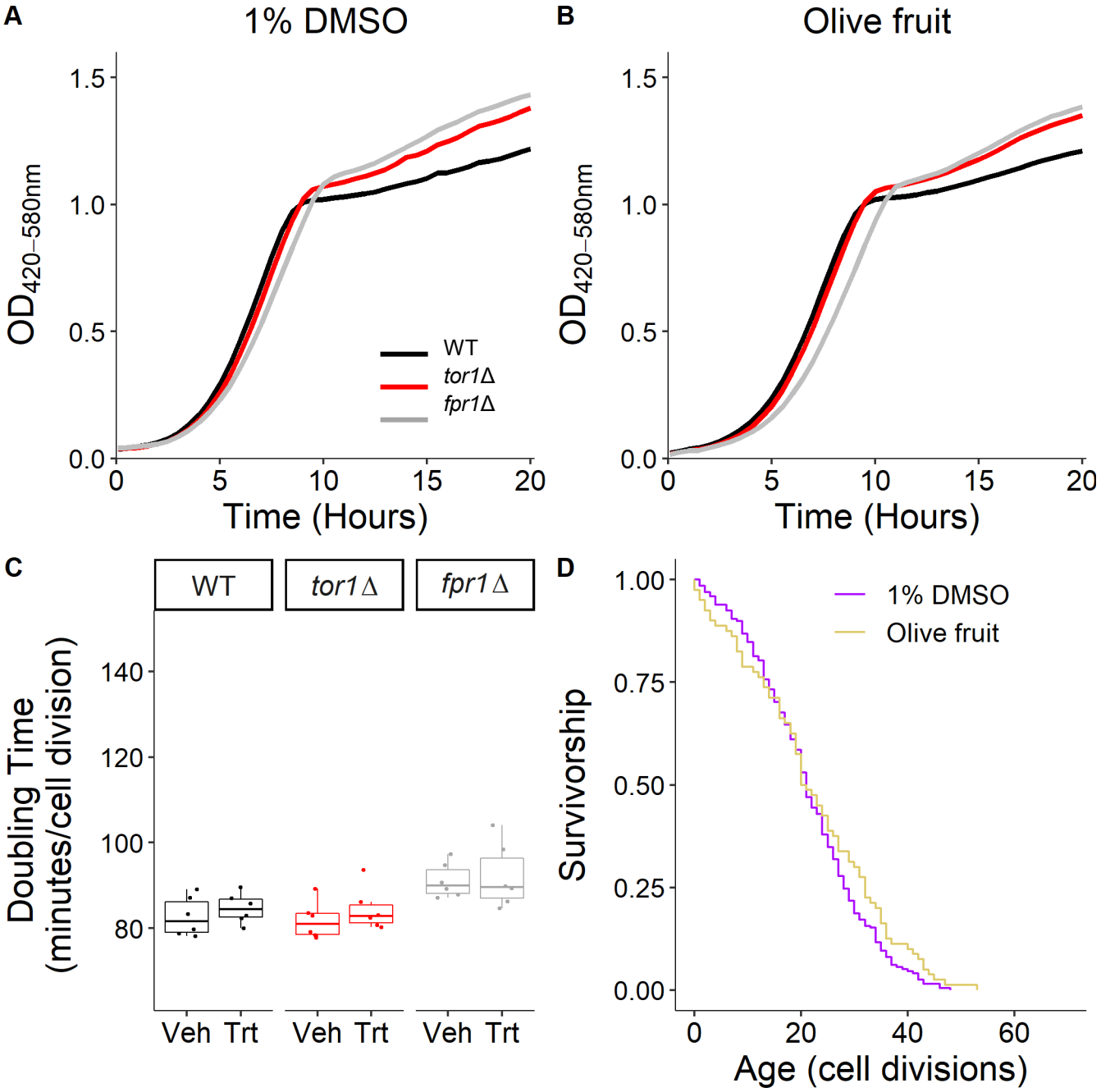

Figure S1-13. **Representative growth curves, doubling times, and replicative lifespan for olive fruit extract.** Representative growth kinetics of WT, *tor1Δ*, and *fpr1Δ* microcultures at **A)** 1% DMSO and **B)** 100 µg/mL olive fruit extract. **C)** Inflection doubling time (DT) of WT, *tor1Δ*, and *fpr1Δ* microcultures. Olive fruit extract does not significantly increase DT (control n = 6, treated n = 6). Treatment compared to vehicle control using Welch's T-test; * p<0.05, ** p<0.01, *** p<0.001. **D)** Olive fruit extract RLS survival curve. For number of cells tested in RLS and Wilcoxon rank sum p-values, see Table 4.

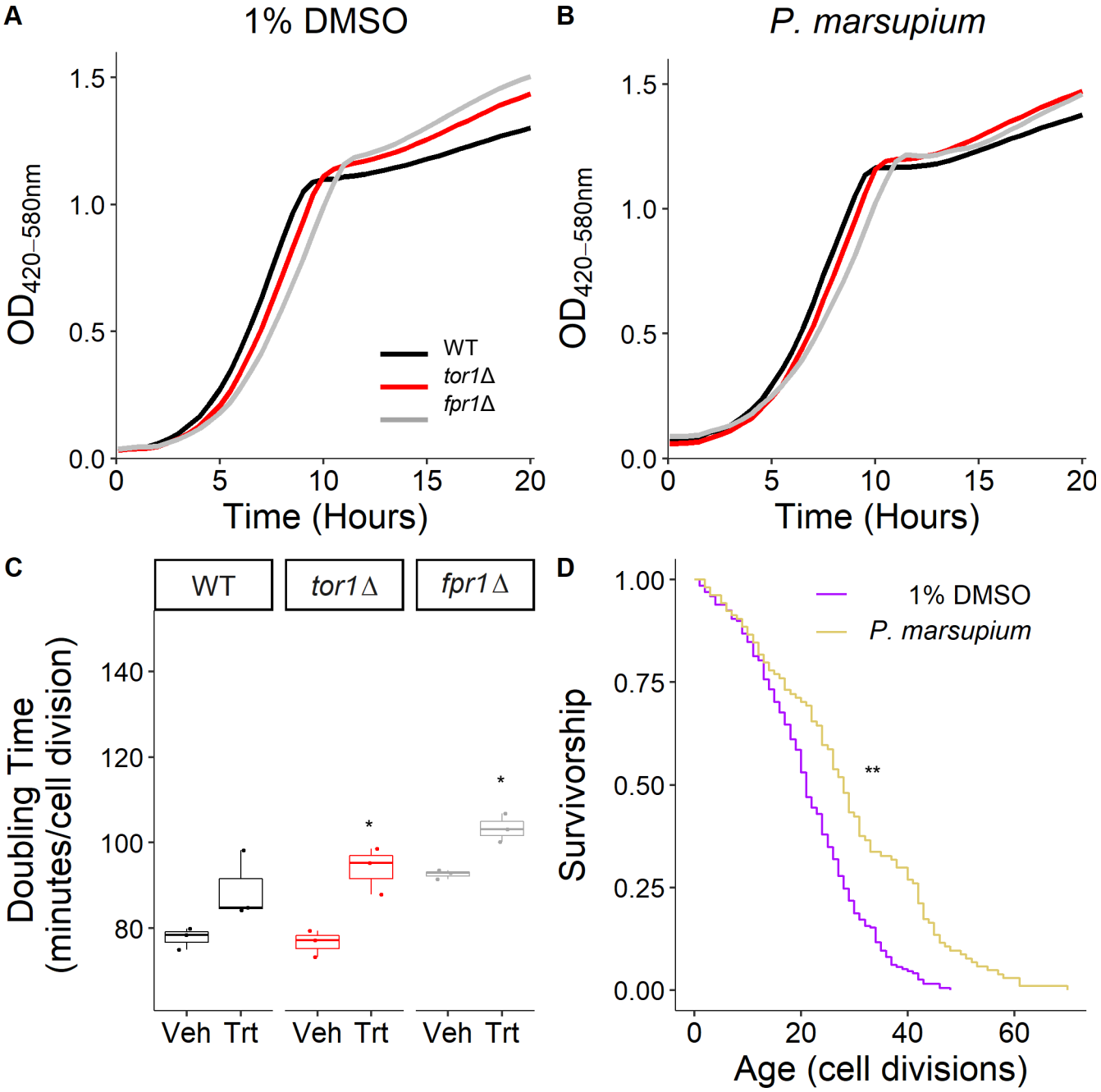

Figure S1-14. **Representative growth curves, doubling times, and replicative lifespan for *Pterocarpus marsupium* extract (PME).** Representative growth kinetics of WT, *tor1Δ*, and *fpr1Δ* microcultures at **A)** 1% DMSO and **B)** 100 µg/mL *Pterocarpus marsupium* extract. **C)** Inflection doubling time (DT) of WT, *tor1Δ*, and *fpr1Δ* microcultures. *Pterocarpus marsupium* extract significantly increases *tor1Δ and fpr1Δ* DT (control n = 3, treated n = 3). Treatment compared to vehicle control using Welch's T-test; * p<0.05, ** p<0.01, *** p<0.001. **D)** *Pterocarpus marsupium* extract replicative lifespan (RLS) survival curve. For number of cells tested in RLS and Wilcoxon rank sum p-values, see Table 4.

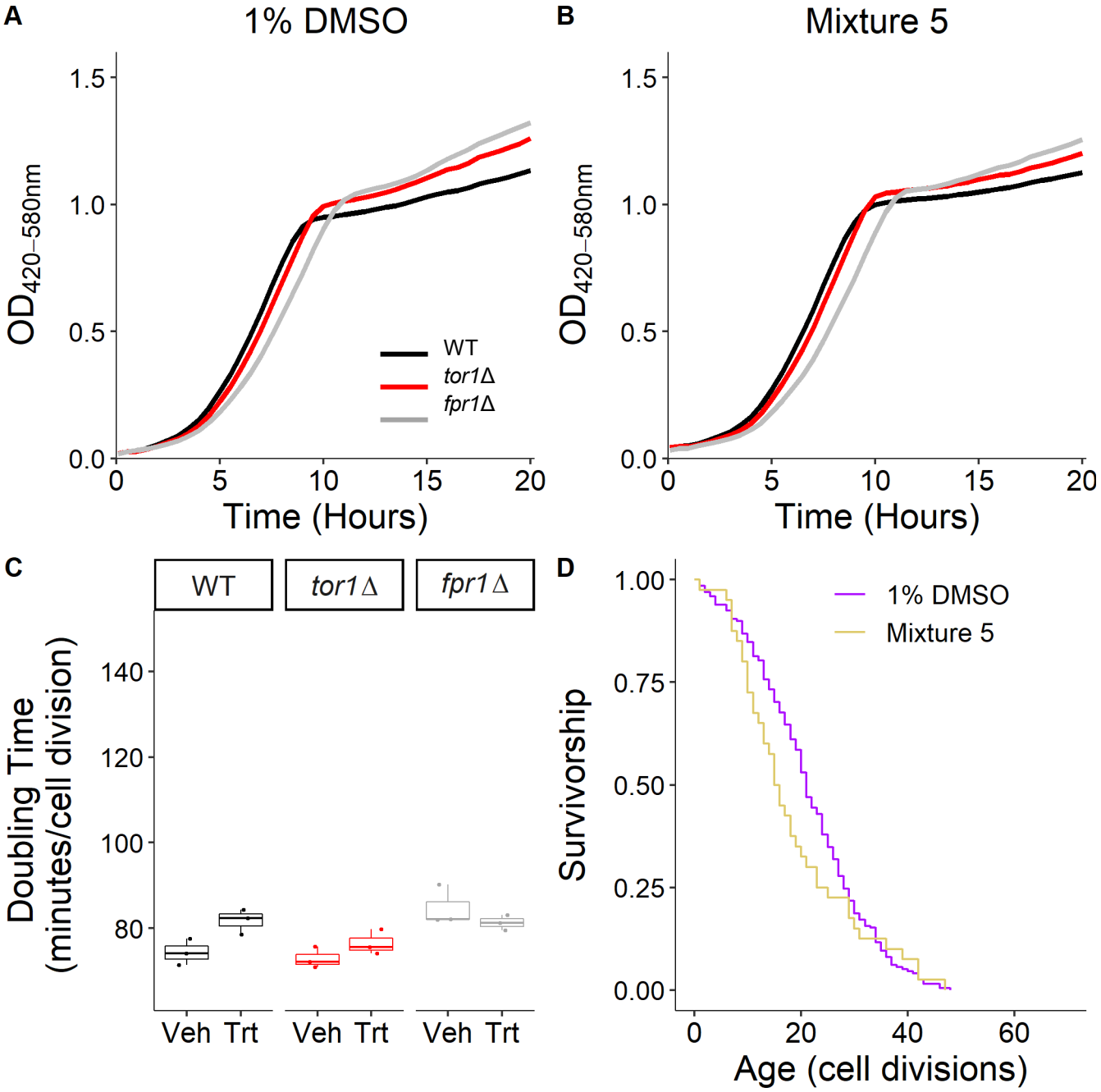

Figure S1-15. **Representative growth curves, doubling times, and replicative lifespan for mixture 5.** Representative growth kinetics of WT, *tor1Δ*, and *fpr1Δ* microcultures at **A)** 1% DMSO and **B)** 100 µg/mL mixture 5. **C)** Inflection doubling time (DT) of WT, *tor1Δ*, and *fpr1Δ* microcultures. Mixture 5 does not significantly increase DT (control n = 3, treated n = 3). Treatment compared to vehicle control using Welch's T-test; * p<0.05, ** p<0.01, *** p<0.001. **D)** Mixture 5 replicative lifespan (RLS) survival curve. For number of cells tested in RLS and Wilcoxon rank sum p-values, see Table 4.

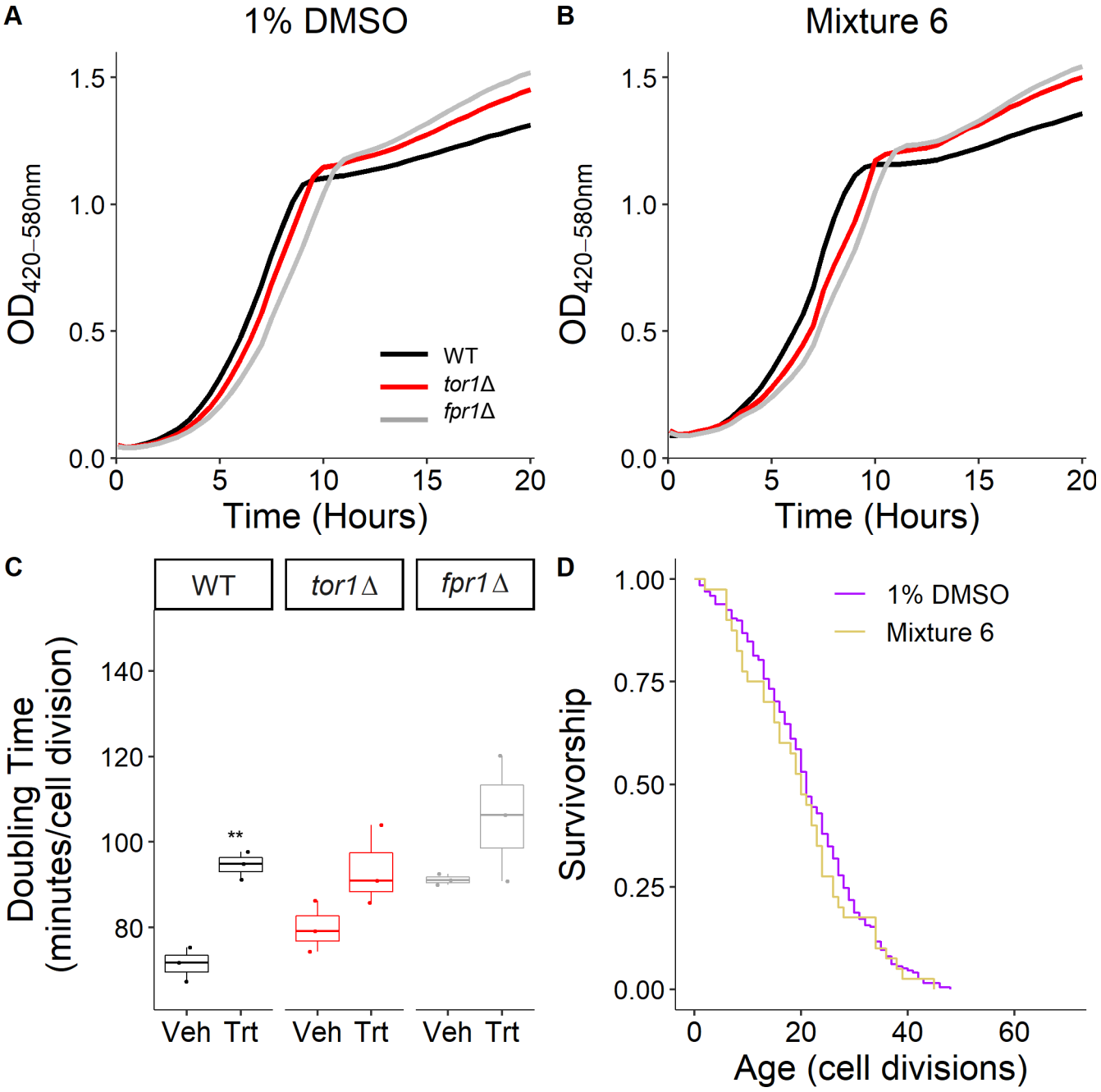

Figure S1-16. **Representative growth curves, doubling times, and replicative lifespan for mixture 6.** Representative growth kinetics of WT, *tor1Δ*, and *fpr1Δ* microcultures at **A)** 1% DMSO and **B)** 100 µg/mL mixture 6.**C)** Inflection doubling time (DT) of WT, *tor1Δ*, and *fpr1Δ* microcultures. Mixture 6 significantly increases WT DT (control n = 3, treated n = 3). Treatment compared to vehicle control using Welch's T-test; * p<0.05, ** p<0.01, *** p<0.001. **D)** Mixture 6 RLS survival curve. For number of cells tested in RLS and Wilcoxon rank sum p-values, see Table 4.

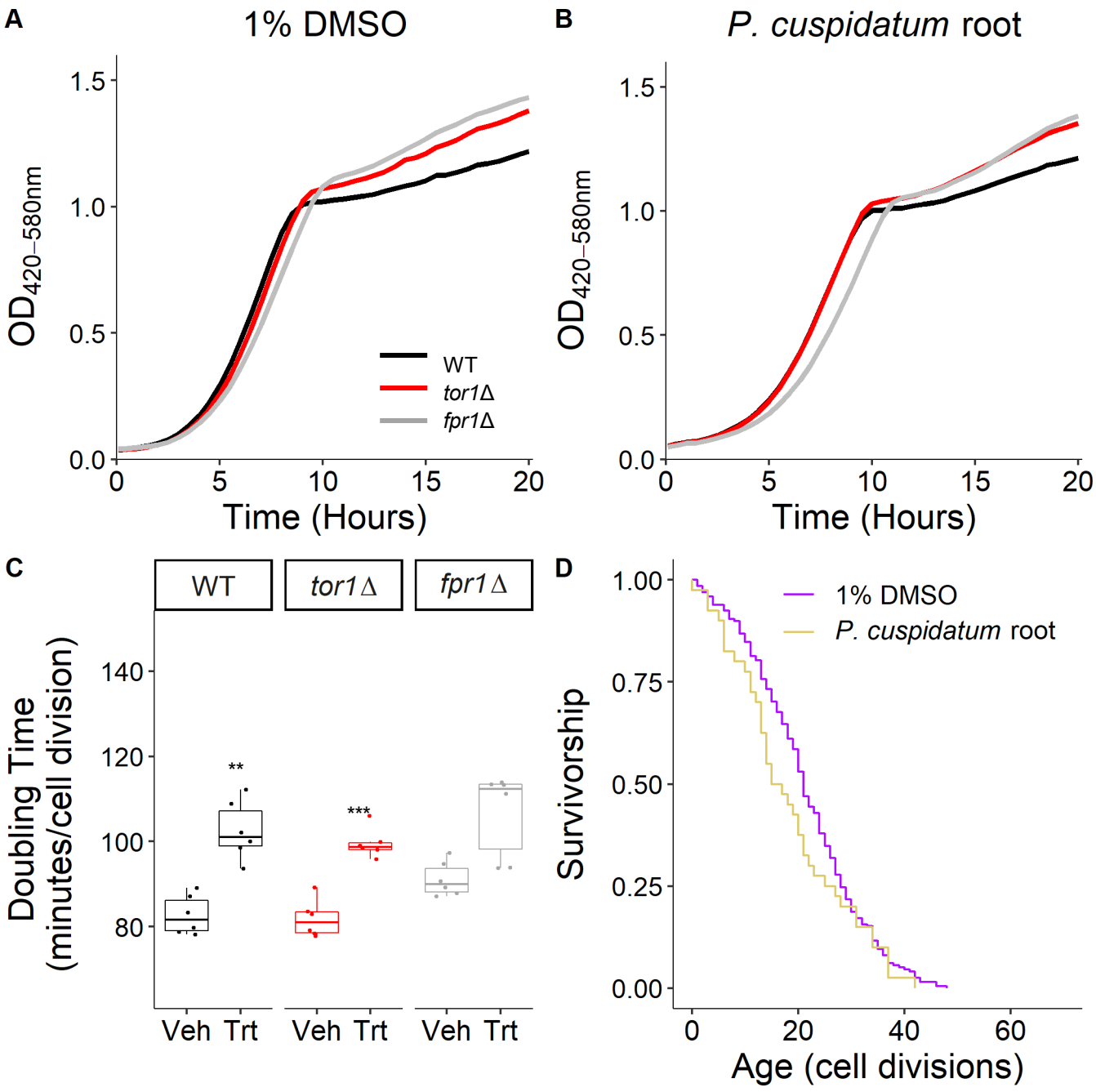

Figure S1-17. **Representative growth curves, doubling times, and replicative lifespan for *Polygonum cuspidatum* root extract (PCE).** Representative growth kinetics of WT, *tor1Δ*, and *fpr1Δ* microcultures at **A)** 1% DMSO and **B)** 100 µg/mL *Polygonum cuspidatum* root. **C)** Inflection DT of WT, *tor1Δ*, and *fpr1Δ* microcultures. *Polygonum cuspidatum* root significantly increases WT and *tor1Δ* DT (control n = 6, treated n = 6). Treatment compared to vehicle control using Welch's T-test; * p<0.05, ** p<0.01, *** p<0.001. **D)** *Polygonum cuspidatum* root replicative lifespan (RLS) survival curve. For number of cells tested in RLS and Wilcoxon rank sum p-values, see Table 4.

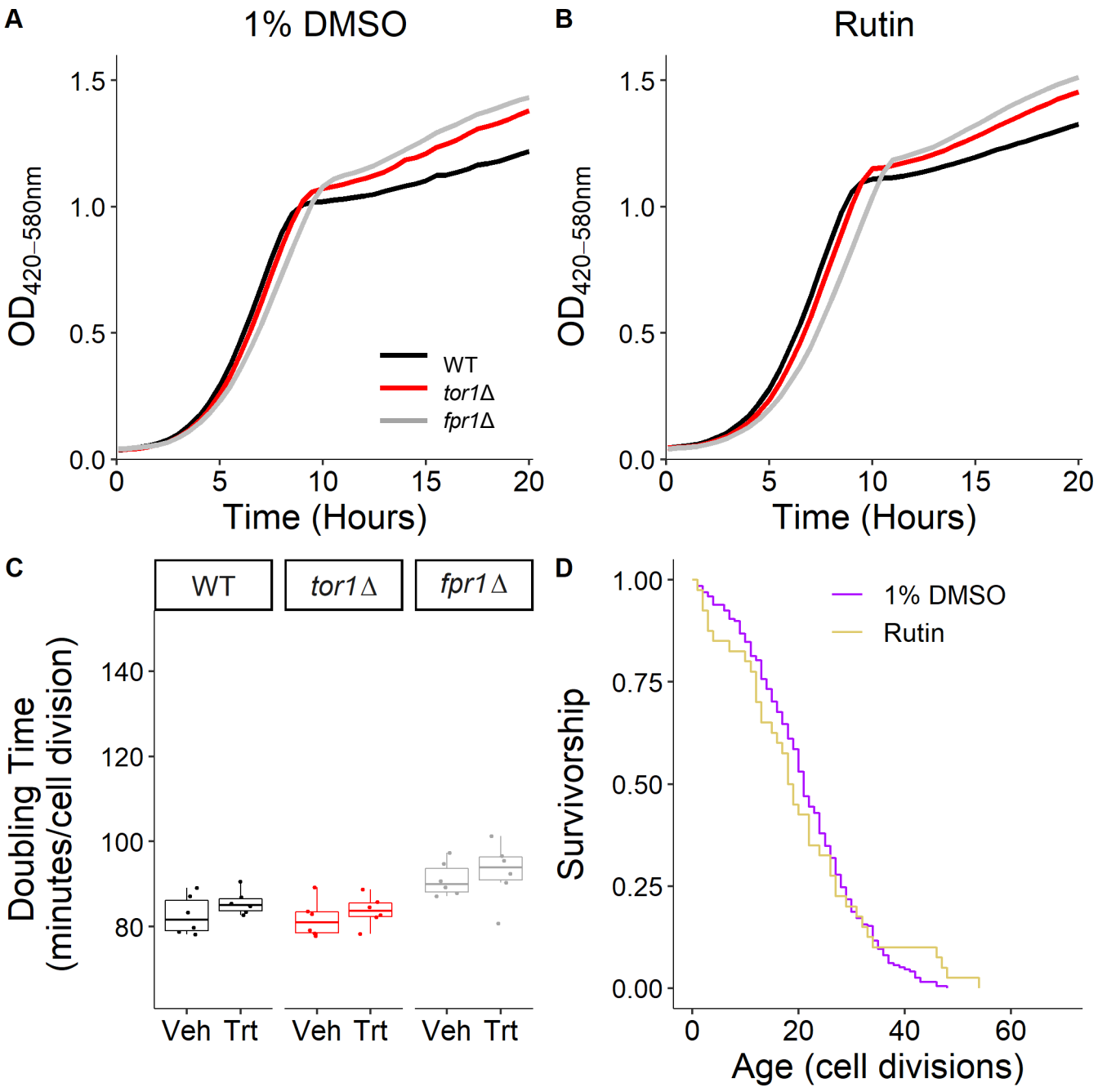

Figure S1-18. **Representative growth curves, doubling times, and replicative lifespan for rutin.** Representative growth kinetics of WT, *tor1Δ*, and *fpr1Δ* microcultures at **A)** 1% DMSO and **B)** 100 µg/mL rutin. **C)** Inflection doubling time (DT) of WT, *tor1Δ*, and *fpr1Δ* microcultures. Rutin does not significantly increase DT (control n = 6, treated n = 6). Treatment compared to vehicle control using Welch's T-test; * p<0.05, ** p<0.01, *** p<0.001. **D)** Rutin replicative lifespan (RLS) survival curve. For number of cells tested in RLS and Wilcoxon rank sum p-values, see Table 4.

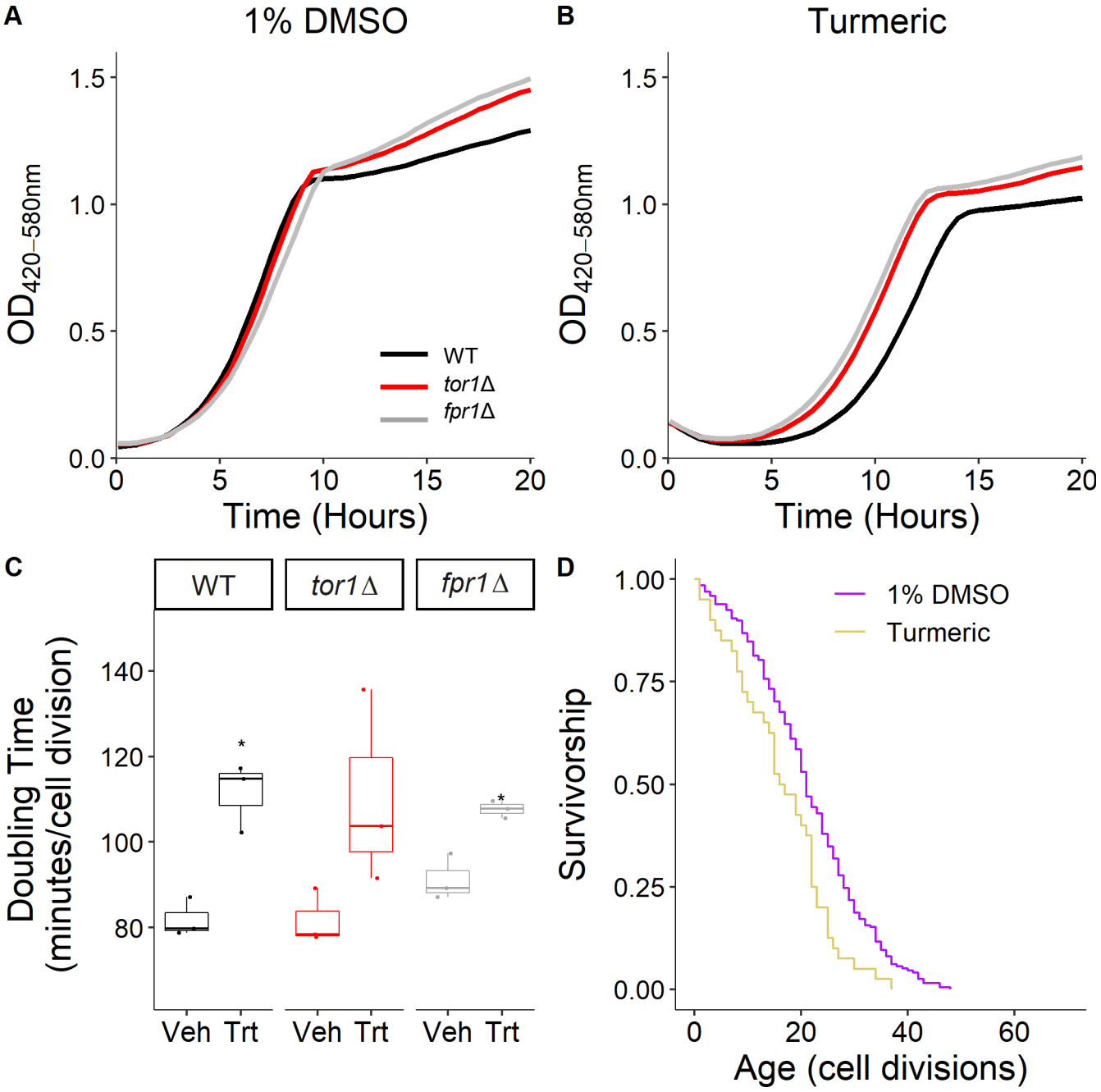

Figure S1-19. **Representative growth curves, doubling times, and replicative lifespan for turmeric extract.** Representative growth kinetics of WT, *tor1Δ*, and *fpr1Δ* microcultures at **A)** 1% DMSO and **B)** 100 µg/mL turmeric extract. **C)** Inflection DT of WT, *tor1Δ*, and *fpr1Δ* microcultures. Turmeric extract significantly increases WT and *fpr1Δ* DT (control n = 3, treated n = 3). Treatment compared to vehicle control using Welch's T-test; * p<0.05, ** p<0.01, *** p<0.001. **D)** Turmeric extract replicative lifespan (RLS) survival curve. For number of cells tested in RLS and Wilcoxon rank sum p- values, see Table 4.

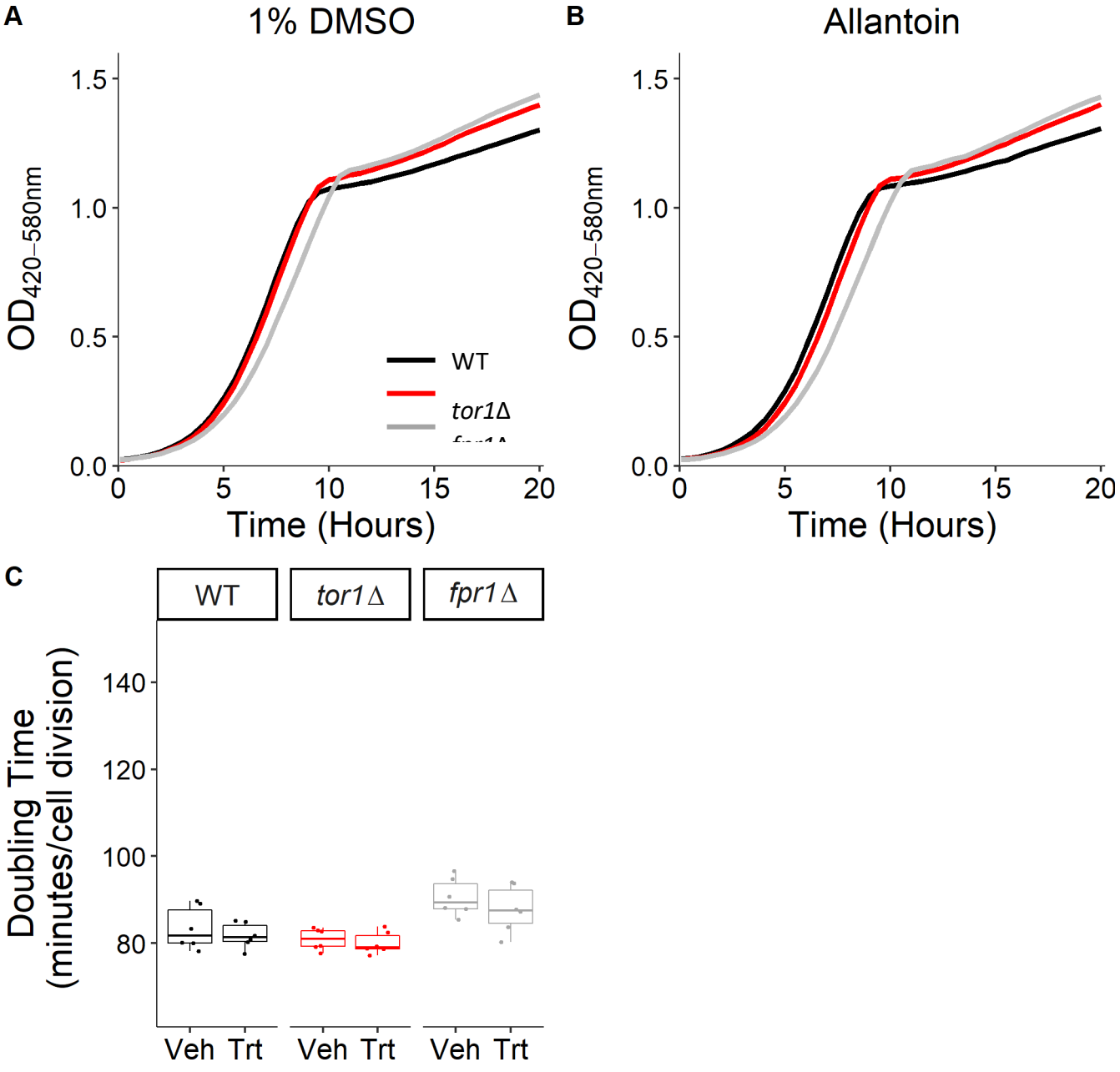

Figure S1-20. **Representative growth curves and doubling times for allantoin.** Representative growth kinetics of WT, *tor1Δ*, and *fpr1Δ* microcultures at **A)** 1% DMSO and **B)** 100 µg/mL allantoin. **C)** Inflection doubling time (DT) of WT, *tor1Δ*, and *fpr1Δ* microcultures. Allantoin does not significantly increase DT (control n = 6, treated n = 6). Treatment compared to vehicle control using Welch's T-test; * p<0.05, ** p<0.01, *** p<0.001.

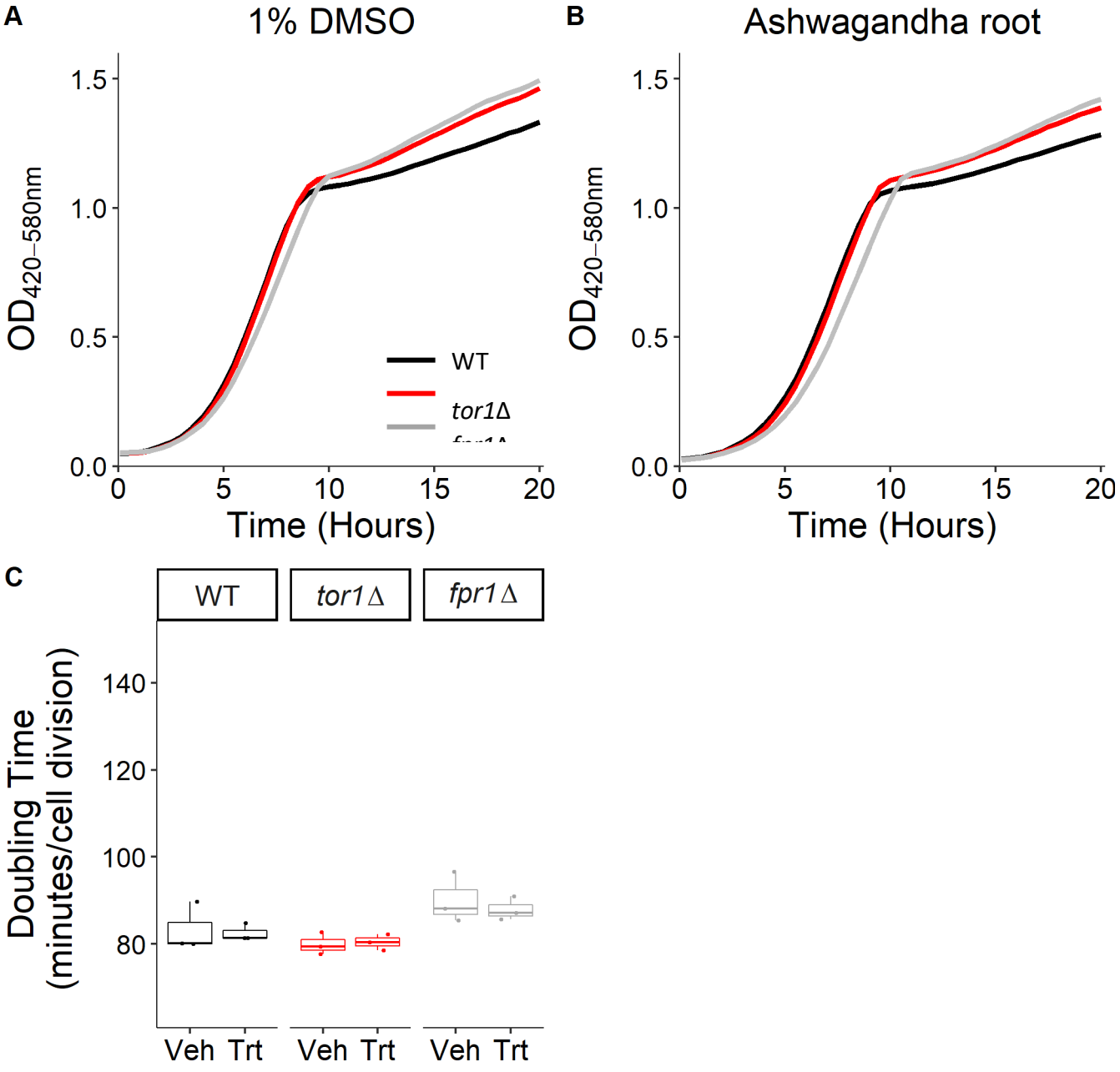

Figure S1-21. **Representative growth curves and doubling times for ashwagandha root.** Representative growth kinetics of WT, *tor1Δ*, and *fpr1Δ* microcultures at **A)** 1% DMSO and **B)** 100 µg/mL ashwagandha root. **C)** Inflection doubling time (DT) of WT, *tor1Δ*, and *fpr1Δ* microcultures. Ashwagandha root does not significantly increase DT (control n =3, treated n = 3). Treatment compared to vehicle control using Welch's T-test; * p<0.05, ** p<0.01, *** p<0.001.

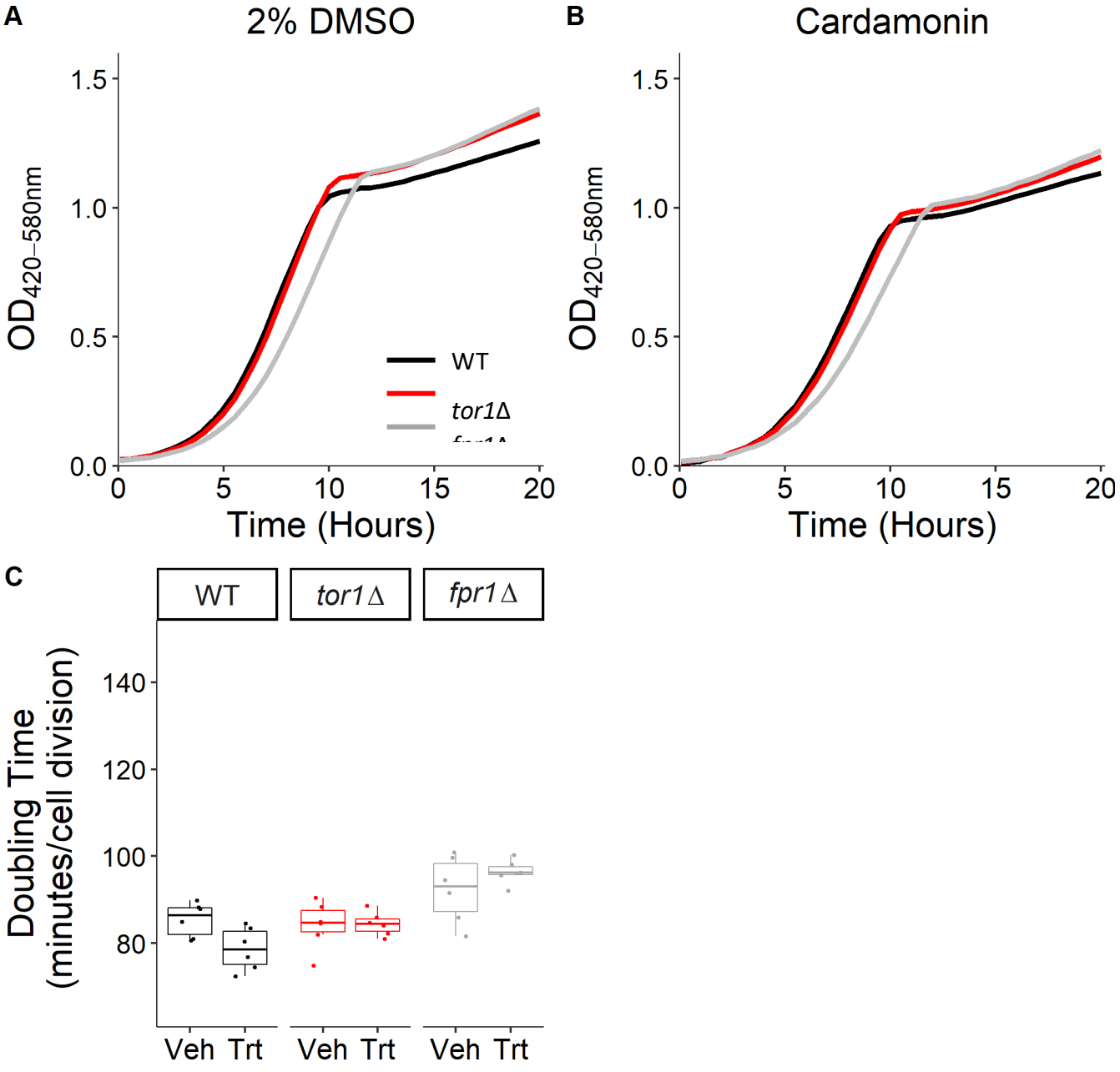

Figure S1-22. **Representative growth curves and doubling times for cardamonin.** Representative growth kinetics of WT, *tor1Δ*, and *fpr1Δ* microcultures at **A)** 2% DMSO and **B)** 100 µg/mL cardamonin. **C)** Inflection doubling time (DT) of WT, *tor1Δ*, and *fpr1Δ* microcultures. Cardamonin does not significantly increase DT (control n = 6 , treated n = 6). Treatment compared to vehicle control using Welch's T-test; * p<0.05, ** p<0.01, *** p<0.001.

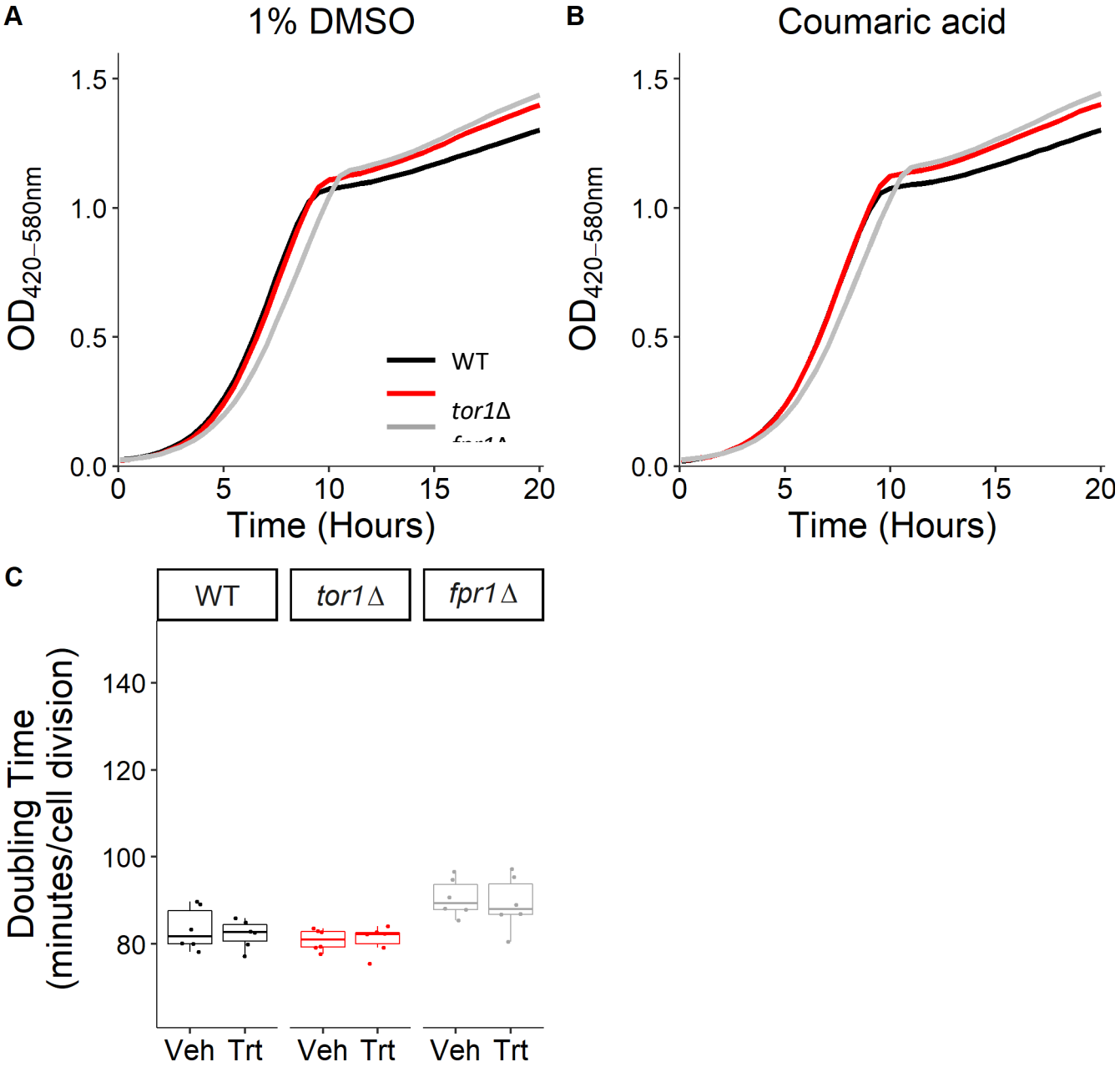

Figure S1-23. **Representative growth curves and doubling times for coumaric acid.** Representative growth kinetics of WT, *tor1Δ*, and *fpr1Δ* microcultures at **A)** 1% DMSO and **B)** 100 µg/mL coumaric acid. **C)** Inflection doubling time (DT) of WT, *tor1Δ*, and *fpr1Δ* microcultures. Coumaric acid does not significantly increase DT (control n = 6, treated n = 6). Treatment compared to vehicle control using Welch's T-test; * p<0.05, ** p<0.01, *** p<0.001.

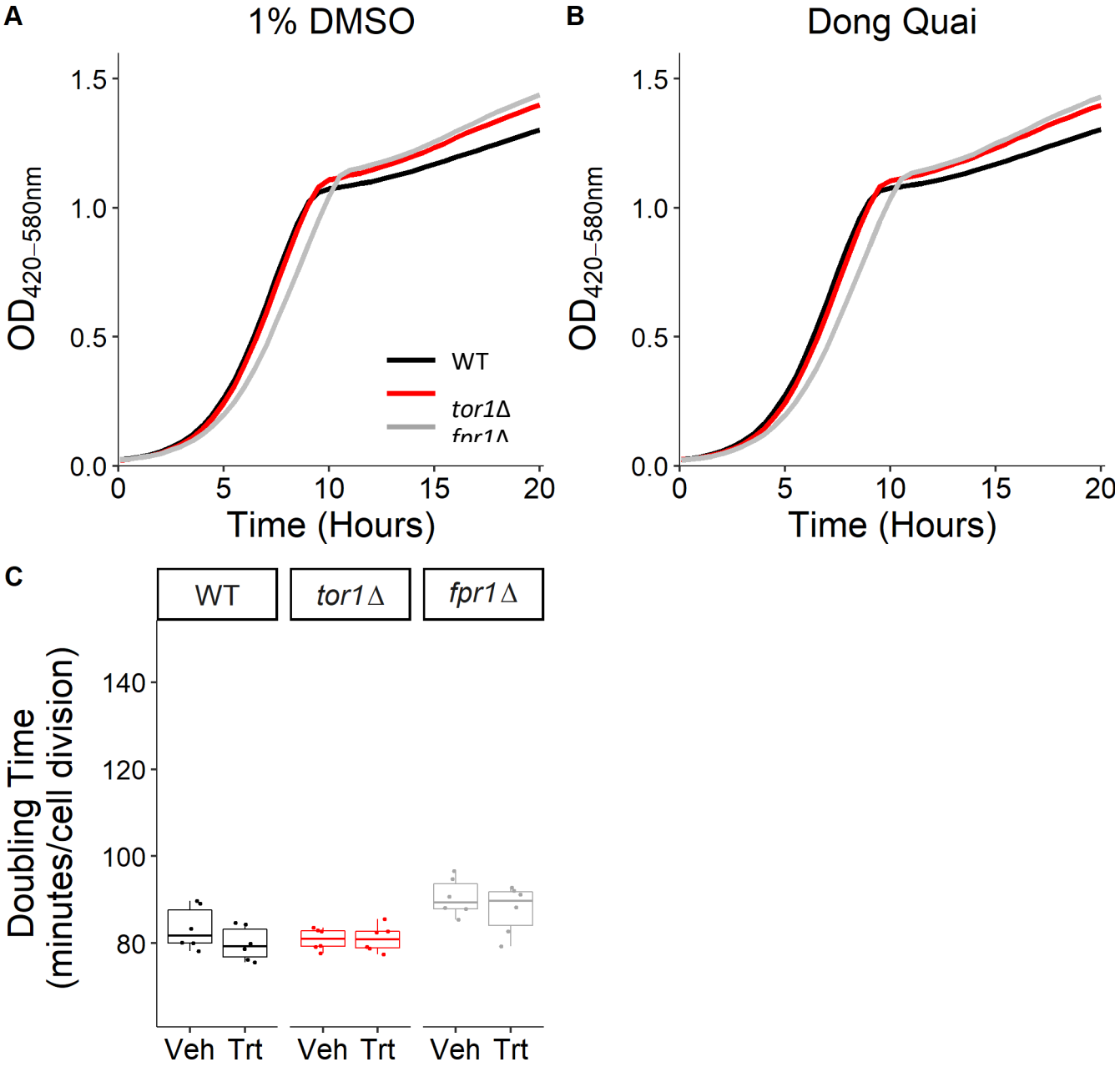

Figure S1-24. **Representative growth curves and doubling times for Dong Quai.** Representative growth kinetics of WT, *tor1Δ*, and *fpr1Δ* microcultures at **A)** 1% DMSO and **B)** 100 µg/mL Dong Quai. **C)** Inflection doubling time (DT) of WT, *tor1Δ*, and *fpr1Δ* microcultures. Dong Quai does not significantly increase DT (control n = 6, treated n = 6). Treatment compared to vehicle control using Welch's T-test; * p<0.05, ** p<0.01, *** p<0.001.

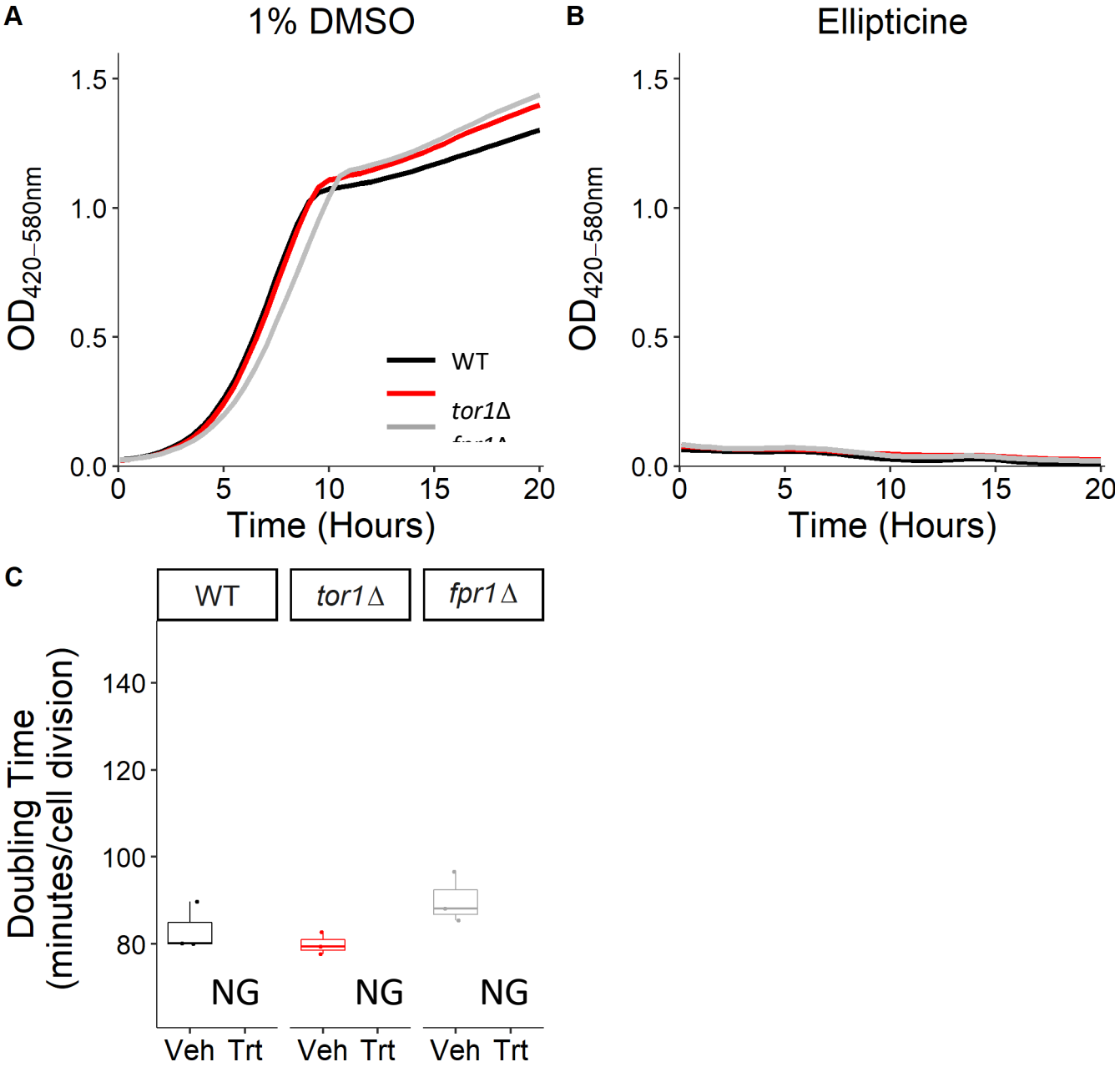

Figure S1-25. **Representative growth curves and doubling times for ellipticine.** Representative growth kinetics of WT, *tor1Δ*, and *fpr1Δ* microcultures at **A)** 1% DMSO and **B)** 100 µg/mL ellipticine. **C)** Inflection doubling time (DT) of WT, *tor1Δ*, and *fpr1Δ* microcultures. Ellipticine suppresses growth such that DT cannot be calculated (control n = 3, treated n = 3). Treatment compared to vehicle control using Welch's T-test; * p<0.05, ** p<0.01, *** p<0.001. NG = No growth, indicated by culture failing to reach OD ≥ 0.3 after 20 hours outgrowth.

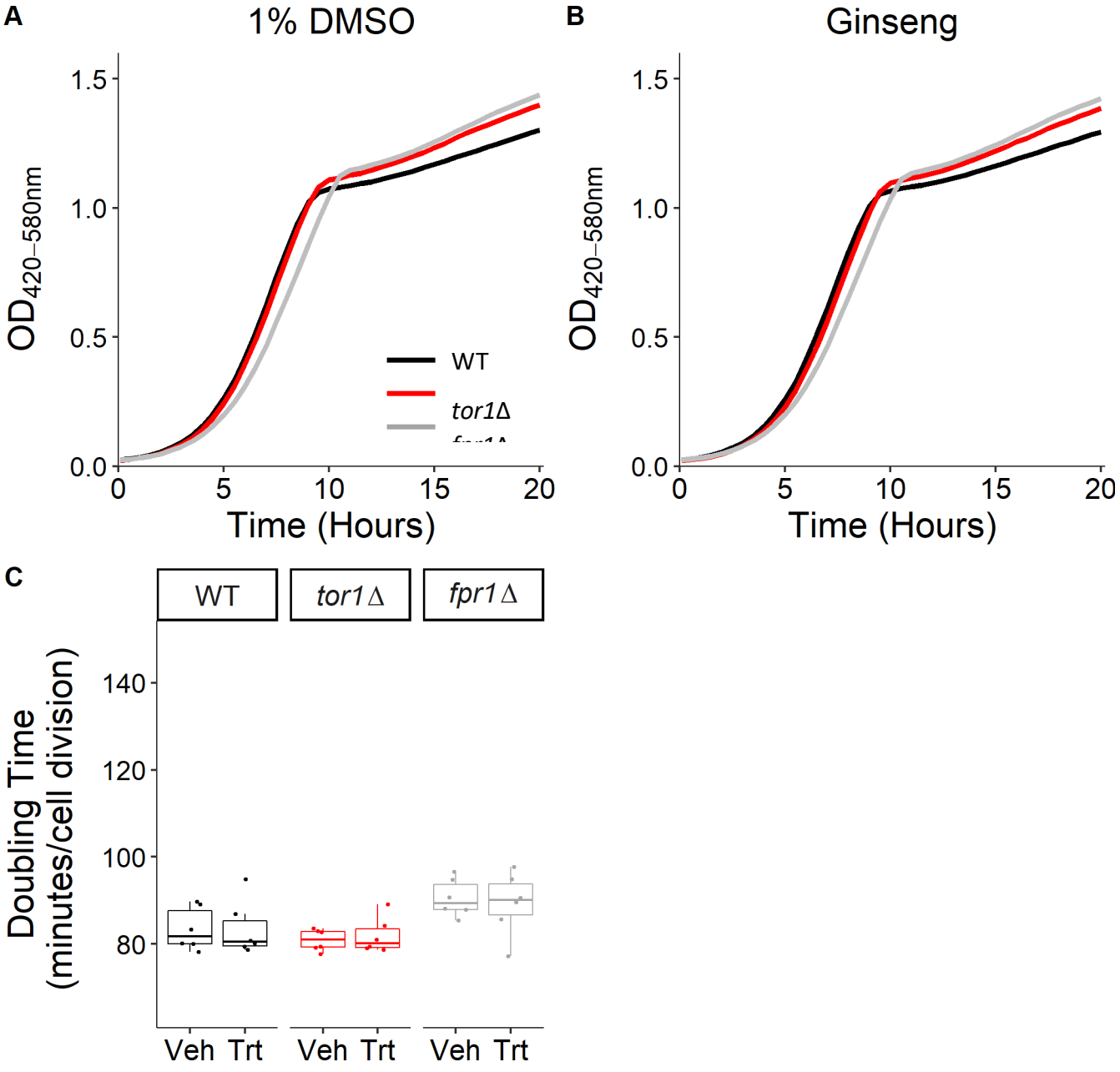

Figure S1-26. **Representative growth curves and doubling times for ginseng extract.** Representative growth kinetics of WT, *tor1Δ*, and *fpr1Δ* microcultures at **A)** 1% DMSO and **B)** 100 µg/mL ginseng extract. **C)** Inflection doubling time (DT) of WT, *tor1Δ*, and *fpr1Δ* microcultures. Ginseng extract does not significantly increase DT (control n = 6, treated n = 6). Treatment compared to vehicle control using Welch's T-test; * p<0.05, ** p<0.01, *** p<0.001.

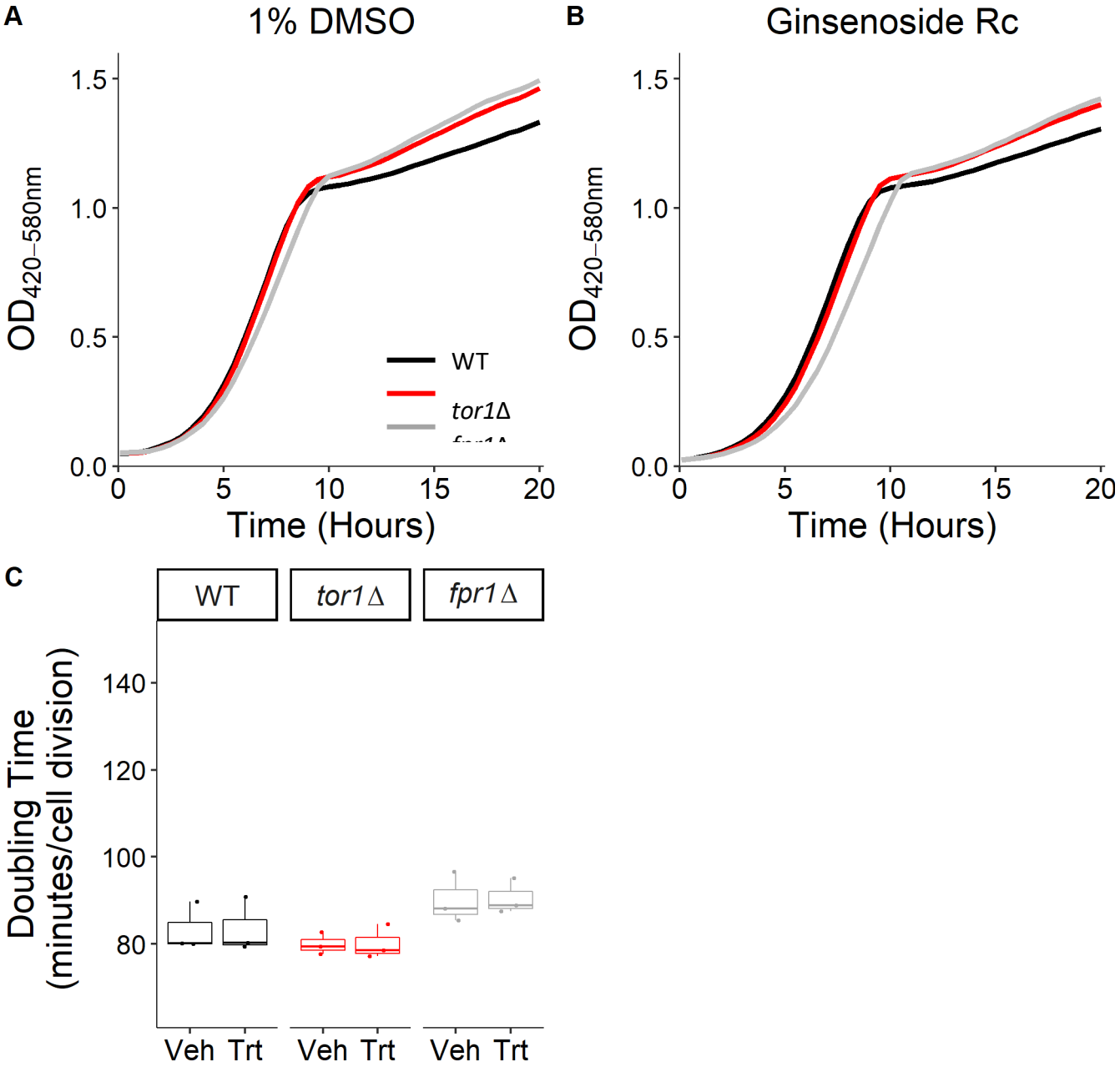

Figure S1-27. **Representative growth curves and doubling times for ginsenoside Rc.** Representative growth kinetics of WT, *tor1Δ*, and *fpr1Δ* microcultures at **A)** 1% DMSO and **B)** 100 µg/mL ginsenoside Rc. **C)** Inflection doubling time (DT) of WT, *tor1Δ*, and *fpr1Δ* microcultures. Ginsenoside Rc does not significantly increase DT (control n = 3, treated n = 3). Treatment compared to vehicle control using Welch's T-test; * p<0.05, ** p<0.01, *** p<0.001.

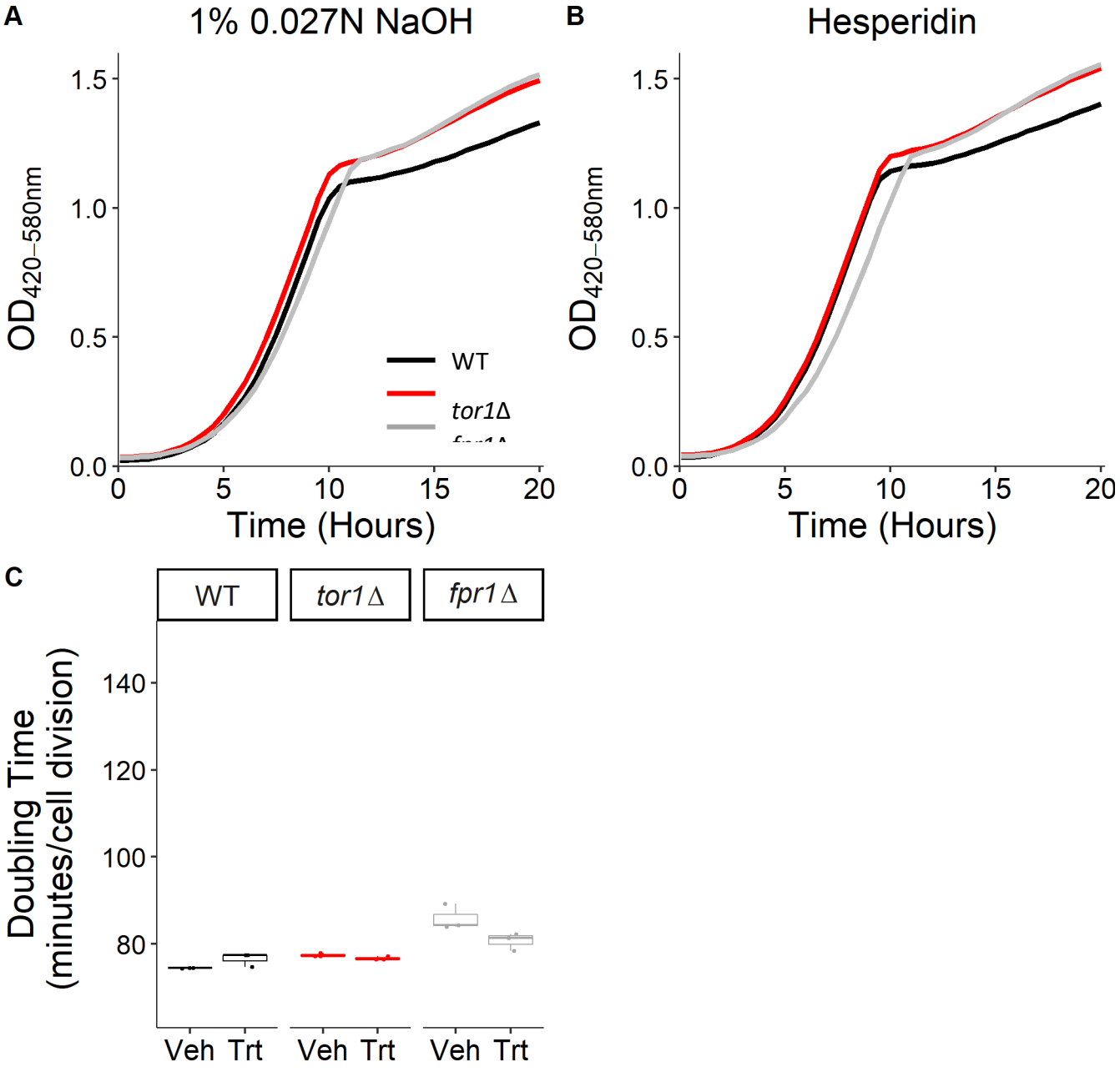

Figure S1-28. **Representative growth curves and doubling times for hesperidin.** Representative growth kinetics of WT, *tor1Δ*, and *fpr1Δ* microcultures at **A)** 1% 0.027N NaOH and **B)** 100 µg/mL hesperidin. **C)** Inflection doubling time (DT) of WT, *tor1Δ*, and *fpr1Δ* microcultures. Hesperidin does not significantly increase DT (control n = 3 , treated n = 3). Treatment compared to vehicle control using Welch's T-test; * p<0.05, ** p<0.01, *** p<0.001.

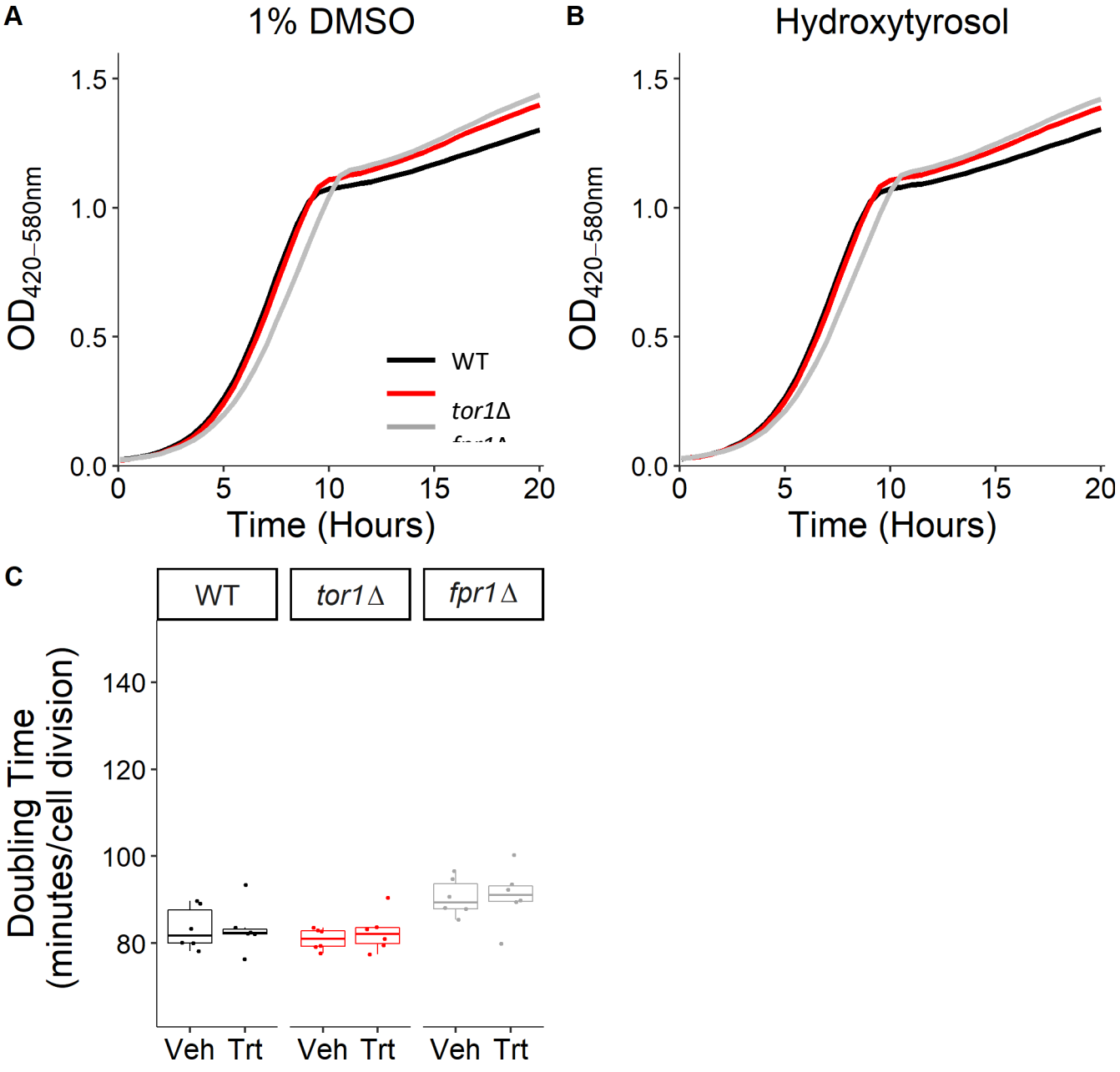

Figure S1-29. **Representative growth curves and doubling times for hydroxytyrosol.** Representative growth kinetics of WT, *tor1Δ*, and *fpr1Δ* microcultures at **A)** 1% DMSO and **B)** 100 µg/mL hydroxytyrosol. **C)** Inflection doubling time (DT) of WT, *tor1Δ*, and *fpr1Δ* microcultures. Hydroxytyrosol does not significantly increase DT (control n = 6, treated n = 6). Treatment compared to vehicle control using Welch's T-test; * p<0.05, ** p<0.01, *** p<0.001.

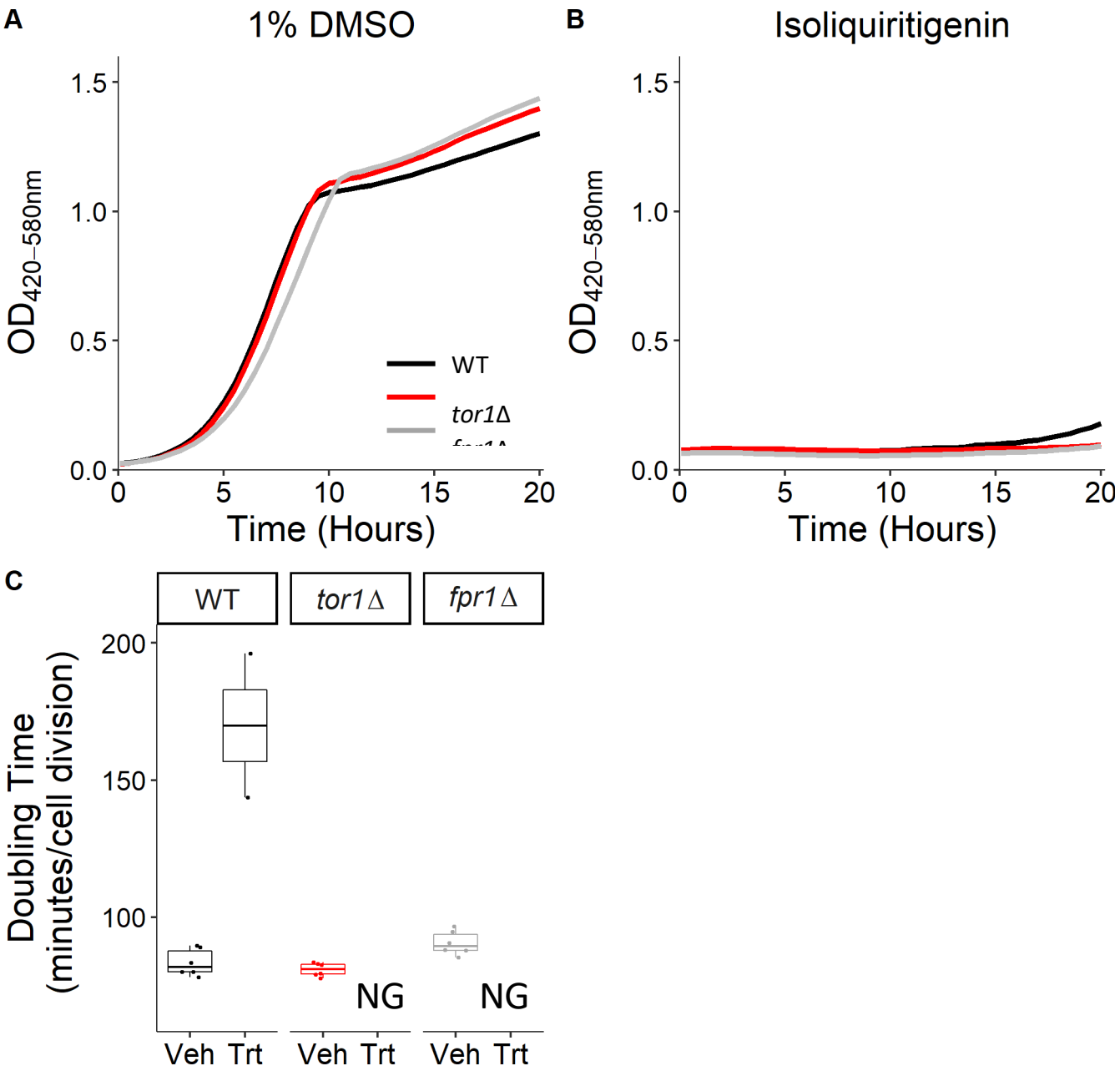

Figure S1-30. **Representative growth curves and doubling times for isoliquiritigenin.** Representative growth kinetics of WT, *tor1Δ*, and *fpr1Δ* microcultures at **A)** 1% DMSO and **B)** 100 µg/mL isoliquiritigenin. **C)** Inflection doubling time (DT) of WT, *tor1Δ*, and *fpr1Δ* microcultures. Isoliquiritigenin suppresses growth such that DT cannot be calculated. Treatment compared to vehicle control using Welch's T-test; * $p<0.05$, ** $p<0.01$, *** $p<0.001$. NG = No growth, indicated by culture failing to reach OD ≥ 0.3 after 20 hours outgrowth.(control n = 6, treated n = 6, of which 2 WT and no *tor1Δ* or *fpr1Δ* cultures grew).

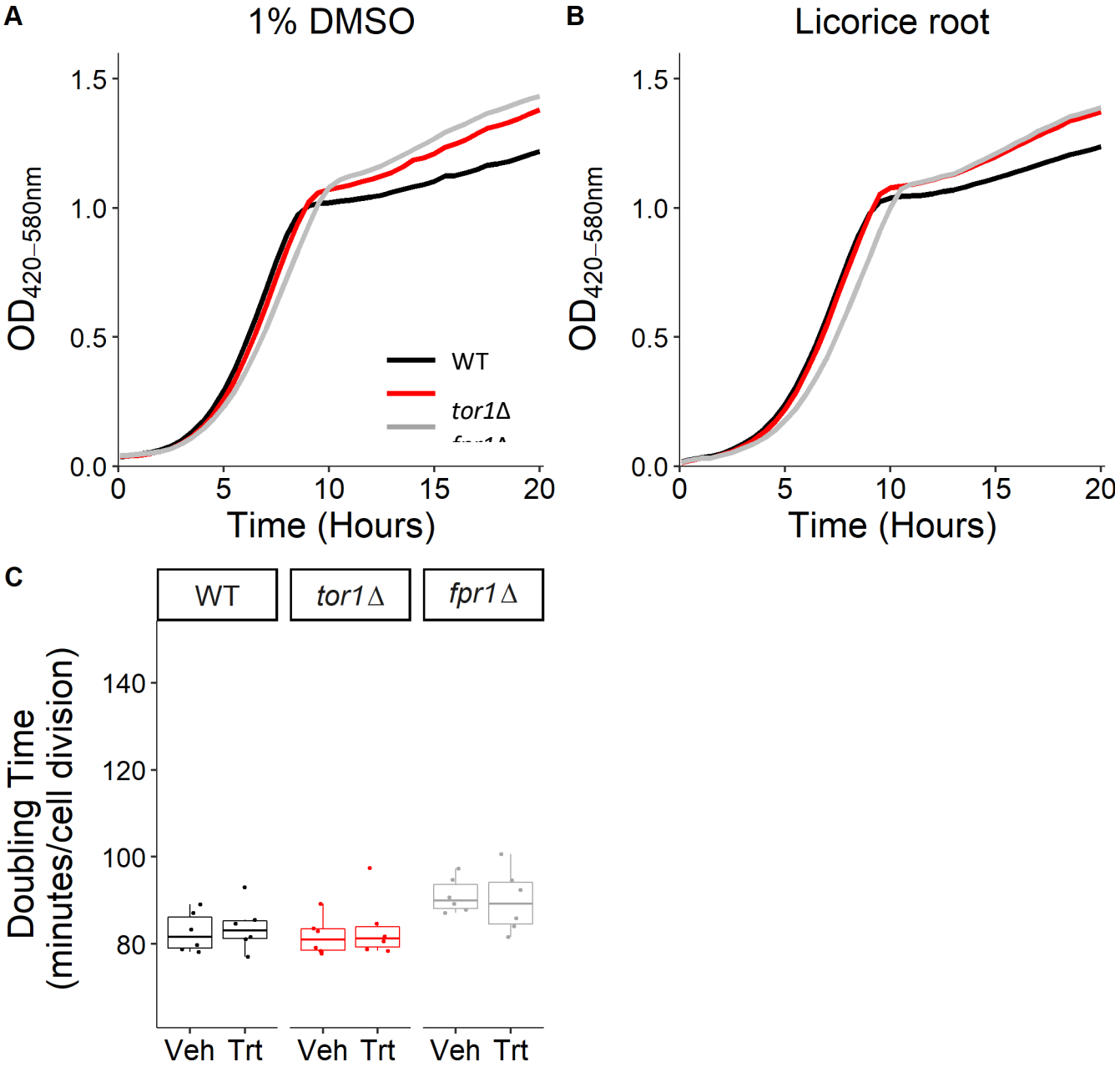

Figure S1-31. **Representative growth curves and doubling times for licorice root.** Representative growth kinetics of WT, *tor1Δ*, and *fpr1Δ* microcultures at **A)** 1% DMSO and **B)** 100 µg/mL licorice root. **C)** Inflection doubling time (DT) of WT, *tor1Δ*, and *fpr1Δ* microcultures. Licorice root does not significantly increase DT (control n = 6, treated n = 6).

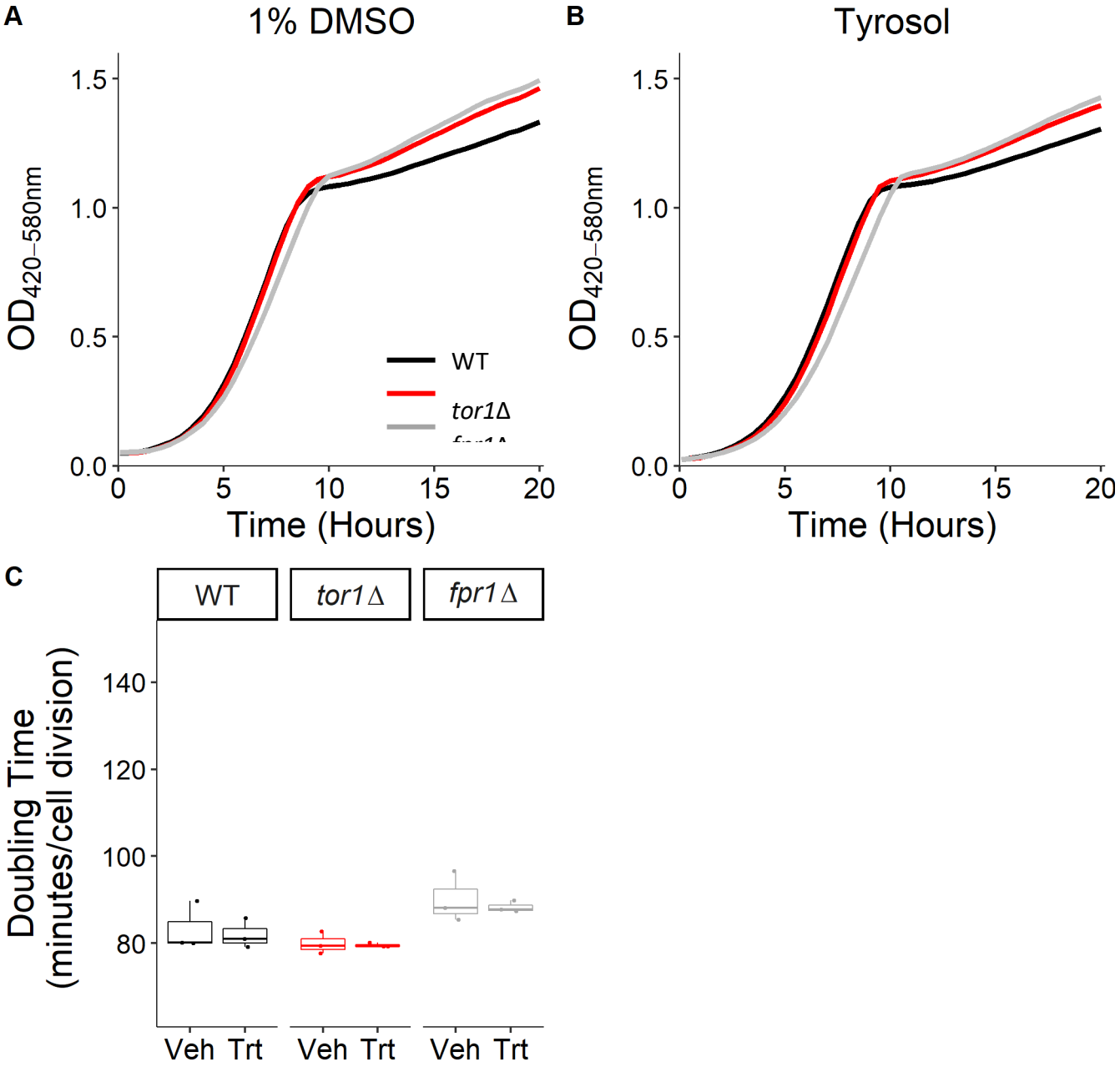

Figure S1-32. **Representative growth curves and doubling times for tyrosol.** Representative growth kinetics of WT, *tor1Δ*, and *fpr1Δ* microcultures at **A)** 1% DMSO and **B)** 100 µg/mL tyrosol. **C)** Inflection doubling time (DT) of WT, *tor1Δ*, and *fpr1Δ* microcultures. Tyrosol does not significantly increase DT (control n = 3, treated n = 3). Treatment compared to vehicle control using Welch's T-test; * p<0.05, ** p<0.01, *** p<0.001.

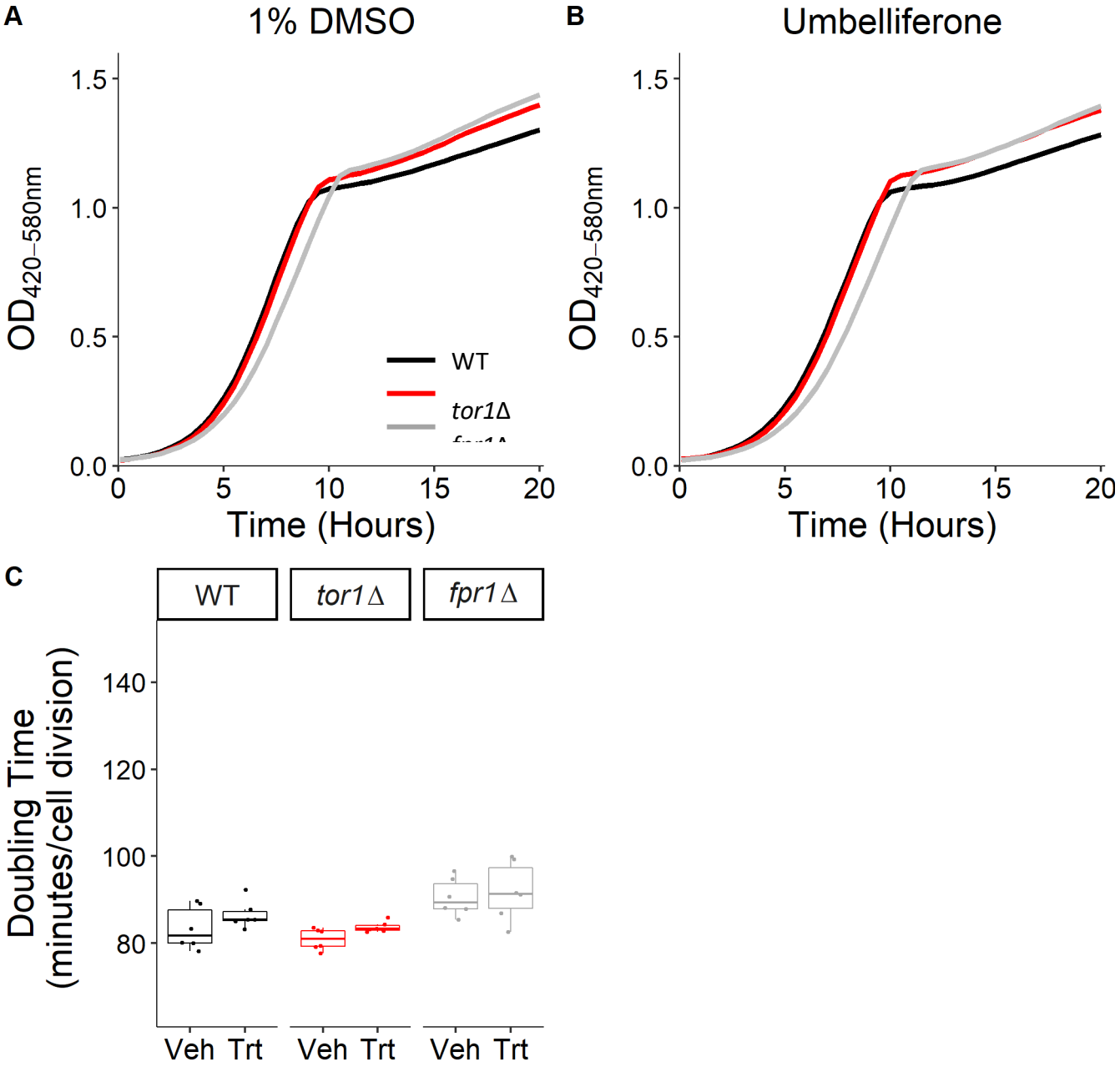

Figure S1-33. **Representative growth curves and doubling times for umbelliferone.** Representative growth kinetics of WT, *tor1Δ*, and *fpr1Δ* microcultures at **A)** 1% DMSO and **B)** 100 µg/mL umbelliferone. **C)** Inflection doubling time (DT) of WT, *tor1Δ*, and *fpr1Δ* microcultures. Umbelliferone does not increase DT (control n = 6, treated n = 6). Treatment compared to vehicle control using Welch's T-test; * p<0.05, ** p<0.01, *** p<0.001.

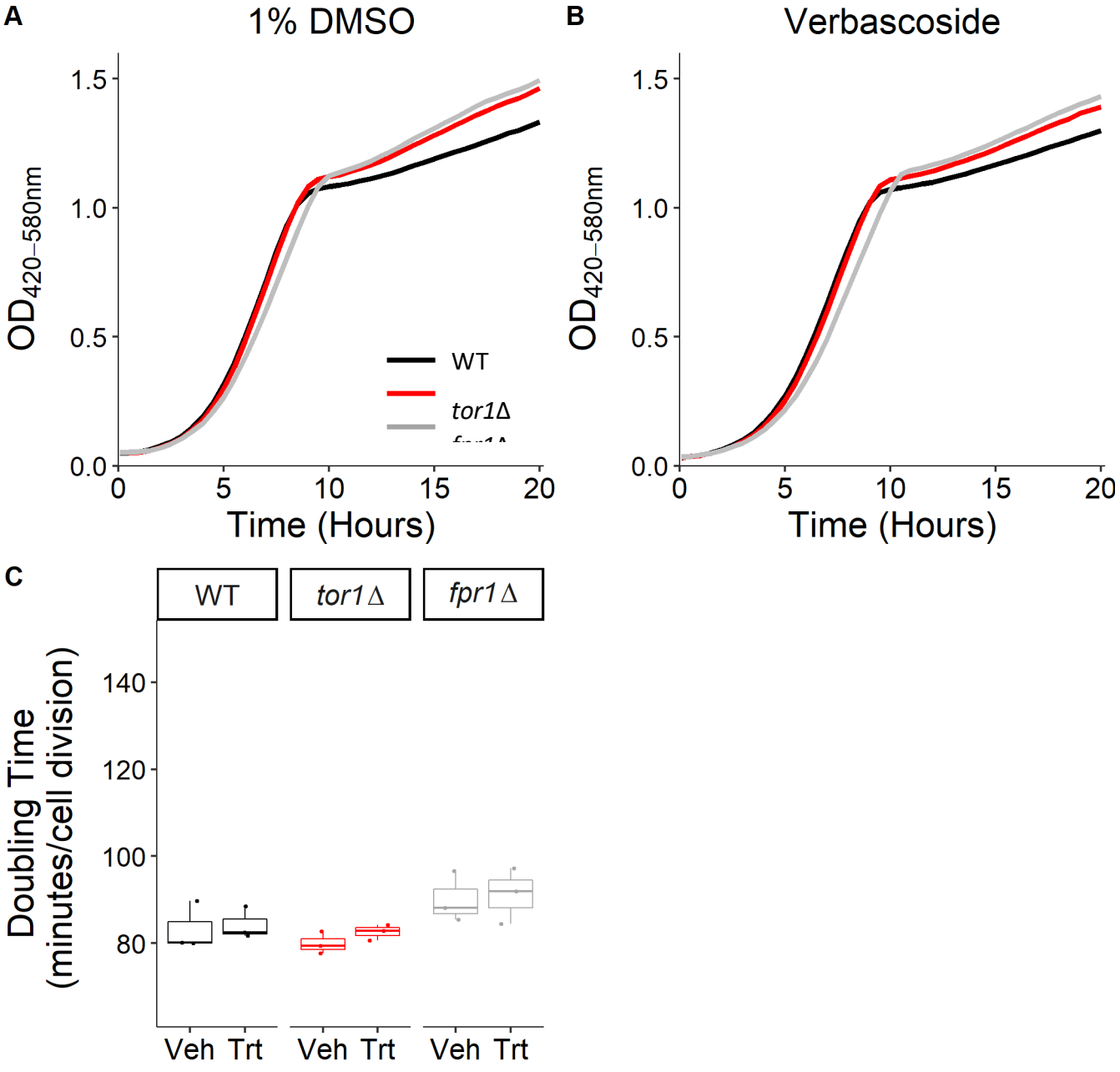

Figure S1-34. **Representative growth curves and doubling times for verbascoside.** Representative growth kinetics of WT, *tor1Δ*, and *fpr1Δ* microcultures at **A)** 1% DMSO and **B)** 100 µg/mL verbascoside. **C)** Inflection doubling time (DT) of WT, *tor1Δ*, and *fpr1Δ* microcultures. Verbascoside does not significantly increase DT (control n = 3, treated n = 3). Treatment compared to vehicle control using Welch's T-test; * p<0.05, ** p<0.01, *** p<0.001.

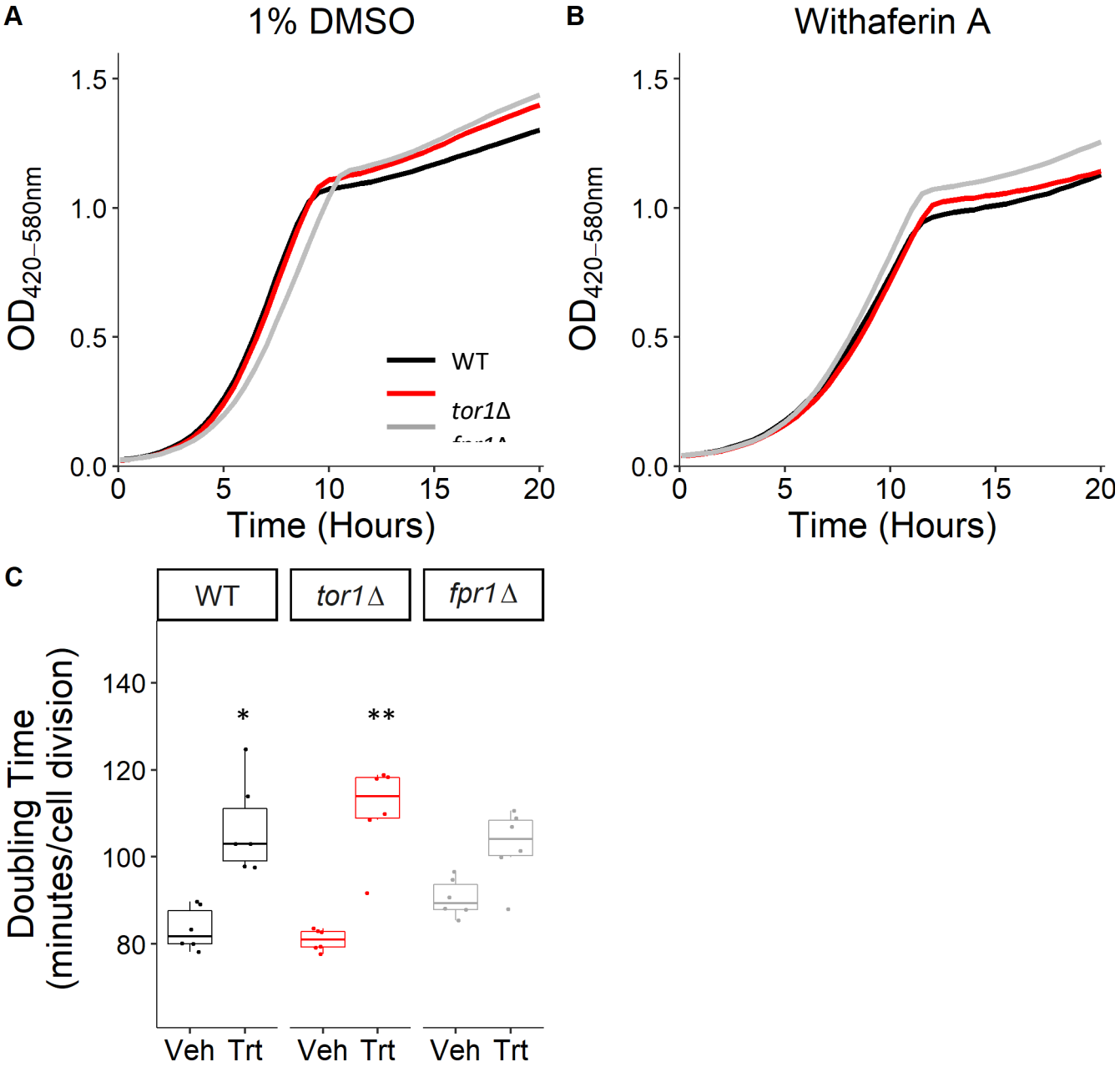

Figure S1-35. **Representative growth curves and doubling times for withaferin A.** Representative growth kinetics of WT, *tor1Δ*, and *fpr1Δ* microcultures at **A)** 1% DMSO and **B)** 100 µg/mL withaferin A. **C)** Inflection doubling time (DT) of WT, *tor1Δ*, and *fpr1Δ* microcultures. Withaferin A significantly increases WT and *tor1Δ* DT (control n = 6, treated n = 6). Treatment compared to vehicle control using Welch's T-test; * p<0.05, ** p<0.01, *** p<0.001.

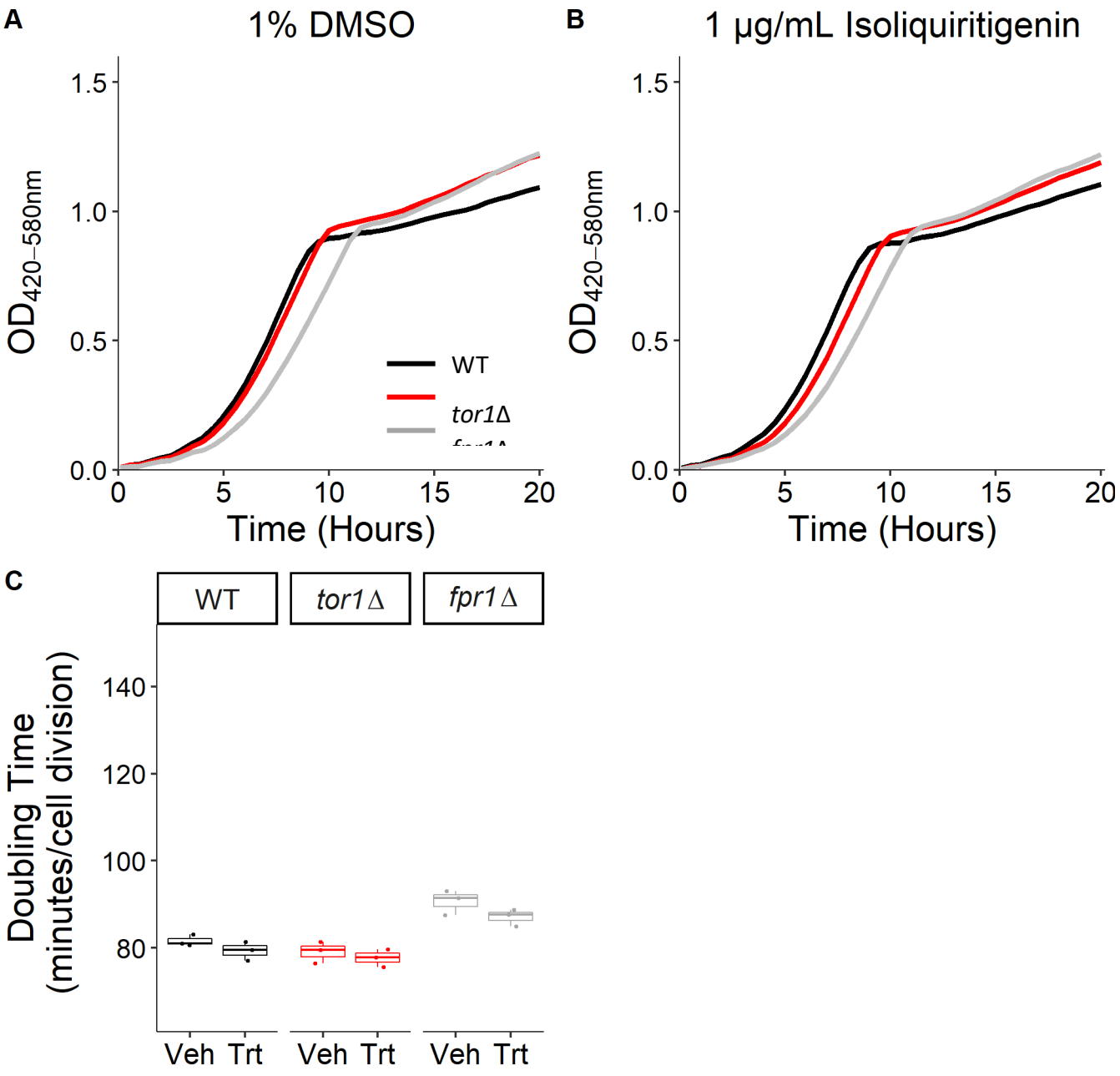

Figure S1-36. **Representative growth curves and doubling times for 1 µg/mL isoliquiritigenin.** Representative growth kinetics of WT, *tor1Δ*, and *fpr1Δ* microcultures at **A)** 1% DMSO and **B)** 1 µg/mL isoliquiritigenin. **C)** Inflection doubling time (DT) of WT, *tor1Δ*, and *fpr1Δ* microcultures. 1 µg/mL Isoliquiritigenin does not significantly increase DT (control n = 3, treated n = 3). Treatment compared to vehicle control using Welch's T-test; * $p<0.05$, ** $p<0.01$, *** $p<0.001$.

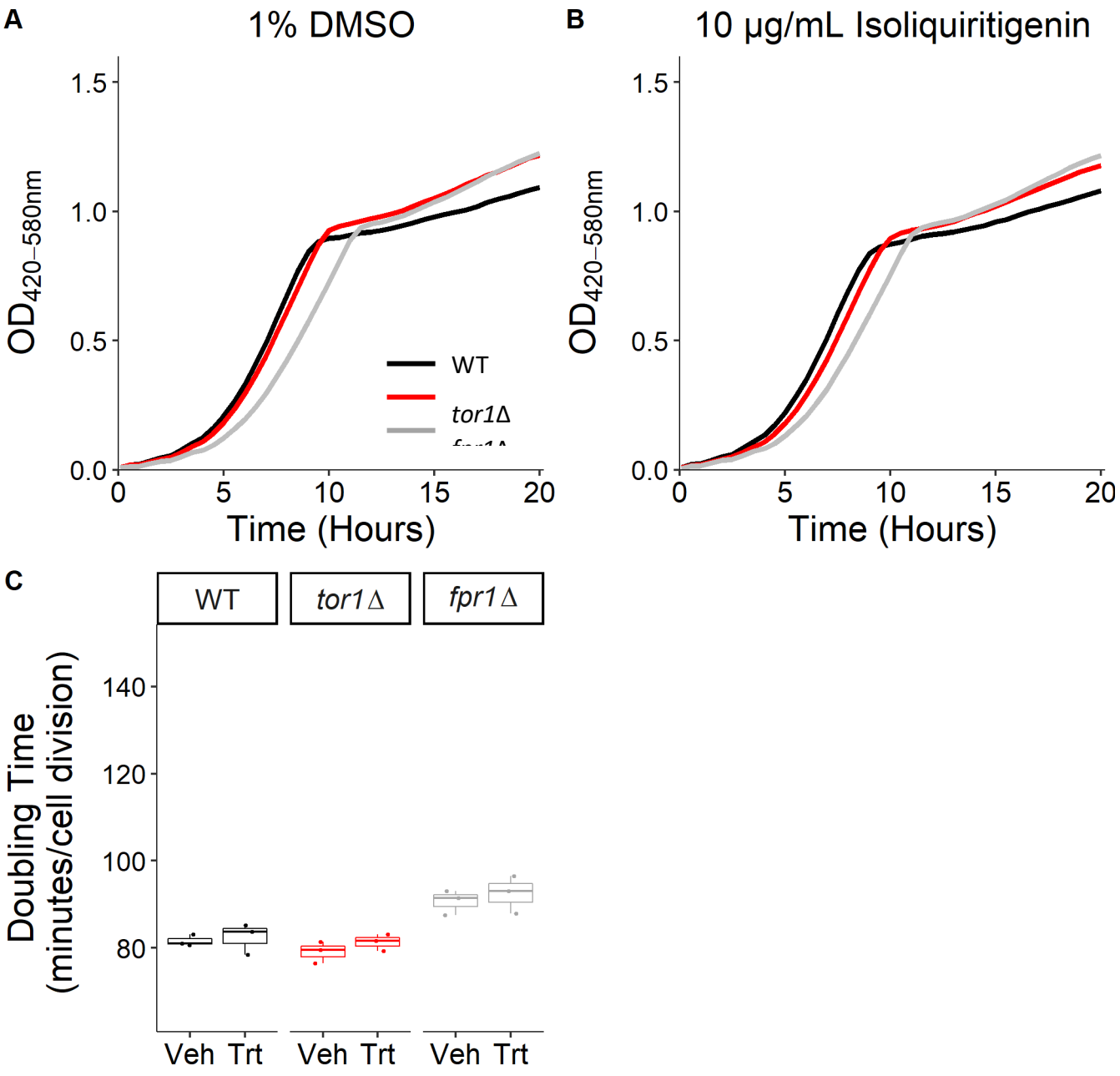

Figure S1-37. **Representative growth curves and doubling times for 10 µg/mL isoliquiritigenin.** Representative growth kinetics of WT, *tor1Δ*, and *fpr1Δ* microcultures at **A)** 1% DMSO and **B)** 10 µg/mL isoliquiritigenin. **C)** Inflection doubling time (DT) of WT, *tor1Δ*, and *fpr1Δ* microcultures. 10 µg/mL isoliquiritigenin does not significantly DT (control n = 3, treated n = 3). Treatment compared to vehicle control using Welch's T-test; * p<0.05, ** p<0.01, *** p<0.001.

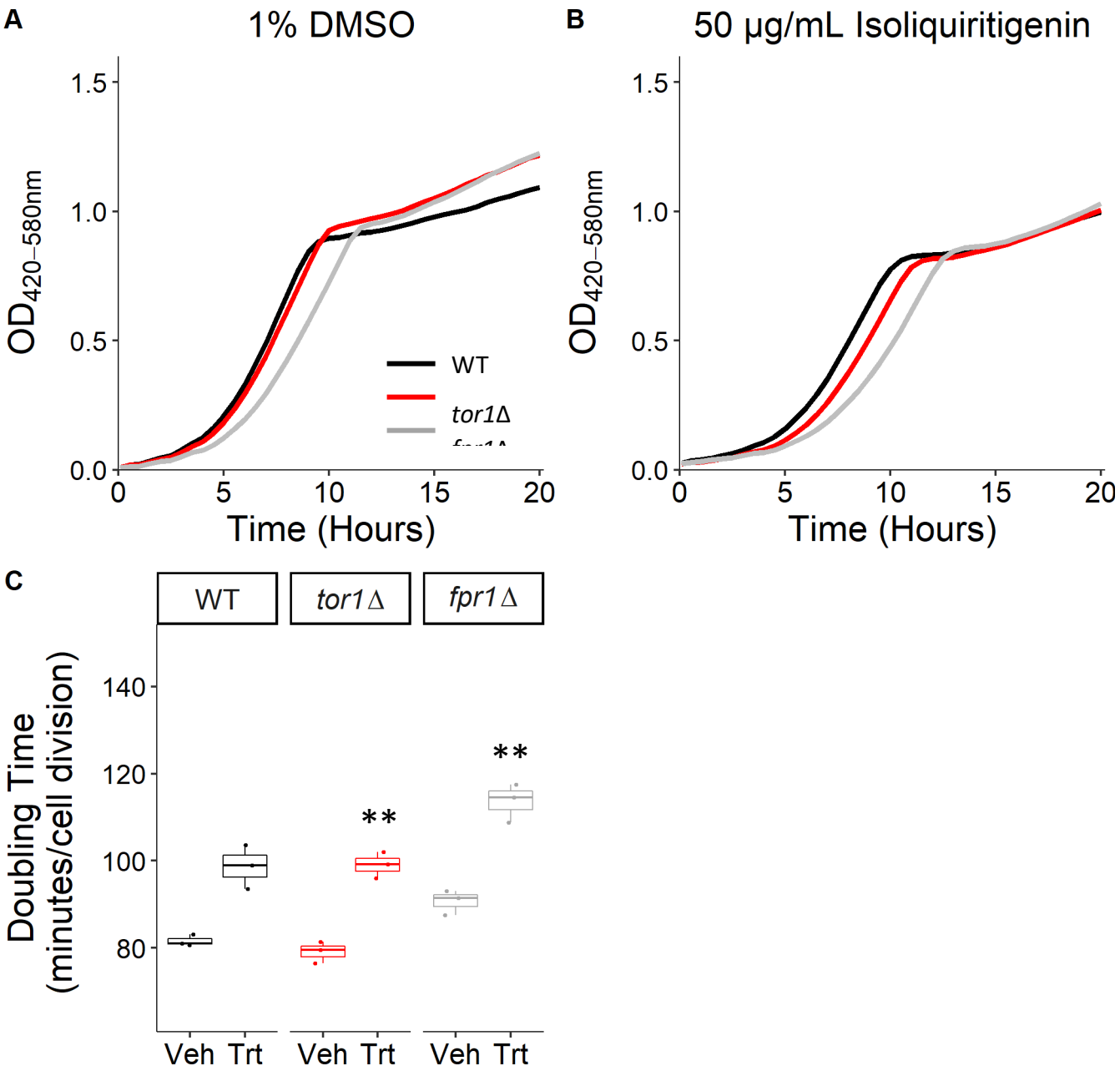

Figure S1-38. **Representative growth curves and doubling times for 50 µg/mL isoliquiritigenin.** Representative growth kinetics of WT, *tor1Δ*, and *fpr1Δ* microcultures at **A)** 1% DMSO and **B)** 50 µg/mL isoliquiritigenin. **C)** Inflection doubling time (DT) of WT, *tor1Δ*, and *fpr1Δ* microcultures. 50 µg/mL isoliquiritigenin significantly increases *tor1Δ* and *fpr1Δ* DT (control n = 3, treated n = 3). Treatment compared to vehicle control using Welch's T-test; * p<0.05, ** p<0.01, *** p<0.001.

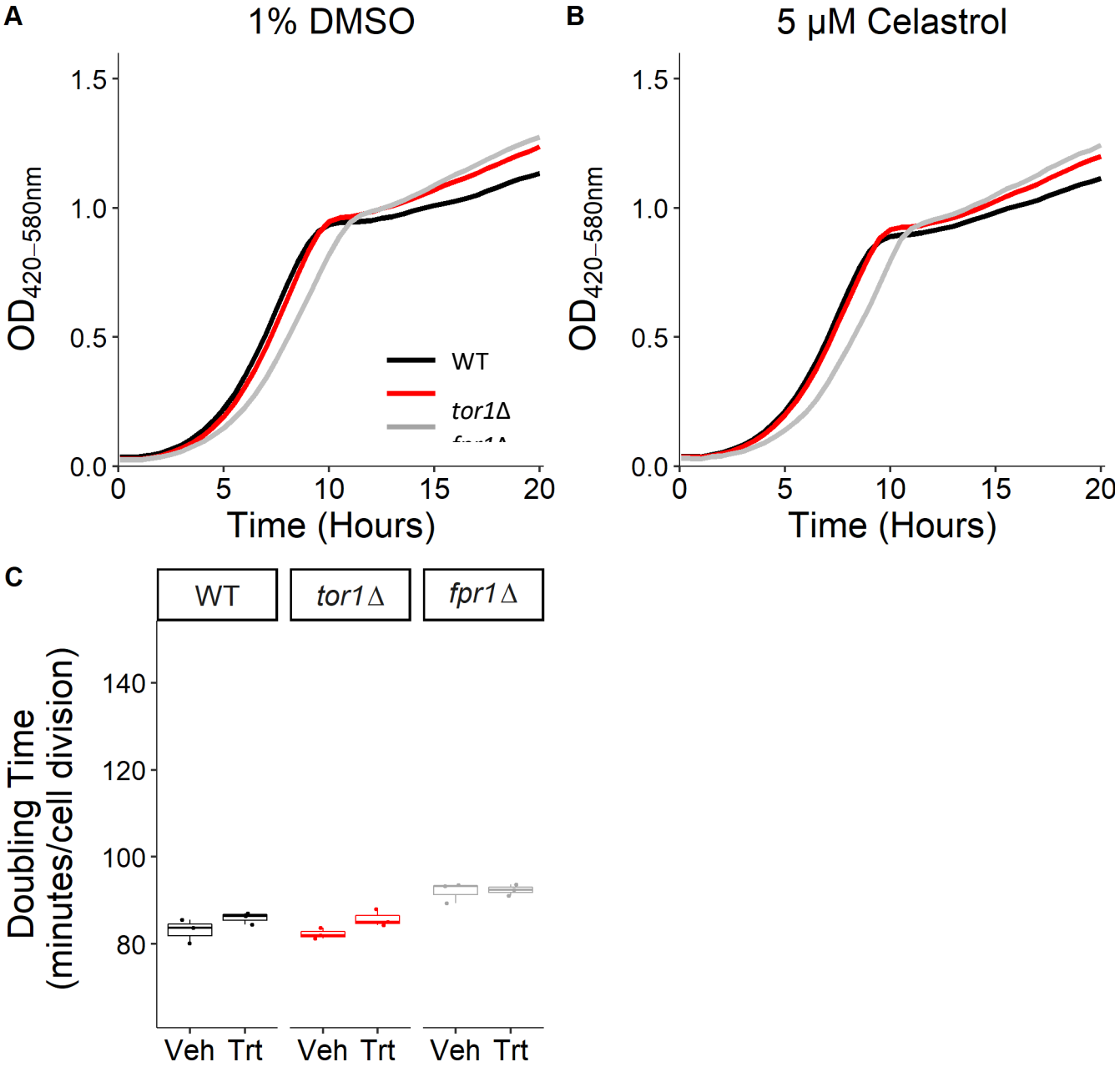

Figure S1-40. **Representative growth curves and doubling times for 5 µM celastrol.** Representative growth kinetics of WT, *tor1Δ*, and *fpr1Δ* microcultures at **A)** 1% DMSO and **B)** 5 µM celastrol. **C)** Inflection doubling time (DT) of WT, *tor1Δ*, and *fpr1Δ* microcultures. 5 µM celastrol does not significantly increase DT (control n = 3, treated n = 3). Treatment compared to vehicle control using Welch's T-test; * p<0.05, ** p<0.01, *** p<0.001.

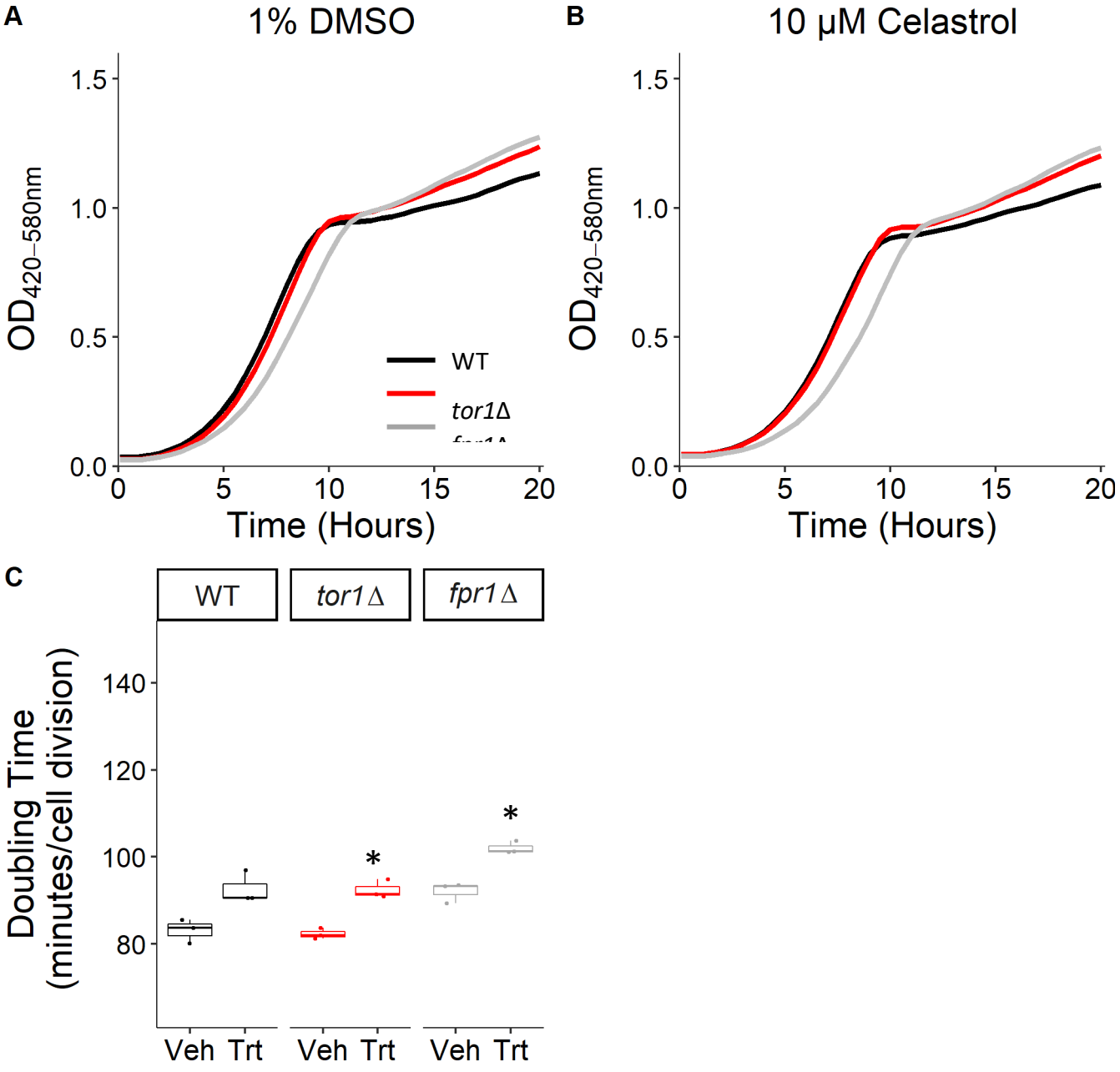

Figure S1-41. **Representative growth curves and doubling times for 10 µM celastrol.** Representative growth kinetics of WT, *tor1Δ*, and *fpr1Δ* microcultures at **A)** 1% DMSO and **B)** 10 µM celastrol. **C)** Inflection doubling time (DT) of WT, *tor1Δ*, and *fpr1Δ* microcultures. 10 µM celastrol significantly increases *tor1Δ* and *fpr1Δ* DT (control n = 3, treated n = 3). Treatment compared to vehicle control using Welch's T-test; * p<0.05, ** p<0.01, *** p<0.001.

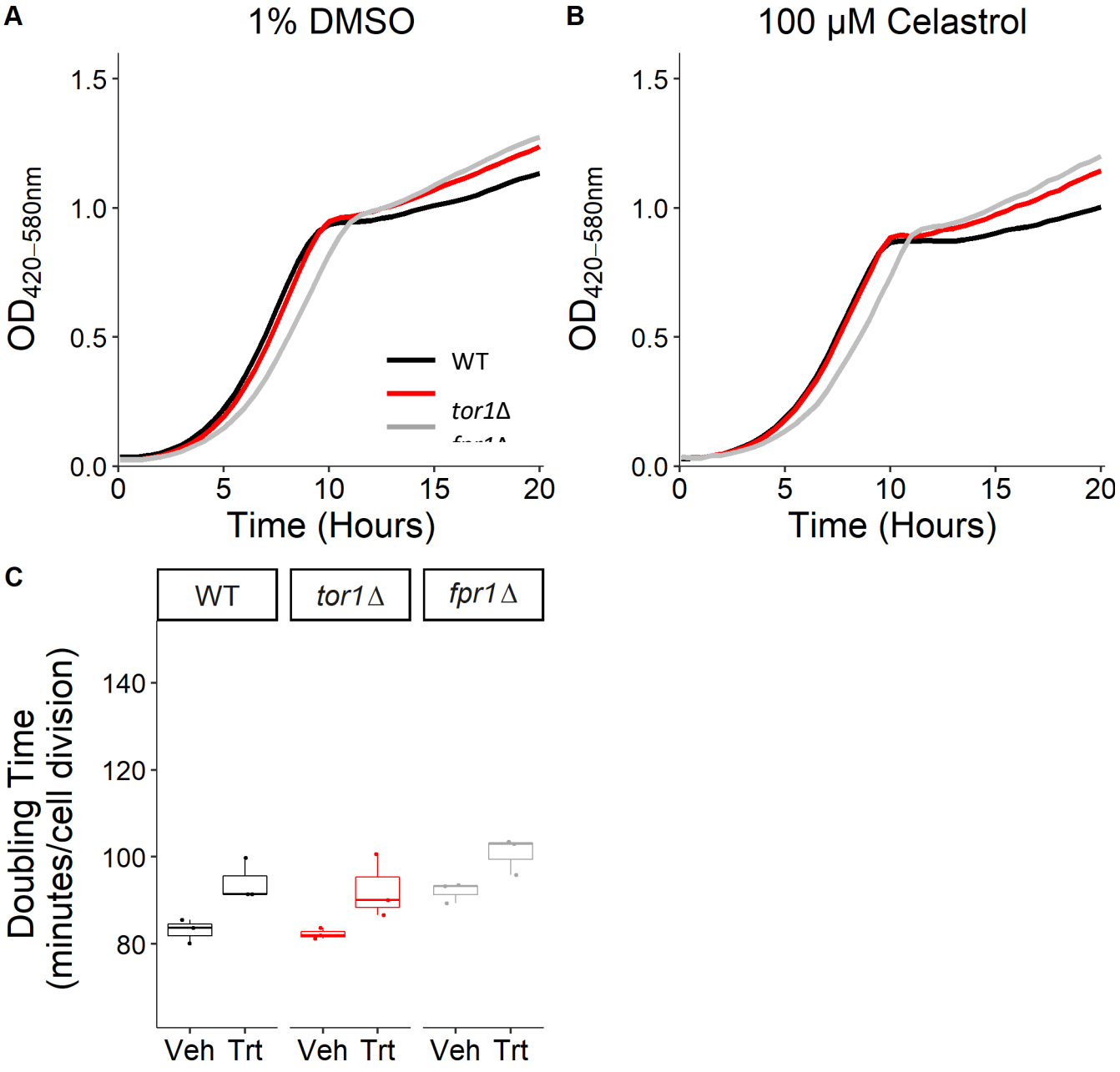

Figure S1-42. **Representative growth curves and doubling times for 100 µM celastrol.** Representative growth kinetics of WT, *tor1Δ*, and *fpr1Δ* microcultures at **A)** 1% DMSO and **B)** 100 µM celastrol. **C)** Inflection doubling time (DT) of WT, *tor1Δ*, and *fpr1Δ* microcultures. 100 µM celastrol does not significantly increase DT (control n = 3, treated n = 3). Treatment compared to vehicle control using Welch's T-test; * p<0.05, ** p<0.01, *** p<0.001.

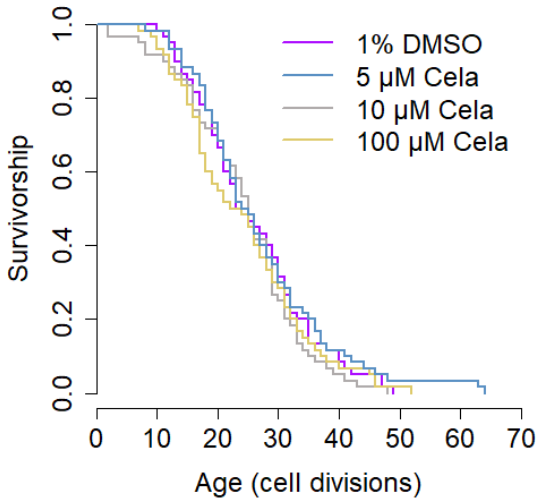

Supplemental Figure 2. RLS dose response for celastrol (BY4741 genetic background). N=60 for each treatment. For number of cells tested and Wilcoxon rank sum p-value, see Table 6.

Chapter 4: Dose-dependent effects of pterostilbene on cellular lifespan and proliferation

Abstract

The advent of the field of geroscience has brought with it significant insights into the connection between aging and disease allowing for the possibility that multiple age-related pathologies could be attenuated by directly modulating biological aging. Invertebrate model organisms have served as a first line of discovery in this area owing to their relatively short lifespans, genetic tractability, and their role in the identification of evolutionary conserved signaling pathways shown to be modulators of aging. The mechanistic Target of Rapamycin (mTOR) signaling pathway has emerged as an important clinical target in this regard with its dysregulation being observed in several pathological conditions, including many cancers, autoimmune disorders, heart failure, neurodegeneration, epilepsy, type 2 diabetes, and autism. Importantly, inhibition of this signaling pathway has been shown to extend lifespan in evolutionary distant organisms suggesting conserved role in longevity regulation. We recently developed a high throughput system to identify candidate TOR inhibitory and pro-longevity compounds in yeast. Leveraging this TOR inhibitory assay and replicative lifespan (RLS) analysis in yeast we have tested a variety of compounds. We recently reported that *Pterocarpus marsupium* extract (PME) extends yeast RLS. Here we describe the lifespan and outgrowth kinetics of pterostilbene treated cells, report on dose-dependent longevity effects, potent cytotoxicity, and a possible role for mitochondrial function in mediating these phenotypes.

Introduction

The advent of the field of geroscience has brought with it significant insights into the connection between aging and disease allowing for the possibility that multiple age-related pathologies could be attenuated by directly modulating biological aging [132, 227]. Invertebrate model organisms have served as a first line of discovery in this area owing to their relatively short lifespans, genetic tractability, and the identification of evolutionary conserved signaling pathways shown to be modulators of aging [19, 228]. As such, interest in identifying interventions that can target these pathways to ameliorate the onset of disease and, potentially, modulate biological aging has increased [229].

mTOR (mechanistic Target of Rapamycin) is a serine/threonine protein kinase and an atypical member of the phosphoinositide 3-kinase (PI3K)-related kinase family. It comprises the catalytic subunit of two functionally distinct protein complexes: mTORC1 (mTOR complex 1) and mTORC2 (mTOR complex 2). mTORC1 functions in numerous cellular processes to promote cell growth and proliferation by mediating the phosphorylation of several downstream effectors enabling the cell to tie environmental nutrient status to cell fate. mTORC2 functions in multiple cellular processes by mediating phosphorylation of several AGC kinase targets: potentiation of mTORC1 signaling via phosphorylation of Akt1; actin cytoskeleton organization via phosphorylation of PKCα/βII; promotion of Na^+ transport via phosphorylation of SGK1. mTORC1 signaling has been well characterized relative to mTORC2 signaling. This is due in large part to the ability to interrogate mTORC1 function via genetic or pharmacological inhibition. Rapamycin is a potent and specific inhibitor of mTORC1 that works by binding to the protein FKBP12 (FPR1 in budding yeast). The FKBP12-rapamycin complex then forms a ternary complex with the mTORC1 catalytic subunit (mTOR) likely resulting in both steric-occlusion of the kinase active site and inhibition of substrate recruitment [21-23]

The mTOR signaling pathway has emerged as an important clinical target with its dysregulation being observed in several pathological conditions, including many cancers [230-235], autoimmune disorders [236, 237], heart failure [238-240], neurodegeneration [241-243], epilepsy [244], type 2 diabetes [245], and autism [246].

mTOR was initially implicated in longevity regulation in the budding yeast *Saccharomyces cerevisiae* when it was found that mutation of mTORC1 substrate S6K1 (*SCH9* in yeast) increased yeast chronological lifespan [30]. Inhibition of mTORC1 has been shown to increase lifespan in yeast [33, 34], nematodes [35], fruit flies [36], and mice [37-39] clearly demonstrating a conserved and central role for mTOR in the regulation of longevity.

One method of lifespan analysis in yeast is the replicative lifespan (RLS) defined as the number of times a daughter cell can bud off from a single mother. Using light microscopy and manually controlled fiber optic needles, individual daughter cells are removed from mother cells on agar plates to determine the replicative lifespan of yeast cells in a variety of environmental conditions. mTOR was discovered as a key regulator of yeast aging in a large-scale RLS analysis of 564 single-gene-deletion strains with the *tor1Δ* extending mean and maximum lifespan by about 20% [27]. Extending this work, the RLS of 4,698 single-gene deletion strains comprising the haploid yeast deletion collection was determined yielding the most comprehensive data set on aging in yeast [87]. Single gene deletions extending lifespan were found to cluster in several functional pathways including the cytosolic and mitochondrial ribosomes and the TCA cycle.

We recently developed a high throughput system to identify candidate TOR inhibitory and pro-longevity compounds in yeast [195]. Utilizing differential growth kinetics of a WT strain, *tor1Δ* mutant and an *fpr1Δ* mutant, the TOR inhibitory status of a compound can be inferred. This system successfully discriminates between first generation allosteric TOR inhibitors like rapamycin and second generation ATP-competitive inhibitors. Leveraging the RLS and TOR inhibitory assays, we have tested a variety of compounds. We recently reported that *Pterocarpus marsupium* extract (PME) extends yeast replicative lifespan [247].

PME is an extract of the heartwood from the Indian kino tree with a long history of use in Ayurvedic medicine. In typical usage a tumbler is made from the heartwood, filled with water, and left to sit overnight. The aqueous preparation is then consumed the following morning. A number of individual compounds have been identified from both aqueous and organic extracts of the heartwood utilizing various techniques [248]. Commonly identified bioactive compounds include the hydroxychalcone

isoliquiritigenin [249-253], the proanthocyanidin epicatechin [249, 250, 254, 255], the flavonol quercetin [249, 250, 256], the alkaloid berberine [249, 250], and the stilbene pterostilbene [249, 250, 252, 253, 255, 257].

Pterostilbene is a natural stilbenoid compound and a dimethylated analog of resveratrol. It is present in foods like blueberries and almonds and is widely available as an unregulated supplement. It has been reported to be more potent and bioavailable than resveratrol and other stilbenes. This is thought to be due to methylation of the phenolic hydroxyls increasing lipophilicity and therefore membrane permeability as well as increasing metabolic stability [258]. Several of these PME constituents have been previously reported to extend lifespan in other model organisms: berberine in mice [185] and flies [259]; quercetin in flies [260] and worms [261, 262]; epicatechin in flies [263]. Here we describe the lifespan and outgrowth kinetics of pterostilbene treated cells, report on dose-dependent longevity effects, potent cytotoxicity, and a possible role for mitochondrial function in mediating these phenotypes.

Results

Pterostilbene inhibits yeast growth independently of mTOR inhibition and can increase or decrease yeast RLS.

We previously reported that PME extends yeast replicative lifespan [264]. Because PME is a plant extract, we wished to resolve which constituents may be conferring the lifespan extending benefit. Epicatechin and quercetin (Figure 1) had no significant effect on lifespan relative to vehicle control when tested at the same dose that PME significantly extends lifespan (100 µg/mL). Both berberine and pterostilbene were toxic at this concentration, and we were unable to perform RLS analysis due to severe growth inhibition. We therefore performed dose response experiments for these two constituents to determine whether lower doses might have positive effects on lifespan. Berberine shortened lifespan at 50 ug/mL and had no effect on lifespan at any of the lower doses tested (Figure 1).

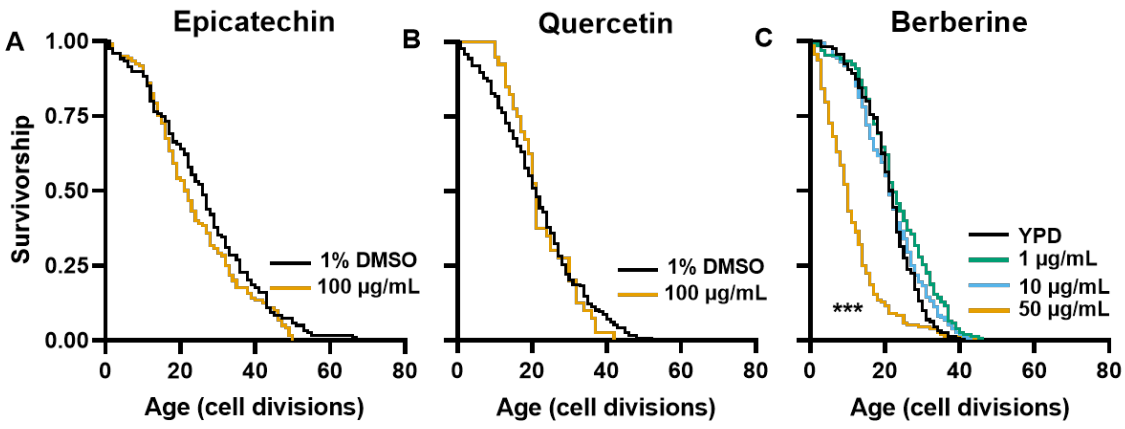

Figure 1. Replicative lifespan (RLS) survival curves for bioactive constituents of Pterocarpus marsupium extract (PME). A)100 µg/mL epicatechin (n = 120) does not significantly alter RLS compared to vehicle control (n = 119) ($p > 0.05$, Wilcoxon rank sum test). **B)** 100 µg/mL quercetin (n = 40) does not significantly alter RLS compared to vehicle control (n = 198) ($p > 0.05$, Wilcoxon rank sum test). **C)** 1 µg/mL (n = 155) and 10 µg/mL (n = 160) Berberine do not significantly alter RLS; 50 µg/mL Berberine (n = 157) significantly reduces RLS compared to YPD control (n = 160) ($p < 0.001$, Wilcoxon rank sum test).

Pterostilbene, in contrast, showed a remarkable dose response profile with respect to lifespan. At doses above 70 μM (~18 μg/mL), pterostilbene significantly reduced lifespan. Interestingly, this effect was reversed at lower concentration, significantly increasing lifespan at both 20 μM (~5 μg/mL) and 40 μM (~10 μg/mL) (**Figure 2**).

While performing the RLS analysis, we noted that cell division times appeared to be significantly extended by pterostilbene in a dose-dependent manner. To quantify this, we assessed the effects of higher dose pterostilbene on yeast growth kinetics using our mTOR inhibitor assay [265]. Doubling time of WT, *tor1Δ*, and *fpr1Δ* microcultures were similarly and significantly increased relative to strain matched vehicle controls (**Figure 3C**). This is inconsistent with the outgrowth kinetic "signature" and doubling times of rapamycin treated cultures (**Figure 3B,D**) suggesting a growth inhibitory mechanism distinct from mTOR inhibition. A comparison of doubling time to lifespan dose-response for pterostilbene indicates a clear relationship between growth inhibition and reduced RLS (**Figure 3E**).

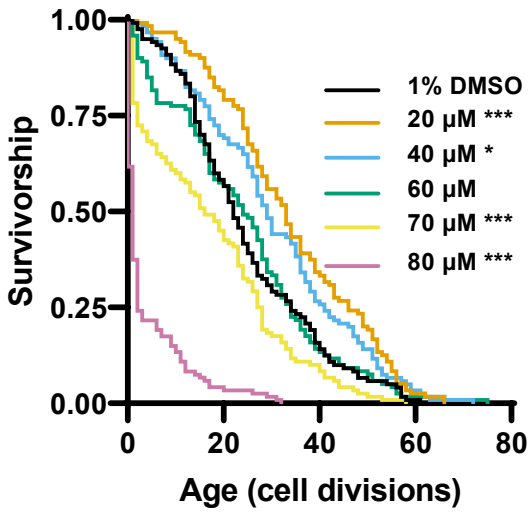

Figure 2. Pterostilbene (PTE) Replicative lifespan (RLS) dose response. 20 and 40 μm PTE significantly extend RLS compared to vehicle control. 60 μM PTE did not significantly alter RLS. 70 μM PTE and 80 μM PTE significantly decreased RLS compared to vehicle control. (Wilcoxon rank sum test, Bonferroni-corrected). For number of cells tested, median lifespans, and p-values, see **Table 1**. *p<0.05, ** p<0.01, *** p<0.001.

High dose pterostilbene inhibits post-diauxic shift growth

While we were unable to obtain RLS data at doses of pterostilbene higher than 80 μM (~21 μg/mL) due to apparent cell cycle arrest in many cells, we observed that some liquid cultures eventually outgrew after a prolonged "lag" period (**Figure 4A**). This extended lag period with undetectable outgrowth exceeded 24 hours at doses above 100 μM (~26 μg/mL) and reached nearly 96 hours at 160 μM (~41 μg/mL).

In addition to the pronounced lag in outgrowth, we also noted a striking "flat lining" phenotype after the diauxic shift, where the maximum optical density of the culture is much lower (~1.0) compared to untreated cells (~1.5) at 160 μM (~41 μg/mL) pterostilbene (**Figure 4A**). We speculated that this may represent a defect in respiratory metabolism in cells treated with high doses of pterostilbene, as the accumulation of biomass after the diauxic shift is primarily a result of a switch from fermentative metabolism to mitochondrial respiration. Consistent with this, an untreated rho^0 strain which has had its mtDNA depleted via exposure to ethidium bromide also displayed the post-diauxic shift "flat line" phenotype (**Figure 4B**). We noted a sudden increase in well-to-well variability in outgrowth kinetics beyond 100 μM PTE (~26 μg/mL). Interestingly, rho^0 cultures only display this well to well variability at 160 μM PTE (~41 μg/mL).

High dose pterostilbene induces mitochondrial instability

To further assess the interaction between mitochondrial function and pterostilbene, we performed a dose response outgrowth experiment in both WT and rho^0 microcultures. As expected, untreated rho^0 cells grow significantly slower than untreated WT cells in YPD. Pterostilbene inhibited growth in a dose-dependent manner in both WT and rho^0 cells. Interestingly, however, the growth inhibition of rho^0 cells was attenuated relative to WT cells such that at doses exceeding ~100 μM (~26 μg/mL) pterostilbene, rho^0 cells actually grew faster than WT cells (**Figure 5**).

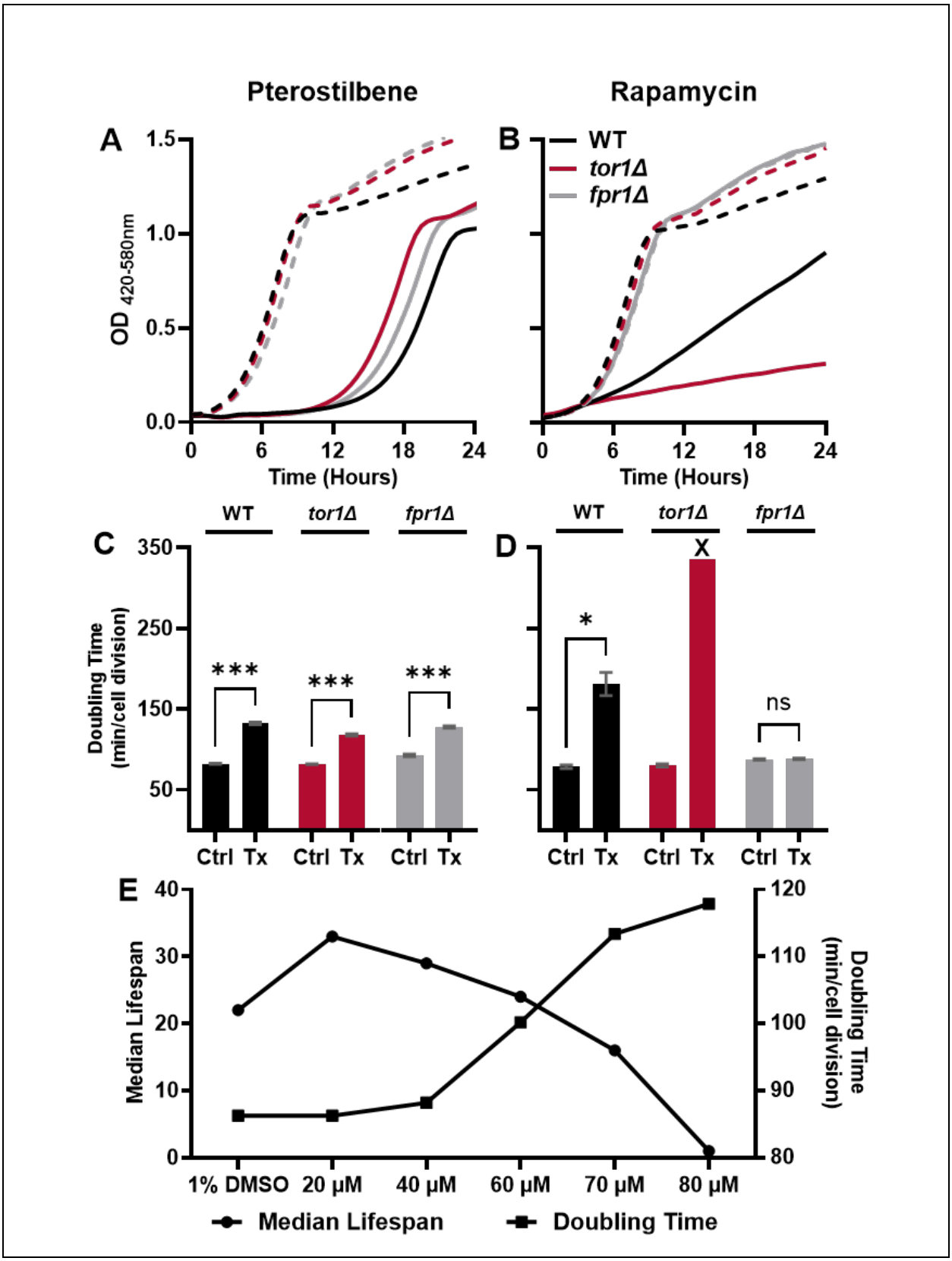
Pterostilbene
Rapamycin
A
B
WT
tor1Δ
fpr1Δ
OD 420-580nm
1.5
1.0
0.5
0.0
0
6
12
18
24
Time (Hours)
C
D
WT
tor1Δ
fpr1Δ
Doubling Time (min/cell division)
350
250
150
50
***
***
***
*
X
ns
Ctrl
Tx
E
Median Lifespan
Doubling Time (min/cell division)
40
30
20
10
0
120
110
100
90
80
1% DMSO
20 μM
40 μM
60 μM
70 μM
80 μM
Median Lifespan
Doubling Time

Figure 3. Representative growth kinetics, doubling times and median lifespans for Pterostilbene (PTE) treated cells. A) Representative growth kinetics of WT, tor1Δ, and fpr1Δ microcultures at 1% DMSO (dashed lines) and 80 μM PTE (solid lines). **B)** Representative growth kinetics of WT, tor1Δ, and fpr1Δ microcultures at 1% DMSO (dashed lines) and 5 ng/mL Rapamycin (solid lines). **C)** Inflection doubling time (DT) of PTE treated WT, tor1Δ, and fpr1Δ microcultures. PTE significantly increases WT, tor1Δ, and fpr1Δ DT (control n = 3, treated n = 3, error bars = SEM). **D)** Inflection doubling time (DT) of Rapamycin treated WT, tor1Δ, and fpr1Δ microcultures. Rapamycin significantly increases WT and tor1Δ but not fpr1Δ DT (control n = 3, treated n = 3, error bars = SEM). Treatment (Tx) compared to strain matched vehicle control (Ctrl) using Welch's T-test; X = doubling time could not be calculated due to limited growth, indicated by OD ≤ 0.3 after 20 h. * $p<0.05$, ** $p<0.01$, *** $p<0.001$. **E)** PTE RLS dose response median lifespans (left axis, circles) and DT (right axis, squares).

To determine whether the post-diauxic shift flat lining was an inherited or a transient effect of pterostilbene exposure, we conducted an experiment exposing cells to high dose pterostilbene. Once these cultures outgrew and displayed the post-diauxic shift "flat lining" they were used as inoculum in a subsequent experiment lacking pterostilbene. There was no lag phase extension observed however, the post-diauxic shift "flat lining" persisted. Cultures that display the post-diauxic shift flat-lining are also unable to grow on plates containing glycerol as the primary carbon source indicating an inability to proliferate when forced to respire.

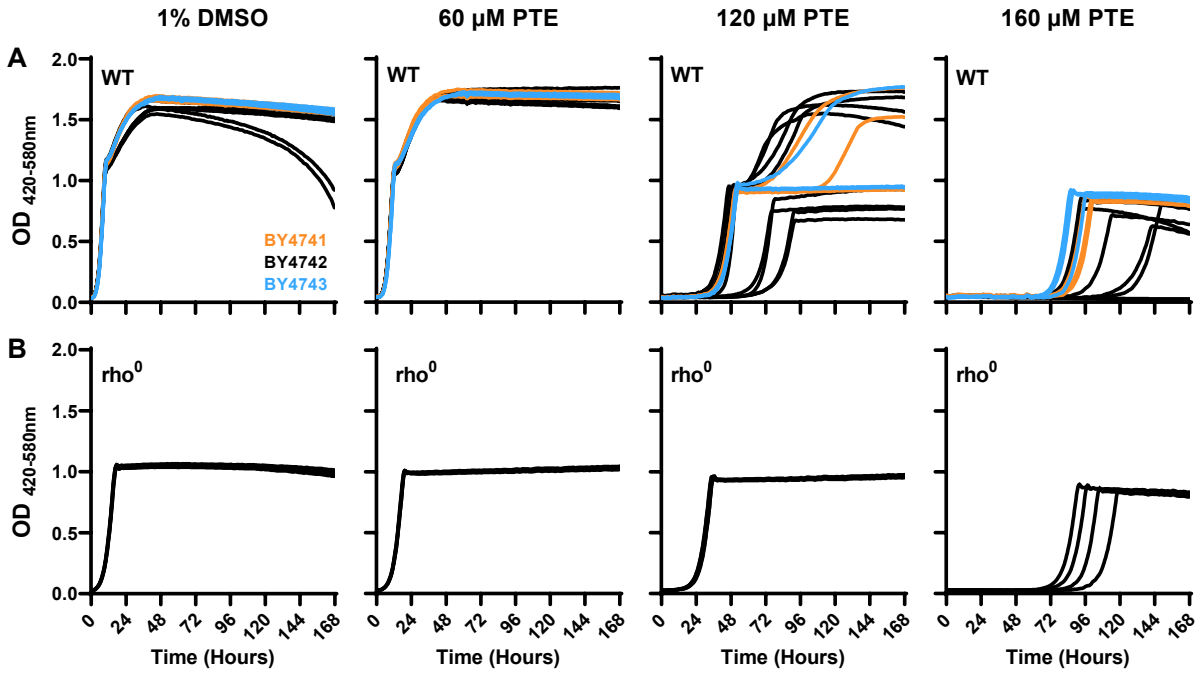

Figure 4. Representative growth kinetics for Pterostilbene (PTE) treated microcultures. A) Representative growth kinetics of BY4741 (orange, n = 3), BY4742 (black, n = 8) and BY4743 (blue, n = 3) WT cultures treated with 60 µM, 120 µM, 160 µM PTE or 1% DMSO. **B)** Representative growth kinetics of rho0 cultures treated with 60 µM, 100 µM, 120 µM, 160 µM PTE or 1% DMSO (n = 4 for all doses).

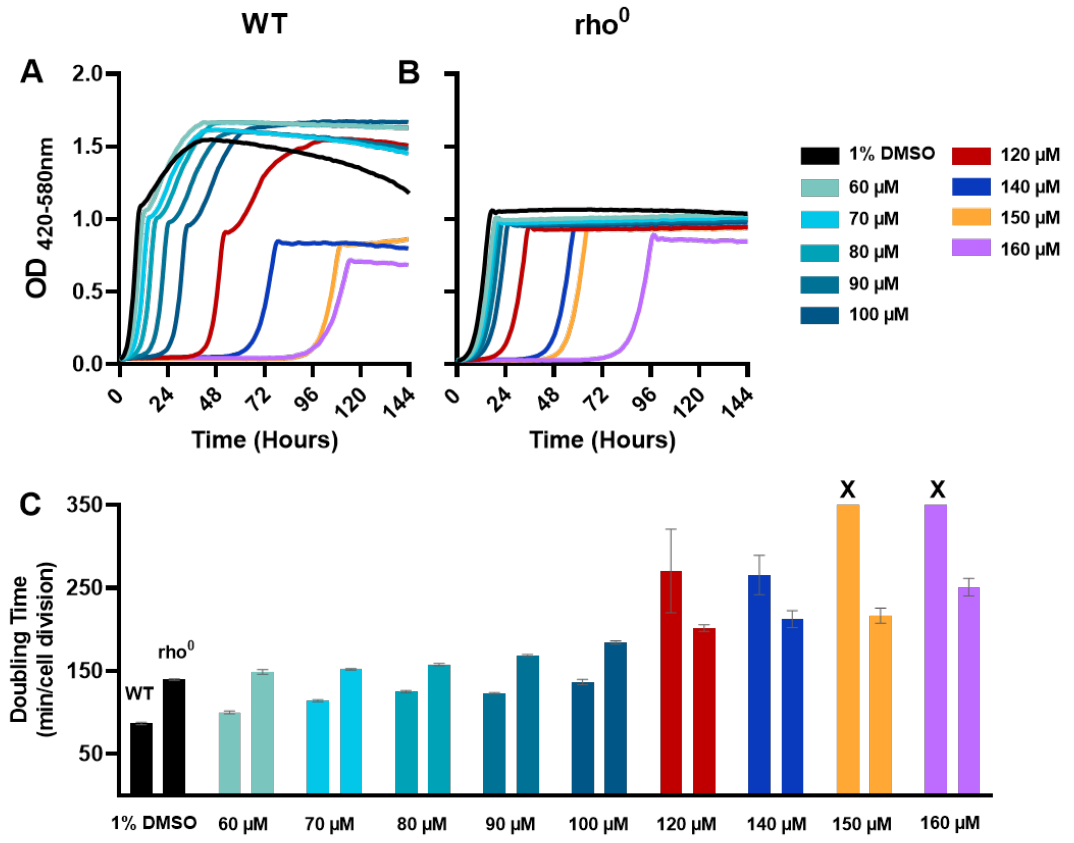

Figure 5. Doubling times and representative growth kinetics for Pterostilbene (PTE) treated microcultures. Representative growth kinetics of **A)** WT and **B)** rho0 cultures treated with 60, 70, 80, 90, 100, 120, 140, 150, and 160 µM PTE or 1% DMSO. **C)** Inflection DT for PTE treated WT (n = 5) and rho0 (n = 4) cultures. Error bars indicate SD. X denotes doubling time not reliably calculated due to lack of growth.

Pterostilbene treatment results in dose dependent cytotoxicity

We conducted time-course flow cytometric analysis of yeast cultures exposed to 80 (~21 µg/mL) or 160 µM (~41 µg/mL) pterostilbene to investigate effects on cell cycle dynamics (Sytox green staining) and cell viability (Propidium iodide and Syto9 staining). These experiments revealed unexpected and rapid cytotoxicity in both WT and rho^0 cells occurring within 1 hour of treatment (**Figure 6**). Consistent with the observation that growth inhibition of pterostilbene treated rho^0 cells is attenuated relative to WT

cells (Figure 5), cytotoxicity of pterostilbene treated rho^0 cells is attenuated relative to dose matched WT cells (Figure 6).

Cell cycle dynamics of untreated WT and rho^0 cells revealed an expansion of the G1 cell population between 4 and 24 hours. This G1 expansion is pronounced in rho^0 cells relative to WT control. The timing of this expansion in the vehicle samples is consistent with typical exit from log phase growth and induction of fermentative growth. On treatment with 80 μM (~21 μg/mL) pterostilbene rho^0 cell cycle dynamics remain largely unaffected relative to DMSO control. This is in contrast to WT cell cycle dynamics at the same dose where G1 expansion is ostensibly delayed until the cytotoxic effect begins to wane (Figure 6). Both WT and rho^0 cells treated with 160 μM (~41 μg/mL) pterostilbene display pronounced and rapid cytotoxicity however this effect is attenuated in rho^0 cells. At this dose cell cycle dynamics remain similar to early control conditions in both strains for the duration of the experiment suggesting a pterostilbene mediated delay in cell cycle transit. Subsequent experiments in WT cells support this notion with clear indications that cell cycle dynamics remain static on pterostilbene treatment until cytotoxicity begins to wane after which G1 expansion is observed (Supplemental Figure 1).

To validate the pronounced cell toxicity observed in the flow cytometry experiments we conducted colony forming unit assays on WT and rho^0 cells. Cultures were exposed to 10, 40, 80 or 160 μM pterostilbene then plated at 15 min, 1 hour and 24 hour timepoints. WT and rho^0 cultures displayed no growth on YPD plates after 15 minutes of exposure to 160 μM pterostilbene confirming the rapidity of the cytotoxic effect (Supplemental Figure 2).

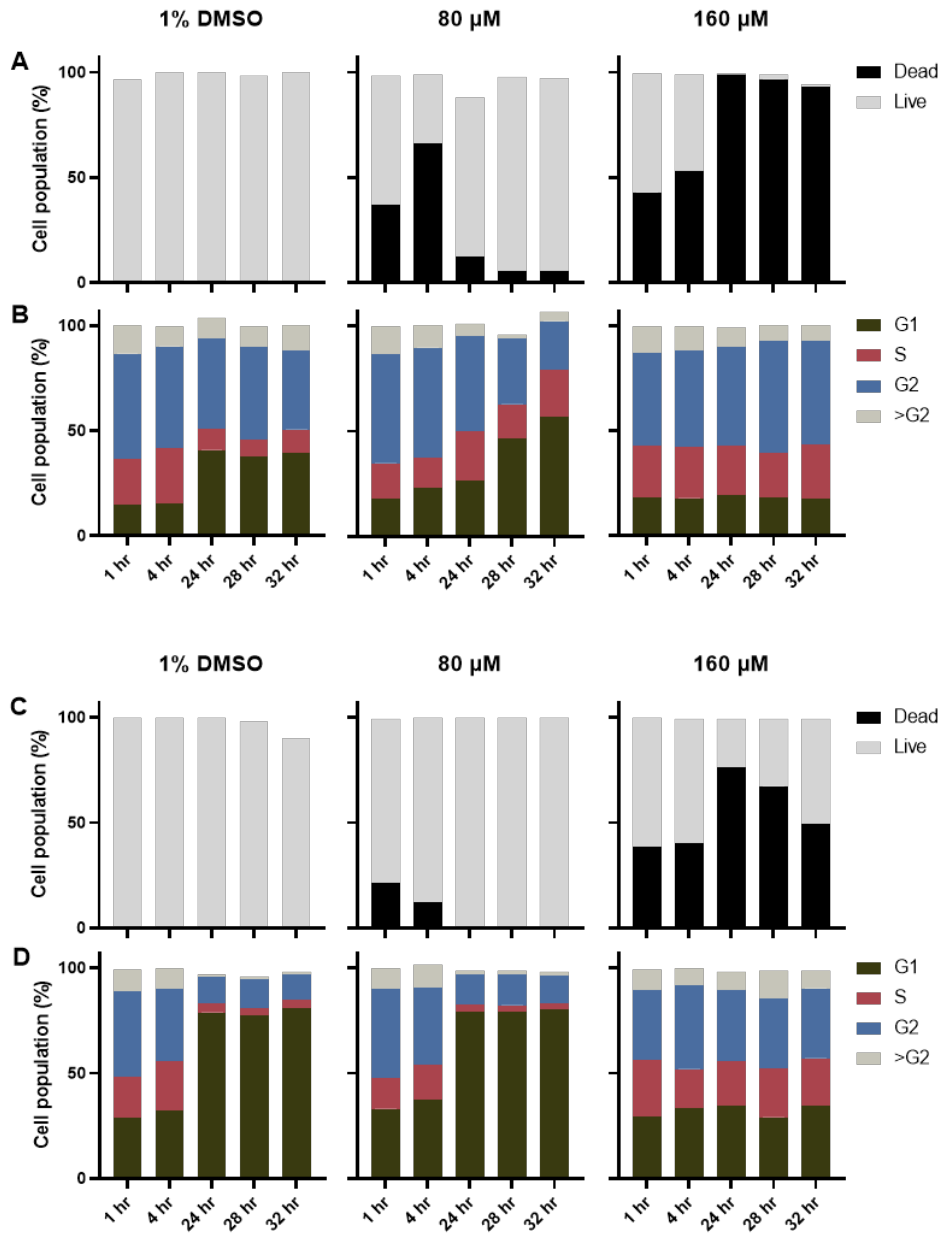

Figure 6. Cell viability and cell cycle dynamics of Pterostilbene treated cells. A) Live/dead frequencies and **B)** cell cycle dynamics of WT cells treated with 1% DMSO, 80 µM or 160 µM PTE. **C)** Live/dead frequencies and **D)** Cell cycle dynamics of rho0 cells treated with 1% DMSO, 80 µM or 160 µM PTE. PTE treatment results in acute, dose dependent cytotoxicity concomitant with cell cycle transit delay relative to vehicle control. These effects are somewhat attenuated in rho0 cells.

Discussion

We previously identified PME as a longevity extending intervention in yeast [264]. PME is a plant extract with a long history of use in Ayurvedic medicine. As a plant extract PME contains a number of phytochemicals one or more of which ostensibly contributes to its lifespan extending benefit in yeast. Berberine was recently identified as a constituent of PME [249, 250]. Other commonly identified components of PME include epicatechin [249, 250, 254, 255], isoliquiritigenin [249-253], quercetin [249, 250, 256], and pterostilbene [249, 250, 252, 253, 255, 257]. We found that pterostilbene can increase or decrease yeast replicative lifespan in a dose dependent fashion.

Pterostilbene has been previously reported as an inhibitor or attenuator of mTOR signaling in various human cell line models including human umbilical vein endothelial cells (HUVECs) [266], human bladder cancer cells [267], and breast cancer cells [268]. Pterostilbene did not suppress yeast growth in a manner consistent with known mTOR inhibitors in our growth kinetic assay. This may reflect differences in pterostilbene activity between human cell lines and yeast, as we previously reported that certain ATP competitive mTOR inhibitors that robustly inhibit mammalian cell proliferation do not show similar growth inhibition in yeast using our system [265]. It is also possible that pterostilbene acts to indirectly inhibit mTOR by acting on upstream components of the pathway that do not have yeast equivalents.

The acute cell toxicity observed at higher doses of pterostilbene may serve to explain the dramatic reduction in lifespan at 80 μM and above. It is worth noting however, that cells that die immediately in response to a drug treatment are not included in the RLS assay, so the reduction in RLS from 80 μM pterostilbene cannot be solely explained by acute lethality of the treatment.

Unexpectedly, we observed that cells grown in higher doses of pterostilbene display a “flat-line” phenotype after the diauxic shift in the outgrowth experiments, which we interpreted as inhibition of mitochondrial respiration. This was confirmed genetically using rho^0 cells lacking mitochondrial DNA, which were unexpectedly somewhat resistant to the growth inhibitory effects of pterostilbene. Pterostilbene exposure only consistently resulted in this flat-line phenotype at doses exceeding 120 μM. This led us to consider two possibilities: that pterostilbene was directly inhibiting mitochondrial respiratory

capacity or that pterostilbene treatment was selecting for respiratory-deficient cells, or both. Growth kinetic analysis revealed that the cells persisting in the pterostilbene culture after outgrowth are permanently respiratory deficient, consistent with pterostilbene selecting for survival of respiratory-deficient cells. Interestingly, rho^0 cells are slightly resistant to pterostilbene mediated growth inhibition as well. One plausible explanation for these observations is that pterostilbene is causing cells to lose mitochondrial DNA during the prolonged “lag phase”, which results in a rho^0 state that is then able to outgrow.

Flow cytometry revealed a rapid and pronounced dose dependent cell toxicity in pterostilbene treated cells. While this toxicity was observed in both WT and rho^0 cells, the effect was attenuated in the rho^0 cells and was concomitant with an observable delay in cell cycle transit. Untreated cells displayed an expansion of the G1 population the timing of which is consistent with induction of normal fermentative growth. Treated cells displayed a dose dependent delay in cell cycle transit that abated only when the toxicity began to wane.

Natural stilbenes like pterostilbene are secondary metabolites generated by plants to protect against stressors such as phytopathogenic fungal/bacterial infection, insect attacks and UV irradiation among others [269]. This could explain the toxicity observed in our yeast-based system. However, a number of *in vitro* studies have reported cytotoxic [270-277] and genotoxic [270-272, 278-280] effects of pterostilbene in both cancer and non-cancerous human cell lines. Generally, pterostilbene was reported to induce dose-dependent cytotoxic effects in various cancer cell lines in a range of 25-100 μM. Data in non-cancerous cell lines is sparse, however reductions in cell viability have been observed [281]. Contrasting with these data are reports that pterostilbene use in murine models is not toxic as well as a clinical trial in humans [282, 283].

As a polyphenol, pterostilbene is already a part of the human diet. It is also on the market as a widely available, unregulated supplement and has been investigated as a chemosensitizer in cancer cell models indicating research interest in its use as a cancer adjuvant. Additionally, the use of stilbenes as natural preservatives is a growing area of interest as synthetic preservatives are increasingly rejected by consumers potentially increasing general consumption of this class of polyphenols [281]. Available data

suggests that pterostilbene is well tolerated *in-vivo* with little effect on measured biochemical or physiological markers [282, 283]. However, there are virtually no studies investigating the cytotoxic and genotoxic effects that have been observed in cell culture models *in-vivo*. This disconnect between *in vitro* and *in vivo* studies is particularly relevant as pterostilbene has been shown to decrease human melanoma growth (murine model) *in vivo* while the same dose detected in the tumor had no effect on growth *in vitro* [284].

There have been multiple reports of stilbenes like resveratrol inhibiting the activity of various cytochrome p450 isoenzymes (CYPs). The CYP superfamily plays a key role in drug metabolism [285]. Inhibition of these enzymes can alter the pharmacokinetics of administered drugs resulting in strong effects on drug plasma or tissue concentrations potentially resulting in serious toxic side effects [286]. The CYP3A subfamily, especially the CYP3A4, is responsible for metabolizing a broad range of drugs including a large number of anti-cancer medicines [287]. Pterostilbene has been shown to dose dependently attenuate CYP3A4 activity *in vitro* however strong inhibition as was seen with other stilbenes including resveratrol was not observed [288, 289]. Pterostilbene has also been shown to strongly inhibit enzymatic activity of some members of the CYP2C subfamily [288, 289]. While toxicity studies have demonstrated that pterostilbene is tolerated *in vivo*, *in vitro* evidence suggests that unregulated pterostilbene supplementation may increase the risk for unwanted toxic side effects in people ingesting certain medications.

Materials and Methods

Yeast strains and culture conditions

Yeast strains used were in the BY4741 (MATa his3Δ1 leu2Δ0 met15Δ0 ura3Δ0), BY4742 (MATα his3Δ1 leu2Δ0 lys2Δ0 ura3Δ0), and BY4743 (MATa/α his3Δ1/his3Δ1 leu2Δ0/leu2Δ0 LYS2/lys2Δ0 met15Δ0/MET15 ura3Δ0/ura3Δ0) genetic backgrounds and have been previously described [195]. For overnight culture and growth analysis, YPD (1% w/v Bacto™ yeast extract (BD), 2% w/v Bacto™ peptone (BD), 2% w/v dextrose) media was used. Yeast was cultured at 30 °C for all experiments.

Outgrowth Analysis

Analysis of maximal growth rate in yeast strains was performed to characterize growth-inhibition of pterostilbene using a Bioscreen C MBR (Growth Curves USA, Piscataway NJ, USA) as previously described [195]. Raw optical density data were smoothed using the R package “smooth.spline.” Doubling times were calculated using the inflection method—identifying the maximum semi-log slope along growth curves within the optical density range linearly correlated with a number of yeast cells—with the online web tool Yeast Outgrowth Data Analyzer (YODA)[129]. All experiments were repeated with at least three biological replicates. The number of biological replicates is indicated in each figure caption. Doubling time was calculated for all cultures where OD ≥ 0.3 after 20-h growth. Otherwise, culture was listed as no growth (NG). Welch’s (unequal variance) t-test with Bonferroni multiple testing correction was used to assess differences relative to experiment-matched vehicle control cultures using R. We applied multiple testing correction using the p.adjust function.

Replicative lifespan analysis

A modified RLS protocol for treatments was developed based on previously described methods [196, 197]. Briefly, cells were grown on freshly prepared YPD plates at 30 °C until single colonies were visible.

Cells were selected from a single colony and lightly patched onto YPD plates supplemented with the designated treatment or vehicle overnight. In the morning, founder cells were aligned and selected as newborn daughter cells using a micromanipulator. Cells were monitored for cell divisions every 90–120 min, and subsequent budded daughter cells were separated and removed as they formed. The process continued until cells stopped dividing. Replicative lifespan was calculated as the number of times each mother cell divided before it underwent permanent cell cycle arrest. Plates were kept in the refrigerator at 4 °C overnight. Plates were kept wrapped in tinfoil except while being dissected to avoid potential light sensitivity of any pterostilbene. All experimenters were blinded to the identity of any of the treatments at the time of dissection. Cells were dissected in groups of 20 and 20-60 cells dissected for each condition tested.

Flow Cytometry

All flow cytometry experiments were conducted in the University of Washington Pathology Flow Cytometry Core Facility using a BD FACSCanto™ II. Forward angle, 90°-side scatter (FSC and SSC) and fluorescence signals were accumulated. The fluorescence signals (pulse area measurements) were screened by a 530/30 nm band-pass filter for SYTOX Green and SYTO 9 and a 670 nM long-pass filter for Propidium Iodide. Instrument calibration and gating were performed as previously described [290].

Table 1. Median RLS (95% confidence intervals), number of cells dissected (n), percent change, and p-value (Wilcoxon rank sum test, Bonferroni-corrected p-value for multiple testing and uncorrected p-value in parentheses) of Pterostilbene compared to vehicle (1% DMSO) control.

Treatment	Concentration	n	Median RLS (95% CI)	% change	Bonferroni-corrected p-value (uncorrected)
DMSO	1%	120	22 (20-25)	-	-
Pterostilbene	20 μM (~5 μg/mL)	120	33 (33-36)	50.0	< 0.001 (< 0.001)
Pterostilbene	40 μM (~10 μg/mL)	120	29 (27-35)	31.8	0.025 (0.005)
Pterostilbene	60 μM (~15 μg/mL)	120	24 (19-28)	9.1	1 (0.763)
Pterostilbene	70 μM (~18 μg/mL)	120	16 (12-23)	-27.3	< 0.001 (< 0.001)
Pterostilbene	80 μM (~21 μg/mL)	120	1 (1-1)	-95.5	< 0.001 (< 0.001)

Supplemental Figures

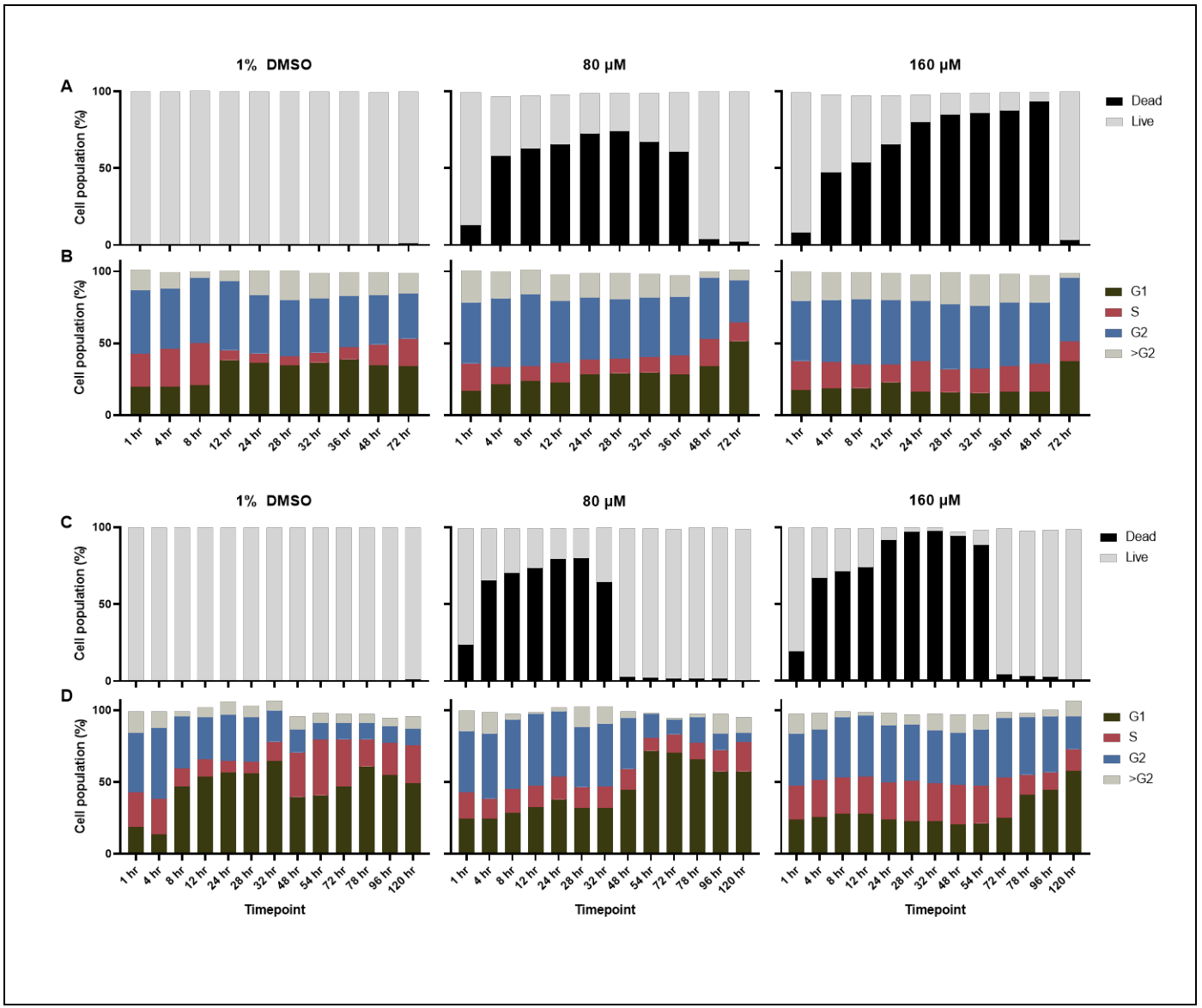

Supplemental Figure 1. Cell viability and cell cycle dynamics of Pterostilbene (PTE) treated cells. A) Live/dead frequencies and **B)** Cell cycle dynamics of WT cells treated with 1% DMSO, 80 μM or 160 μM PTE in a 72 hour experiment. **C)** Live/dead frequencies and **D)** Cell cycle dynamics of WT cells treated with 1% DMSO, 80 μM or 160 μM PTE in a 120 hour experiment. PTE treatment results in acute, dose dependent cytotoxicity concomitant with cell cycle transit delay relative to vehicle control.

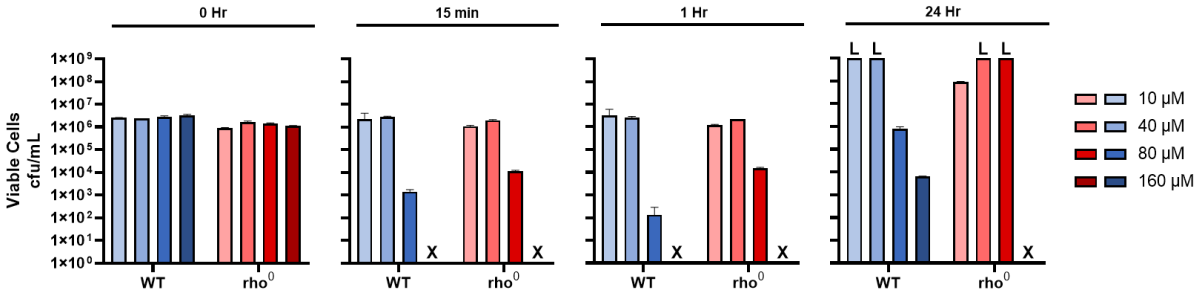

Supplemental Figure 2. Cell viability of pterostilbene (PTE) treated cells. Colony forming unit assay reveals PTE mediated cytotoxicity occurs within 15 minutes of exposure in both WT and rho0 cells. Rho0 cells are somewhat resistant to this effect. X denotes no growth; L denotes a lawn. Error bars indicate SD.

Chapter 5: Conclusion

Over the last century advances in modern medicine have facilitated stunning increases in life expectancy with the global average rising to 72 years in 2020. Longer life is concomitant with a period of decline in the later years characterized by the onset and progression of multiple age associated diseases resulting in reduced quality of life. As a field, geroscience is focused on elucidating the molecular mechanisms of biological aging. Identifying pharmacological interventions that directly target these molecular mechanisms thereby increasing healthspan and lifespan is a growing area of research [229]. The mTOR signaling pathway has emerged as an important clinical target in this regard.

Rodent models are a widely used standard in terms of translatability to human aging. For example, the Interventions Testing Program (ITP) is a multi-site program designed to identify agents that extend lifespan and healthspan in mice. Programs like this are crucial in establishing the translatability of putative longevity promoting compounds. However, rodent lifespan averages ~3 years making this model less than ideal for compound *discovery*. In this context, leveraging invertebrate model systems for compound discovery makes sense given the conserved nature of nutrient sensing pathways involved in longevity regulation, their genetic tractability, and relatively short lifespans. Indeed, much of our understanding of aging biology comes from the use of invertebrate model systems. Utilization of invertebrate systems for compound discovery enables less time consuming, higher throughput experiments. This, in turn helps to advance the field as it opens up the possibility for screening large numbers of compounds for longevity effects at relatively low cost with the added benefit of serving programs like the ITP with evidence-based candidate pro-longevity compounds. Despite the fact that lifespan and screening studies in yeast are less expensive and less time consuming than studies in rodents, roundworms or fruitflies, utilization of this system has lagged. This is evidenced by the fact that 48.5% of experiments contained in the DrugAge database are performed in *C. elegans* and 30% of experiments in the database are performed in *D. melanogaster* while yeast based studies make up only 2.4% of studies.

This thesis presents a novel, high-throughput method of identifying candidate pro-longevity compounds that will advance the use of *S. cerevisae* in the context of aging biology research. We first

present the development of a yeast-based growth assay to identify putative mTOR inhibitors that is sensitive enough to discern between allosteric and ATP-competitive modes of inhibition. We then leverage this system along with replicative life-span analysis to identify putative longevity compounds in a screen of natural products and natural product mixtures identifying *Pterocarpus marsupium* extract (PME) as a pro-longevity compound mixture. Finally, we investigate the effects on yeast growth and lifespan of a group of compounds found to be constituents of PME.

While the material presented herein demonstrates the potential of leveraging a yeast based system for drug discovery, there are notable drawbacks in the utilization of this system stemming from biological constraints imposed by the use of *S. cerevisiae* as a model organism. We have observed two instances where our yeast based system does not properly resolve known ATP-competitive mTOR inhibitors identified as such in mammals. This is consistent with a previous report observing differential sensitivity between and yeast and mammals [291]. This discrepancy is likely due to sequence differences between mammalian and yeast proteins. ATP-competitive mTOR inhibitors bind the mTOR kinase ATP-binding site. In mTOR this structure is characterized by a hydrophobic cleft in which kinase inhibitors form hydrogen bonds with various residues. Previous studies have established that the differential sensitivity of ATP-competitive mTOR inhibitors within a single model system arise from differential binding affinity to the ATP-binding site [23]. This limitation does not preclude the use of this system for drug discovery but does indicate that further testing, in mammalian cell culture for example, may be warranted in some cases prior to making a determination of mTOR inhibitory status.

Sirtuins are a family of protein deacetylases homologous to the yeast silent information regulator (SIR) 2. Increased expression of Sir2 orthologs is sufficient to extend lifespan in yeast, worms, and flies [292]. Interest in sirtuins as anti-aging drug targets stems partly from the observation that the stilbene resveratrol activates Sir2 *in-vitro* and that resveratrol treatment has been reported to increase lifespan in yeast, worms and flies [293]. These claims were widely spread in popular media where red wine was touted as healthy because it contained resveratrol, glazing over the fact that sirtuin biology is complex and the effects of sirtuin activation may be tissue or context dependent. In yeast, Sir2 overexpression increases replicative life span but shortens chronological lifespan [294]. Additionally, the initial reports of

Sir2-dependent life-span extension from resveratrol in yeast, worms and flies have been difficult to replicate [295]. *In-vivo,* different labs have reported that resveratrol can activate, inhibit or have no effect on sirtuins. Resveratrol is also reported to have numerous molecular targets making it difficult to identify a dominant mechanism of action.

Pterostilbene is an analog of resveratrol that has been touted as more effective than resveratrol due to its increased bioavailability. In keeping with the conflicting observations seen on resveratrol treatment, we find that pterostilbene can increase or decrease yeast replicative lifespan. The mechanism by which pterostilbene effects lifespan is not known. A next step in this regard would be to test the effects of pterostilbene on sir2delta cells. Additionally, pterostilbene rapidly induces potent cytotoxicity at higher doses and inhibits yeast growth at doses that also extend cellular life span.

The story of resveratrol is a cautionary tale that should inform how we move forward with pterostilbene. Pterostilbene is an example of an attractive putative anti-aging drug that could possibly do harm in the wrong context (i.e. patients taking certain medications).

The most exciting next step is the continued search for novel mTOR inhibitors. Rapamycin was first isolated from a soil sample on Rapa Nui (Easter Island). Our group has developed a yeast based assay to identify novel mTOR inhibitors. Screening libraries of already approved compounds is the lowest hanging fruit in this regard. However, the more exciting alternative in my opinion is to screen libraries of compounds isolated from plant and animal sources in a sort of bench chemist to bench scientist pipeline.

Bibliography

1. Riley, J.C., *Estimates of Regional and Global Life Expectancy, 1800–2001.* Population and Development Review, 2005. **31**(3): p. 537--543. PMID or DOI: 10.1111/j.1728-4457.2005.00083.x.
2. United Nations Department of Economic and Social Affairs, P.D., *World Population Prospects 2022: Summary of Results*. UN DESA/POP/2022/TR/NO.3.
3. Niccoli, T. and L. Partridge, *Ageing as a Risk Factor for Disease.* Current Biology, 2012. **22**(17): p. R741--R752. PMID or DOI: Anonymous:c37.
4. *65+ in the United States: 2010*, U.S.C. Bureau, Editor. 2014, U.S. Government Pritning Office: Washington, DC.
5. Roberts, A.W., Stella U. Ogunwole, Laura Blakeslee, and Megan A. Rabe, *The Population 65 years and Older in the United States: 2016*, U.S.C. Bureau, Editor. 2018, American Community Survey Reports: Washington, DC.
6. Kaeberlein, M., *How healthy is the healthspan concept?* GeroScience, 2018. **40**(4): p. 361--364. PMID or DOI: Kaeberlein:2018c37.
7. Osborne, T.B., L.B. Mendel, and E.L. Ferry, *The Effect of Retardation of Growth Upon the Breeding Period and Duration of Life of Rats.* Science, 1917. **45**(1160): p. 294--295. PMID or DOI: 10.1126/science.45.1160.294.
8. Sherman, H.C. and H.L. Campbell, *Rate of Growth and Length of Life.* Proceedings of the National Academy of Sciences, 1935. **21**(5): p. 235--239. PMID or DOI: 10.1073/pnas.21.5.235.
9. Sherman, H.C. and H.L. Campbell, *The Influence of Food upon Longevity.* Proceedings of the National Academy of Sciences, 1928. **14**(11): p. 852--855. PMID or DOI: 10.1073/pnas.14.11.852.
10. McDonald, R.B. and J.J. Ramsey, *Honoring Clive McCay and 75 Years of Calorie Restriction Research.* The Journal of Nutrition, 2010. **140**(7): p. 1205--1210. PMID or DOI: 10.3945/jn.110.122804.
11. McCay, C.M., M.F. Crowell, and L.A. Maynard, *The Effect of Retarded Growth Upon the Length of Life Span and Upon the Ultimate Body Size.* The Journal of Nutrition, 1935. **10**(1): p. 63--79. PMID or DOI: 10.1093/jn/10.1.63.
12. Kirkwood, T.B.L. and R. Holliday, *The evolution of ageing and longevity.* Proceedings of the Royal Society of London. Series B. Biological Sciences, 1979. **205**(1161): p. 531--546. PMID or DOI: 10.1098/rspb.1979.0083.
13. Harman, D., *Aging: A Theory Based on Free Radical and Radiation Chemistry.* Journal of Gerontology, 1956. **11**(3): p. 298--300. PMID or DOI: 10.1093/geronj/11.3.298.
14. Klass, M.R., *A method for the isolation of longevity mutants in the nematode Caenorhabditis elegans and initial results.* Mechanisms of Ageing and Development, 1983. **22**(3-4): p. 279--286. PMID or DOI: 10.1016/0047-6374(83)90082-9.
15. Klass, M.R., *Aging in the nematode Caenorhabditis elegans: Major biological and environmental factors influencing life span.* Mechanisms of Ageing and Development, 1977. **6**(6): p. 413--429. PMID or DOI: 10.1016/0047-6374(77)90043-4.
16. Friedman, D.B. and T.E. Johnson, *A mutation in the age-1 gene in Caenorhabditis elegans lengthens life and reduces hermaphrodite fertility.* Genetics, 1988. **118**(1): p. 75--86. PMID or DOI: undefined.
17. Kenyon, C., et al., *A C. elegans mutant that lives twice as long as wild type.* Nature, 1993. **366**(6454): p. 366461a0. PMID or DOI: 10.1038/366461a0.
18. Kimura, K.D., et al., *daf-2, an Insulin Receptor-Like Gene That Regulates Longevity and Diapause in Caenorhabditis elegans.* Science, 1997. **277**(5328): p. 942--946. PMID or DOI: 10.1126/science.277.5328.942.
19. Kaeberlein, M., et al., *Regulation of yeast replicative life span by TOR and Sch9 in response to nutrients.* Science, 2005. **310**(5751): p. 1193-6. PMID or DOI: 16293764.
20. Loewith, R., et al., *Two TOR Complexes, Only One of which Is Rapamycin Sensitive, Have Distinct Roles in Cell Growth Control.* Molecular Cell, 2002. **10**(3): p. 457--468. PMID or DOI: 10.1016/s1097-2765(02)00636-6.

21. Chen, J., et al., *Identification of an 11-kDa FKBP12-rapamycin-binding domain within the 289-kDa FKBP12-rapamycin-associated protein and characterization of a critical serine residue.* Proceedings of the National Academy of Sciences, 1995. **92**(11): p. 4947--4951. PMID or DOI: 10.1073/pnas.92.11.4947.
22. Choi, J., et al., *Structure of the FKBP12-Rapamycin Complex Interacting with Binding Domain of Human FRAP.* Science, 1996. **273**(5272): p. 239--242. PMID or DOI: 10.1126/science.273.5272.239.
23. Yang, H., et al., *mTOR kinase structure, mechanism and regulation.* Nature, 2013. **497**(7448): p. 217--23. PMID or DOI: 10.1038/nature12122.
24. Gaubitz, C., et al., *Molecular Basis of the Rapamycin Insensitivity of Target Of Rapamycin Complex 2.* Mol Cell, 2015. **58**(6): p. 977-88. PMID or DOI: 26028537.
25. Sarbassov, D.D., et al., *Prolonged Rapamycin Treatment Inhibits mTORC2 Assembly and Akt/PKB.* Molecular Cell, 2006. **22**(2): p. 159--168. PMID or DOI: 10.1016/j.molcel.2006.03.029.
26. Benavides-Serrato, A., et al., *Specific blockade of Rictor-mTOR association inhibits mTORC2 activity and is cytotoxic in glioblastoma.* PLoS ONE, 2017. **12**(4): p. e0176599. PMID or DOI: 10.1371/journal.pone.0176599.
27. Kaeberlein, M., et al., *Regulation of Yeast Replicative Life Span by TOR and Sch9 in Response to Nutrients.* Science, 2005. **310**(5751): p. 1193--1196. PMID or DOI: 10.1126/science.1115535.
28. Hansen, M., et al., *Lifespan extension by conditions that inhibit translation in Caenorhabditis elegans.* 2007. PMID or DOI:
29. Kapahi, P., et al., *Regulation of Lifespan in Drosophila by Modulation of Genes in the TOR Signaling Pathway.* Current Biology, 2004. **14**(10): p. 885-890. PMID or DOI:
30. Fabrizio, P., et al., *Regulation of longevity and stress resistance by Sch9 in yeast.* 2001. PMID or DOI: 10.1126/science.1059497.
31. Vellai, T., et al., *Genetics: Influence of TOR kinase on lifespan in C. elegans.* 2003. PMID or DOI: 10.1038/426620a.
32. Jia, K., D. Chen, and D.L. Riddle, *The TOR pathway interacts with the insulin signaling pathway to regulate C. elegans larval development, metabolism and life span.* Development (Cambridge, England), 2004. **131**(16): p. 3897--906. PMID or DOI: 10.1242/dev.01255.
33. Powers, R.W., et al., *Extension of chronological life span in yeast by decreased TOR pathway signaling.* Genes \& Development, 2006. **20**(2): p. 174-184. PMID or DOI: 10.1101/gad.1381406.
34. Medvedik, O., et al., *MSN2 and MSN4 link calorie restriction and TOR to sirtuin-mediated lifespan extension in Saccharomyces cerevisiae.* PLoS biology, 2007. **5**(10): p. e261. PMID or DOI: 10.1371/journal.pbio.0050261.
35. Robida-Stubbs, S., et al., *TOR signaling and rapamycin influence longevity by regulating SKN-1/Nrf and DAF-16/FoxO.* Cell metabolism, 2012. **15**(5): p. 713--24. PMID or DOI: 10.1016/j.cmet.2012.04.007.
36. Bjedov, I., et al., *Mechanisms of Life Span Extension by Rapamycin in the Fruit Fly Drosophila melanogaster.* Cell Metabolism, 2010. **11**(1): p. 35--46. PMID or DOI: 10.1016/j.cmet.2009.11.010.
37. Harrison, D.E., et al., *Rapamycin fed late in life extends lifespan in genetically heterogeneous mice.* Nature, 2009. **460**(7253): p. 392-5. PMID or DOI: 19587680. PMC2786175.
38. Miller, R.A., et al., *Rapamycin, But Not Resveratrol or Simvastatin, Extends Life Span of Genetically Heterogeneous Mice.* The Journals of Gerontology: Series A, 2011. **66A**(2): p. 191--201. PMID or DOI: 10.1093/gerona/glq178.
39. Anisimov, V.N., et al., *Rapamycin increases lifespan and inhibits spontaneous tumorigenesis in inbred female mice.* Cell Cycle, 2011. **10**(24): p. 4230--4236. PMID or DOI: 10.4161/cc.10.24.18486.
40. López-Otín, C., et al., *The hallmarks of aging.* Cell, 2013. **153**(6): p. 1194--217. PMID or DOI: 10.1016/j.cell.2013.05.039.
41. Koga, H., S. Kaushik, and A.M. Cuervo, *Protein homeostasis and aging: The importance of exquisite quality control.* Ageing Research Reviews, 2011. **10**(2): p. 205--215. PMID or DOI: 10.1016/j.arr.2010.02.001.
42. Gonskikh, Y. and N. Polacek, *Alterations of the translation apparatus during aging and stress response.* Mechanisms of Ageing and Development, 2017. **168**: p. 30--36. PMID or DOI: 10.1016/j.mad.2017.04.003.
43. Roux, P.P. and I. Topisirovic, *Signaling Pathways Involved in the Regulation of mRNA Translation.* Molecular and Cellular Biology, 2018. **38**(12): p. e00070--18. PMID or DOI: 10.1128/mcb.00070-18.

44. Zhao, J., et al., *mTOR inhibition activates overall protein degradation by the ubiquitin proteasome system as well as by autophagy.* Proceedings of the National Academy of Sciences, 2015. **112**(52): p. 15790--15797. PMID or DOI: 10.1073/pnas.1521919112.
45. Dhillon, R.S. and J.M. Denu, *Using comparative biology to understand how aging affects mitochondrial metabolism.* Molecular and Cellular Endocrinology, 2017. **455**: p. 54--61. PMID or DOI: 10.1016/j.mce.2016.12.020.
46. Morita, M., et al., *mTORC1 Controls Mitochondrial Activity and Biogenesis through 4E-BP-Dependent Translational Regulation.* Cell Metabolism, 2013. **18**(5): p. 698--711. PMID or DOI: 10.1016/j.cmet.2013.10.001.
47. Lindqvist, L.M., et al., *Cross-talk between protein synthesis, energy metabolism and autophagy in cancer.* Current Opinion in Genetics \& Development, 2018. **48**: p. 104--111. PMID or DOI: 10.1016/j.gde.2017.11.003.
48. Bartolomé, A., et al., *MTORC1 Regulates both General Autophagy and Mitophagy Induction after Oxidative Phosphorylation Uncoupling.* Molecular and Cellular Biology, 2017. **37**(23): p. e00441--17. PMID or DOI: 10.1128/mcb.00441-17.
49. Wiley, Christopher D. and J. Campisi, *From Ancient Pathways to Aging Cells—Connecting Metabolism and Cellular Senescence.* Cell Metabolism, 2016. **23**(6): p. 1013--1021. PMID or DOI: 10.1016/j.cmet.2016.05.010.
50. Papadopoli, D., et al., *mTOR as a central regulator of lifespan and aging.* F1000Research, 2019. **8**: p. F1000 Faculty Rev--998. PMID or DOI: 10.12688/f1000research.17196.1.
51. Narita, M., et al., *Spatial Coupling of mTOR and Autophagy Augments Secretory Phenotypes.* Science, 2011. **332**(6032): p. 966--970. PMID or DOI: 10.1126/science.1205407.
52. Iglesias-Bartolome, R., et al., *mTOR Inhibition Prevents Epithelial Stem Cell Senescence and Protects from Radiation-Induced Mucositis.* Cell Stem Cell, 2012. **11**(3): p. 401--414. PMID or DOI: 10.1016/j.stem.2012.06.007.
53. Kolesnichenko, M., et al., *Attenuation of TORC1 signaling delays replicative and oncogenic RAS-induced senescence.* Cell Cycle, 2012. **11**(12): p. 2391--2401. PMID or DOI: 10.4161/cc.20683.
54. Longo, V.D., et al., *Replicative and chronological aging in Saccharomyces cerevisiae.* Cell Metab, 2012. **16**(1): p. 18-31. PMID or DOI: 22768836. 3392685.
55. Kaeberlein, M., *Lessons on longevity from budding yeast.* Nature, 2010. **464**(7288): p. 513-9. PMID or DOI: 20336133. 3696189.
56. Fabrizio, P., et al., *Regulation of longevity and stress resistance by Sch9 in yeast.* Science, 2001. **292**(5515): p. 288-90. PMID or DOI: 11292860.
57. Johnson, S.C., P.S. Rabinovitch, and M. Kaeberlein, *mTOR is a key modulator of ageing and age-related disease.* Nature, 2013. **493**(7432): p. 338-45. PMID or DOI: 23325216. 3687363.
58. Johnson, S.C., et al., *Modulating mTOR in aging and health.* Interdiscip Top Gerontol, 2015. **40**: p. 107-27. PMID or DOI: 25341517.
59. Powers, R.W., 3rd, et al., *Extension of chronological life span in yeast by decreased TOR pathway signaling.* Genes Dev, 2006. **20**(2): p. 174-84. PMID or DOI: 16418483. 1356109.
60. Robida-Stubbs, S., et al., *TOR signaling and rapamycin influence longevity by regulating SKN-1/Nrf and DAF-16/FoxO.* Cell metabolism, 2012. **15**(5): p. 713-24. PMID or DOI: 22560223. 3348514.
61. Bjedov, I., et al., *Mechanisms of life span extension by rapamycin in the fruit fly Drosophila melanogaster.* Cell Metab, 2010. **11**(1): p. 35-46. PMID or DOI: 20074526. 2824086.
62. Johnson, S.C., et al., *Preserving youth: does rapamycin deliver?* Sci Transl Med, 2013. **5**(211): p. 211fs40. PMID or DOI: 24225941. 4019780.
63. Anisimov, V.N., et al., *Rapamycin increases lifespan and inhibits spontaneous tumorigenesis in inbred female mice.* Cell Cycle, 2011. **10**(24): p. 4230-6. PMID or DOI: 22107964.
64. Popovich, I.G., et al., *Lifespan extension and cancer prevention in HER-2/neu transgenic mice treated with low intermittent doses of rapamycin.* Cancer Biol Ther, 2014. **15**(5): p. 586-92. PMID or DOI: 24556924. PMC4026081.
65. Halloran, J., et al., *Chronic inhibition of mammalian target of rapamycin by rapamycin modulates cognitive and non-cognitive components of behavior throughout lifespan in mice.* Neuroscience, 2012. **223**: p. 102-13. PMID or DOI: 22750207. PMC3454865.

66. Majumder, S., et al., *Lifelong rapamycin administration ameliorates age-dependent cognitive deficits by reducing IL-1beta and enhancing NMDA signaling.* Aging cell, 2012. **11**(2): p. 326-35. PMID or DOI: 22212527. 3306461.
67. Neff, F., et al., *Rapamycin extends murine lifespan but has limited effects on aging.* J Clin Invest, 2013. **123**(8): p. 3272-91. PMID or DOI: 23863708. 3726163.
68. Flynn, J.M., et al., *Late-life rapamycin treatment reverses age-related heart dysfunction.* Aging Cell, 2013. **12**(5): p. 851-62. PMID or DOI: 23734717. 4098908.
69. Dai, D.F., et al., *Altered proteome turnover and remodeling by short-term caloric restriction or rapamycin rejuvenate the aging heart.* Aging Cell, 2014. **13**(3): p. 529-39. PMID or DOI: 24612461. 4040127.
70. Chen, C., Y. Liu, and P. Zheng, *mTOR regulation and therapeutic rejuvenation of aging hematopoietic stem cells.* Sci Signal, 2009. **2**(98): p. ra75. PMID or DOI: 19934433.
71. Urfer, S.R., et al., *A randomized controlled trial to establish effects of short-term rapamycin treatment in 24 middle-aged companion dogs.* Geroscience, 2017. PMID or DOI: 28374166.
72. Mannick, J.B., et al., *mTOR inhibition improves immune function in the elderly.* Sci Transl Med, 2014. **6**(268): p. 268ra179. PMID or DOI: 25540326.
73. Bitto, A., et al., *Transient rapamycin treatment can increase lifespan and healthspan in middle-aged mice.* Elife, 2016. **5**: p. e16351. PMID or DOI: 27549339. PMC4996648.
74. Blagosklonny, M.V., *Increasing healthy lifespan by suppressing aging in our lifetime: preliminary proposal.* Cell cycle, 2010. **9**(24): p. 4788-94. PMID or DOI: 21150328.
75. Kaeberlein, M., K.E. Creevy, and D.E. Promislow, *The dog aging project: translational geroscience in companion animals.* Mamm Genome, 2016. **27**(7-8): p. 279-88. PMID or DOI: 27143112. PMC4936929.
76. Kaeberlein, M., P.S. Rabinovitch, and G.M. Martin, *Healthy Aging: The Ultimate Preventative Medicine.* Science, 2015. **350**(6265): p. 1191-1193. PMID or DOI:
77. Loewith, R., et al., *Two TOR complexes, only one of which is rapamycin sensitive, have distinct roles in cell growth control.* Mol Cell, 2002. **10**(3): p. 457-68. PMID or DOI: 12408816.
78. Wullschleger, S., R. Loewith, and M.N. Hall, *TOR signaling in growth and metabolism.* Cell, 2006. **124**(3): p. 471-84. PMID or DOI: 16469695.
79. Heitman, J., N.R. Movva, and M.N. Hall, *Targets for cell cycle arrest by the immunosuppressant rapamycin in yeast.* Science, 1991. **253**(5022): p. 905-9. PMID or DOI: 1715094.
80. Lorenz, M.C. and J. Heitman, *TOR mutations confer rapamycin resistance by preventing interaction with FKBP12-rapamycin.* J Biol Chem, 1995. **270**(46): p. 27531-7. PMID or DOI: 7499212.
81. Benton, B.M., J.H. Zang, and J. Thorner, *A novel FK506- and rapamycin-binding protein (FPR3 gene product) in the yeast Saccharomyces cerevisiae is a proline rotamase localized to the nucleolus.* J Cell Biol, 1994. **127**(3): p. 623-39. PMID or DOI: 7525596. PMC2120238.
82. Saxton, R.A. and D.M. Sabatini, *mTOR Signaling in Growth, Metabolism, and Disease.* Cell, 2017. **168**(6): p. 960-976. PMID or DOI: 28283069. PMC5394987.
83. Jacinto, E., et al., *Mammalian TOR complex 2 controls the actin cytoskeleton and is rapamycin insensitive.* Nat Cell Biol, 2004. **6**(11): p. 1122-8. PMID or DOI: 15467718.
84. Lamming, D.W., et al., *Rapamycin-induced insulin resistance is mediated by mTORC2 loss and uncoupled from longevity.* Science, 2012. **335**(6076): p. 1638-43. PMID or DOI: 22461615. 3324089.
85. Helliwell, S.B., et al., *TOR1 and TOR2 are structurally and functionally similar but not identical phosphatidylinositol kinase homologues in yeast.* Mol Biol Cell, 1994. **5**(1): p. 105-18. PMID or DOI: 8186460.
86. Kunz, J., et al., *Target of rapamycin in yeast, TOR2, is an essential phosphatidylinositol kinase homolog required for G1 progression.* Cell, 1993. **73**(3): p. 585-96. PMID or DOI: 8387896.
87. McCormick, M.A., et al., *A Comprehensive Analysis of Replicative Lifespan in 4,698 Single-Gene Deletion Strains Uncovers Conserved Mechanisms of Aging.* Cell Metab, 2015. **22**(5): p. 895-906. PMID or DOI: 26456335. PMC4862740.
88. Beaupere, C., et al., *CAN1 Arginine Permease Deficiency Extends Yeast Replicative Lifespan via Translational Activation of Stress Response Genes.* Cell Rep, 2017. **18**(8): p. 1884-1892. PMID or DOI: 28228255. PMC5327506.
89. Folkes, A.J., et al., *The identification of 2-(1H-indazol-4-yl)-6-(4-methanesulfonyl-piperazin-1-ylmethyl)-4-morpholin-4-yl-t hieno[3,2-d]pyrimidine (GDC-0941) as a potent, selective, orally bioavailable inhibitor of*

class I PI3 kinase for the treatment of cancer. J Med Chem, 2008. **51**(18): p. 5522-32. PMID or DOI: 18754654.
90. Chresta, C.M., et al., *AZD8055 is a potent, selective, and orally bioavailable ATP-competitive mammalian target of rapamycin kinase inhibitor with in vitro and in vivo antitumor activity.* Cancer Res, 2010. **70**(1): p. 288-98. PMID or DOI: 20028854.
91. Knight, S.D., et al., *Discovery of GSK2126458, a Highly Potent Inhibitor of PI3K and the Mammalian Target of Rapamycin.* ACS Med Chem Lett, 2010. **1**(1): p. 39-43. PMID or DOI: 24900173. PMC4007793.
92. O'Donnell, J.S., et al., *PI3K-AKT-mTOR inhibition in cancer immunotherapy, redux.* Semin Cancer Biol, 2017. PMID or DOI: 28467889.
93. Liu, Q., et al., *Selective ATP-competitive inhibitors of TOR suppress rapamycin-insensitive function of TORC2 in Saccharomyces cerevisiae.* ACS Chem Biol, 2012. **7**(6): p. 982-7. PMID or DOI: 22496512. PMC3376217.
94. Beevers, C.S., et al., *Curcumin disrupts the Mammalian target of rapamycin-raptor complex.* Cancer Res, 2009. **69**(3): p. 1000-8. PMID or DOI: 19176385. PMC4307947.
95. Beevers, C.S., et al., *Curcumin inhibits the mammalian target of rapamycin-mediated signaling pathways in cancer cells.* Int J Cancer, 2006. **119**(4): p. 757-64. PMID or DOI: 16550606.
96. Zhang, Q., et al., *Green tea extract and (-)-epigallocatechin-3-gallate inhibit mast cell-stimulated type I collagen expression in keloid fibroblasts via blocking PI-3K/AkT signaling pathways.* J Invest Dermatol, 2006. **126**(12): p. 2607-13. PMID or DOI: 16841034.
97. Van Aller, G.S., et al., *Epigallocatechin gallate (EGCG), a major component of green tea, is a dual phosphoinositide-3-kinase/mTOR inhibitor.* Biochem Biophys Res Commun, 2011. **406**(2): p. 194-9. PMID or DOI: 21300025.
98. Saiki, S., et al., *Caffeine induces apoptosis by enhancement of autophagy via PI3K/Akt/mTOR/p70S6K inhibition.* Autophagy, 2011. **7**(2): p. 176-87. PMID or DOI: 21081844. PMC3039768.
99. Reinke, A., et al., *Caffeine targets TOR complex I and provides evidence for a regulatory link between the FRB and kinase domains of Tor1p.* J Biol Chem, 2006. **281**(42): p. 31616-26. PMID or DOI: 16923813.
100. Anastasius, N., et al., *Evidence that low-dose, long-term genistein treatment inhibits oestradiol-stimulated growth in MCF-7 cells by down-regulation of the PI3-kinase/Akt signalling pathway.* J Steroid Biochem Mol Biol, 2009. **116**(1-2): p. 50-5. PMID or DOI: 19406242.
101. Wiczk, A., et al., *Sulforaphane, a cruciferous vegetable-derived isothiocyanate, inhibits protein synthesis in human prostate cancer cells.* Biochim Biophys Acta, 2012. **1823**(8): p. 1295-305. PMID or DOI: 22640870.
102. Xie, R., et al., *Alpha-lipoic acid pre- and post-treatments provide protection against in vitro ischemia-reperfusion injury in cerebral endothelial cells via Akt/mTOR signaling.* Brain Res, 2012. **1482**: p. 81-90. PMID or DOI: 22982730.
103. Li, Z., et al., *Alpha-lipoic acid supplementation reduces mTORC1 signaling in skeletal muscle from high fat fed, obese Zucker rats.* Lipids, 2014. **49**(12): p. 1193-201. PMID or DOI: 25366515.
104. Jiang, L., et al., *Glucosamine protects nucleus pulposus cells and induces autophagy via the mTOR-dependent pathway.* J Orthop Res, 2014. **32**(11): p. 1532-42. PMID or DOI: 25087910.
105. Meng, F.D., et al., *Synergistic effects of snail and quercetin on renal cell carcinoma Caki-2 by altering AKT/mTOR/ERK1/2 signaling pathways.* Int J Clin Exp Pathol, 2015. **8**(6): p. 6157-68. PMID or DOI: 26261493. PMC4525827.
106. Lu, Q., et al., *Quercetin inhibits the mTORC1/p70S6K signaling-mediated renal tubular epithelial-mesenchymal transition and renal fibrosis in diabetic nephropathy.* Pharmacol Res, 2015. **99**: p. 237-47. PMID or DOI: 26151815.
107. Fan, X., et al., *Berberine alleviates ox-LDL induced inflammatory factors by up-regulation of autophagy via AMPK/mTOR signaling pathway.* J Transl Med, 2015. **13**: p. 92. PMID or DOI: 25884210. PMC4365560.
108. Park, D., et al., *Resveratrol induces autophagy by directly inhibiting mTOR through ATP competition.* Sci Rep, 2016. **6**: p. 21772. PMID or DOI: 26902888. PMC4763238.
109. Murakami, C.J., et al., *A method for high-throughput quantitative analysis of yeast chronological life span.* J Gerontol A Biol Sci Med Sci, 2008. **63**(2): p. 113-21. PMID or DOI: 18314444.
110. Murakami, C. and M. Kaeberlein, *Quantifying yeast chronological life span by outgrowth of aged cells.* J Vis Exp, 2009(27). PMID or DOI: 19421136. 2762921.

111. Delaney, J.R., et al., *Stress profiling of longevity mutants identifies Afg3 as a mitochondrial determinant of cytoplasmic mRNA translation and aging.* Aging Cell, 2013. **12**(1): p. 156-66. PMID or DOI: 23167605. 3687586.
112. Steffen, K.K., et al., *Yeast life span extension by depletion of 60s ribosomal subunits is mediated by Gcn4.* Cell, 2008. **133**(2): p. 292-302. PMID or DOI: 18423200. 2749658.
113. Beretta, L., et al., *Rapamycin blocks the phosphorylation of 4E-BP1 and inhibits cap-dependent initiation of translation.* EMBO J, 1996. **15**(3): p. 658-64. PMID or DOI: 8599949. PMC449984.
114. Kaeberlein, M., *mTOR Inhibition: From Aging to Autism and Beyond.* Scientifica (Cairo), 2013. **2013**: p. 849186. PMID or DOI: 24379984. 3860151.
115. Wu, T.J., et al., *Identification of a Non-Gatekeeper Hot Spot for Drug-Resistant Mutations in mTOR Kinase.* Cell Rep, 2015. **11**(3): p. 446-59. PMID or DOI: 25865887. PMC4761412.
116. Wanke, V., et al., *Caffeine extends yeast lifespan by targeting TORC1.* Mol Microbiol, 2008. **69**(1): p. 277-85. PMID or DOI: 18513215.
117. Rallis, C., S. Codlin, and J. Bahler, *TORC1 signaling inhibition by rapamycin and caffeine affect lifespan, global gene expression, and cell proliferation of fission yeast.* Aging Cell, 2013. **12**(4): p. 563-73. PMID or DOI: 23551936. PMC3798131.
118. Sutphin, G.L., et al., *Caffeine extends life span, improves healthspan, and delays age-associated pathology in Caenorhabditis elegans.* Longev Healthspan, 2012. **1**: p. 9. PMID or DOI: 24764514. 3922918.
119. Bridi, J.C., et al., *Lifespan Extension Induced by Caffeine in Caenorhabditis elegans is Partially Dependent on Adenosine Signaling.* Front Aging Neurosci, 2015. **7**: p. 220. PMID or DOI: 26696878. PMC4672644.
120. Loftfield, E., et al., *Association of Coffee Consumption With Overall and Cause-Specific Mortality in a Large US Prospective Cohort Study.* Am J Epidemiol, 2015. **182**(12): p. 1010-22. PMID or DOI: 26614599.
121. Je, Y. and E. Giovannucci, *Coffee consumption and total mortality: a meta-analysis of twenty prospective cohort studies.* Br J Nutr, 2014. **111**(7): p. 1162-73. PMID or DOI: 24279995.
122. Liu, M., et al., *Resveratrol inhibits mTOR signaling by promoting the interaction between mTOR and DEPTOR.* J Biol Chem, 2010. **285**(47): p. 36387-94. PMID or DOI: 20851890. PMC2978567.
123. Brito, P.M., et al., *Resveratrol inhibits the mTOR mitogenic signaling evoked by oxidized LDL in smooth muscle cells.* Atherosclerosis, 2009. **205**(1): p. 126-34. PMID or DOI: 19108833.
124. Tillu, D.V., et al., *Resveratrol engages AMPK to attenuate ERK and mTOR signaling in sensory neurons and inhibits incision-induced acute and chronic pain.* Mol Pain, 2012. **8**: p. 5. PMID or DOI: 22269797. PMC3284441.
125. Kaeberlein, M., et al., *Substrate-specific activation of sirtuins by resveratrol.* J Biol Chem, 2005. **280**(17): p. 17038-45. PMID or DOI: 15684413.
126. Fay, J.C. and J.A. Benavides, *Evidence for domesticated and wild populations of Saccharomyces cerevisiae.* PLoS Genet, 2005. **1**(1): p. 66-71. PMID or DOI: 16103919. PMC1183524.
127. Liti, G., et al., *Population genomics of domestic and wild yeasts.* Nature, 2009. **458**(7236): p. 337-41. PMID or DOI: 19212322. PMC2659681.
128. Winzeler, E.A., et al., *Functional characterization of the S. cerevisiae genome by gene deletion and parallel analysis.* Science, 1999. **285**(5429): p. 901-6. PMID or DOI: 10436161.
129. Olsen, B., C.J. Murakami, and M. Kaeberlein, *YODA: software to facilitate high-throughput analysis of chronological life span, growth rate, and survival in budding yeast.* BMC Bioinformatics, 2010. **11**: p. 141. PMID or DOI: 20298554. 2850362.
130. Sierra, F. and R. Kohanski, *Geroscience and the trans-NIH Geroscience Interest Group, GSIG.* Geroscience, 2017. **39**(1): p. 1-5. PMID or DOI: 28299635.
131. Lee, M.B. and M. Kaeberlein, *Translational geroscience: From invertebrate models to companion animal and human interventions.* Translational Medicine of Aging, 2018. **2**: p. 15-29. PMID or DOI:
132. Lopez-Otin, C., et al., *The hallmarks of aging.* Cell, 2013. **153**(6): p. 1194-217. PMID or DOI: 23746838. 3836174.
133. Kennedy, B.K., et al., *Geroscience: linking aging to chronic disease.* Cell, 2014. **159**(4): p. 709-13. PMID or DOI: 25417146.
134. Mortimer, R.K. and J.R. Johnston, *Life span of individual yeast cells.* Nature, 1959. **183**(4677): p. 1751-2. PMID or DOI: 13666896.

135. Lin, S.J., P.A. Defossez, and L. Guarente, *Requirement of NAD and SIR2 for life-span extension by calorie restriction in Saccharomyces cerevisiae.* Science, 2000. **289**(5487): p. 2126-8. PMID or DOI: 11000115
136. Jiang, J.C., et al., *An intervention resembling caloric restriction prolongs life span and retards aging in yeast.* Faseb J, 2000. **14**(14): p. 2135-7. PMID or DOI: 11024000.
137. Kaeberlein, M., M. McVey, and L. Guarente, *The SIR2/3/4 complex and SIR2 alone promote longevity in Saccharomyces cerevisiae by two different mechanisms.* Genes Dev, 1999. **13**(19): p. 2570-80. PMID or DOI: 10521401. 317077.
138. Kaeberlein, M., et al., *Sir2-independent life span extension by calorie restriction in yeast.* PLoS Biol, 2004. **2**(9): p. E296. PMID or DOI: 15328540. 514491.
139. Kirchman, P.A., et al., *Interorganelle signaling is a determinant of longevity in Saccharomyces cerevisiae.* Genetics, 1999. **152**(1): p. 179-90. PMID or DOI: 10224252.
140. Lai, C.Y., et al., *A mutation in the ATP2 gene abrogates the age asymmetry between mother and daughter cells of the yeast Saccharomyces cerevisiae.* Genetics, 2002. **162**(1): p. 73-87. PMID or DOI: 12242224. 1462265.
141. Miceli, M.V., et al., *Loss of mitochondrial membrane potential triggers the retrograde response extending yeast replicative lifespan.* Front Genet, 2011. **2**: p. 102. PMID or DOI: 22303396. 3266616.
142. Veatch, J.R., et al., *Mitochondrial dysfunction leads to nuclear genome instability via an iron-sulfur cluster defect.* Cell, 2009. **137**(7): p. 1247-58. PMID or DOI: 19563757.
143. Hughes, C.E., et al., *Cysteine Toxicity Drives Age-Related Mitochondrial Decline by Altering Iron Homeostasis.* Cell, 2020. **180**(2): p. 296-310 e18. PMID or DOI: 31978346.
144. Hughes, A.L. and D.E. Gottschling, *An early age increase in vacuolar pH limits mitochondrial function and lifespan in yeast.* Nature, 2012. **492**(7428): p. 261-5. PMID or DOI: 23172144. 3521838.
145. Henderson, K.A., A.L. Hughes, and D.E. Gottschling, *Mother-daughter asymmetry of pH underlies aging and rejuvenation in yeast.* Elife, 2014. **3**: p. e03504. PMID or DOI: 25190112. PMC4175738.
146. Chen, K.L., et al., *Loss of vacuolar acidity results in iron-sulfur cluster defects and divergent homeostatic responses during aging in Saccharomyces cerevisiae.* Geroscience, 2020. PMID or DOI: 31975050.
147. Murakami, C., et al., *pH neutralization protects against reduction in replicative lifespan following chronological aging in yeast.* Cell Cycle, 2012. **11**(16): p. 3087-96. PMID or DOI: 22871733. 3442919.
148. Mouton, S.N., et al., *A physicochemical perspective of aging from single-cell analysis of pH, macromolecular and organellar crowding in yeast.* Elife, 2020. **9**. PMID or DOI: 32990592. PMC7556870.
149. Kruegel, U., et al., *Elevated proteasome capacity extends replicative lifespan in Saccharomyces cerevisiae.* PLoS Genet, 2011. **7**(9): p. e1002253. PMID or DOI: 21931558. 3169524.
150. Yao, Y., et al., *Proteasomes, Sir2, and Hxk2 form an interconnected aging network that impinges on the AMPK/Snf1-regulated transcriptional repressor Mig1.* PLoS Genet, 2015. **11**(1): p. e1004968. PMID or DOI: 25629410. 4309596.
151. Hu, Z., et al., *Ssd1 and Gcn2 suppress global translation efficiency in replicatively aged yeast while their activation extends lifespan.* Elife, 2018. **7**. PMID or DOI: 30117416. PMC6097839.
152. Aris, J.P., et al., *Autophagy and leucine promote chronological longevity and respiration proficiency during calorie restriction in yeast.* Exp Gerontol, 2013. **48**(10): p. 1107-19. PMID or DOI: 23337777. PMC3728276.
153. Sinclair, D.A. and L. Guarente, *Extrachromosomal rDNA circles--a cause of aging in yeast.* Cell, 1997. **91**(7): p. 1033-42. PMID or DOI: 9428525.
154. Crane, M.M., et al., *DNA damage checkpoint activation impairs chromatin homeostasis and promotes mitotic catastrophe during aging.* Elife, 2019. **8**. PMID or DOI: 31714209. PMC6850777.
155. Myers, A. and G.J. Lithgow, *Drugs that target aging: how do we discover them?* Expert Opin Drug Discov, 2019. **14**(6): p. 541-548. PMID or DOI: 30973028. PMC6497572.
156. Barardo, D., et al., *The DrugAge database of aging-related drugs.* Aging Cell, 2017. **16**(3): p. 594-597. PMID or DOI: 28299908. PMC5418190.
157. Tacutu, R., et al., *Human Ageing Genomic Resources: new and updated databases.* Nucleic Acids Res, 2018. **46**(D1): p. D1083-D1090. PMID or DOI: 29121237. PMC5753192.
158. Lee, M.B., et al., *A system to identify inhibitors of mTOR signaling using high-resolution growth analysis in Saccharomyces cerevisiae.* Geroscience, 2017. **39**(4): p. 419-428. PMID or DOI: 28707282. PMC5636783.

159. McCubrey, J.A., et al., *Effects of resveratrol, curcumin, berberine and other nutraceuticals on aging, cancer development, cancer stem cells and microRNAs.* Aging (Albany NY), 2017. **9**(6): p. 1477-1536. PMID or DOI: 28611316. PMC5509453.
160. Westerheide, S.D., et al., *Celastrols as inducers of the heat shock response and cytoprotection.* J Biol Chem, 2004. **279**(53): p. 56053-60. PMID or DOI: 15509580.
161. Kiaei, M., et al., *Celastrol blocks neuronal cell death and extends life in transgenic mouse model of amyotrophic lateral sclerosis.* Neurodegener Dis, 2005. **2**(5): p. 246-54. PMID or DOI: 16909005.
162. Chellappa, K., et al., *The leptin sensitizer celastrol reduces age-associated obesity and modulates behavioral rhythms.* Aging Cell, 2019. **18**(3): p. e12874. PMID or DOI: 30821426. PMC6516176.
163. Ahmad, F., et al., *Hypoglycemie activity of Pterocarpus marsupium wood.* Journal of ethnopharmacology, 1991. **35**(1): p. 71-75. PMID or DOI:
164. Maruthupandian, A. and V. Mohan, *Antidiabetic, antihyperlipidaemic and antioxidant activity of Pterocarpus marsupium Roxb. in alloxan induced diabetic rats.* Int J Pharm Tech Res, 2011. **3**(3): p. 1681-1687. PMID or DOI:
165. Halagappa, K., H.N. Girish, and B.P. Srinivasan, *The study of aqueous extract of Pterocarpus marsupium Roxb. on cytokine TNF-α in type 2 diabetic rats.* Indian journal of pharmacology, 2010. **42**(6): p. 392-396. PMID or DOI: 21189913.
166. Maurya, R., et al., *Constituents of Pterocarpus marsupium: an ayurvedic crude drug.* Phytochemistry, 2004. **65**(7): p. 915-920. PMID or DOI: WOS:000221135300019.
167. Devgun, M., A. Nanda, and S.H. Ansari, *Pterocarpus marsupium roxb. - A Comprehensive Review.* Phcog Rev, 2009. **3**(6): p. 359-363. PMID or DOI:
168. Tiwari, M., M. Sharma, and H.N. Khare, *Chemical constituents and medicinal uses of Pterocarpus marsupium roxb.* Flora and Fauna, 2015. **21**(1): p. 55-59. PMID or DOI:
169. Li, Y.R., S. Li, and C.C. Lin, *Effect of resveratrol and pterostilbene on aging and longevity.* Biofactors, 2018. **44**(1): p. 69-82. PMID or DOI: 29210129.
170. Si, H., C.Q. Lai, and D. Liu, *Dietary epicatechin, a novel anti-aging bioactive small molecule.* Curr Med Chem, 2019. PMID or DOI: 31886745.
171. Si, H., et al., *Dietary epicatechin promotes survival of obese diabetic mice and Drosophila melanogaster.* J Nutr, 2011. **141**(6): p. 1095-100. PMID or DOI: 21525262. PMC3095141.
172. Proshkina, E., et al., *Geroprotective and Radioprotective Activity of Quercetin, (-)-Epicatechin, and Ibuprofen in Drosophila melanogaster.* Front Pharmacol, 2016. **7**: p. 505. PMID or DOI: 28066251. PMC5179547.
173. Bartholome, A., et al., *Epigallocatechin gallate-induced modulation of FoxO signaling in mammalian cells and C. elegans: FoxO stimulation is masked via PI3K/Akt activation by hydrogen peroxide formed in cell culture.* Arch Biochem Biophys, 2010. **501**(1): p. 58-64. PMID or DOI: 20513639.
174. Massie, H.R., V.R. Aiello, and T.R. Williams, *Inhibition of iron absorption prolongs the life span of Drosophila.* Mech Ageing Dev, 1993. **67**(3): p. 227-37. PMID or DOI: 8326745.
175. Demidenko, Z.N. and M.V. Blagosklonny, *At concentrations that inhibit mTOR, resveratrol suppresses cellular senescence.* Cell Cycle, 2009. **8**(12): p. 1901-4. PMID or DOI: 19471118.
176. Mao, L., et al., *Berberine decelerates glucose metabolism via suppression of mTOR-dependent HIF-1α protein synthesis in colon cancer cells.* Oncology Reports, 2018. **39**(5): p. 2436-2442. PMID or DOI:
177. Qin, H., et al., *ERK-dependent mTOR pathway is involved in berberine-induced autophagy in hepatic steatosis.* Journal of Molecular Endocrinology, 2016. **57**(4): p. 251-260. PMID or DOI:
178. Wang, N., et al., *Berberine induces autophagic cell death and mitochondrial apoptosis in liver cancer cells: the cellular mechanism.* Journal of Cellular Biochemistry, 2010. **111**: p. 1426-1436. PMID or DOI:
179. Wu, T.-J., et al., *Identification of a Non-Gatekeeper Hot Spot for Drug-Resistant Mutations in mTOR Kinase.* Cell reports, 2015. **11**(3): p. 446-459. PMID or DOI: 25865887.
180. Nakashima, A. and F. Tamanoi, *Conservation of the Tsc/Rheb/TORC1/S6K/S6 Signaling in Fission Yeast.* The Enzymes, 2010. **28**: p. 167-187. PMID or DOI: 25814783.
181. Huang, J. and B.D. Manning, *The TSC1-TSC2 complex: a molecular switchboard controlling cell growth.* The Biochemical journal, 2008. **412**(2): p. 179-190. PMID or DOI: 18466115.

182. Bar, D.Z., et al., *Cell size and fat content of dietary-restricted Caenorhabditis elegans are regulated by ATX-2, an mTOR repressor.* Proceedings of the National Academy of Sciences of the United States of America, 2016. **113**(32): p. E4620-E4629. PMID or DOI: 27457958.
183. Howitz, K.T., et al., *Small molecule activators of sirtuins extend Saccharomyces cerevisiae lifespan.* Nature, 2003. **425**(6954): p. 191-196. PMID or DOI:
184. Miller, R.A., et al., *Rapamycin, but not resveratrol or simvastatin, extends life span of genetically heterogeneous mice.* The journals of gerontology. Series A, Biological sciences and medical sciences, 2011. **66**(2): p. 191-201. PMID or DOI: 20974732. 3021372.
185. Dang, Y., et al., *Berberine ameliorates cellular senescence and extends the lifespan of mice via regulating p16 and cyclin protein expression.* Aging Cell, 2020. **19**(1): p. e13060. PMID or DOI: 31773901. PMC6974710.
186. Zhang, L., et al., *Significant longevity-extending effects of EGCG on Caenorhabditis elegans under stress.* Free Radical Biology and Medicine, 2009. **46**(3): p. 414-421. PMID or DOI:
187. Basu, A. and E.A. Lucas, *Mechanisms and Effects of Green Tea on Cardiovascular Health.* Nutrition Reviews, 2007. **65**(8): p. 361-375. PMID or DOI:
188. Yang, C.S. and X. Wang, *Green Tea and Cancer Prevention.* Nutrition and Cancer, 2010. **62**(7): p. 931-937. PMID or DOI:
189. Yuan, X., et al., *Green Tea Liquid Consumption Alters the Human Intestinal and Oral Microbiome.* Molecular Nutrition & Food Research, 2018. **62**(12): p. 1800178. PMID or DOI:
190. Chen, T., et al., *Green Tea Polyphenols Modify the Gut Microbiome in db/db Mice as Co-Abundance Groups Correlating with the Blood Glucose Lowering Effect.* Molecular Nutrition & Food Research, 2019. **63**(8): p. 1801064. PMID or DOI:
191. Nash, A.K., et al., *The gut mycobiome of the Human Microbiome Project healthy cohort.* Microbiome, 2017. **5**(1): p. 153. PMID or DOI: 10.1186/s40168-017-0373-4.
192. Brachmann, C.B., et al., *Designer deletion strains derived from Saccharomyces cerevisiae S288C: A useful set of strains and plasmids for PCR‐mediated gene disruption and other applications.* Yeast, 1998. **14**(2): p. 115-132. PMID or DOI:
193. Burtner, C.R., et al., *A molecular mechanism of chronological aging in yeast.* Cell Cycle, 2009. **8**(8): p. 1256-1270. PMID or DOI: WOS:000265594200028.
194. Murakami, C.J., et al., *Composition and acidification of the culture medium influences chronological aging similarly in vineyard and laboratory yeast.* PLoS One, 2011. **6**(9): p. e24530. PMID or DOI: 21949725. 3176285.
195. Lee, M.B., et al., *A system to identify inhibitors of mTOR signaling using high-resolution growth analysis in Saccharomyces cerevisiae.* GeroScience, 2017. PMID or DOI:
196. Steffen, K.K., B.K. Kennedy, and M. Kaeberlein, *Measuring Replicative Life Span in the Budding Yeast.* Journal of Visualized Experiments : JoVE, 2009(28): p. 1209. PMID or DOI:
197. Beaupere, C., et al., *Genetic screen identifies adaptive aneuploidy as a key mediator of ER stress resistance in yeast.* Proc Natl Acad Sci U S A, 2018. **115**(38): p. 9586-9591. PMID or DOI: 30185560. PMC6156608.
198. Calvert, S., et al., *A network pharmacology approach reveals new candidate caloric restriction mimetics in C. elegans.* Aging Cell, 2016. **15**(2): p. 256-66. PMID or DOI: 26676933. PMC4783339.
199. Brown, M.K., J.L. Evans, and Y. Luo, *Beneficial effects of natural antioxidants EGCG and alpha-lipoic acid on life span and age-dependent behavioral declines in Caenorhabditis elegans.* Pharmacol Biochem Behav, 2006. **85**(3): p. 620-8. PMID or DOI: 17156833.
200. Benedetti, M.G., et al., *Compounds that confer thermal stress resistance and extended lifespan.* Exp Gerontol, 2008. **43**(10): p. 882-91. PMID or DOI: 18755260. PMC2603168.
201. Bauer, J.H., et al., *An accelerated assay for the identification of lifespan-extending interventions in Drosophila melanogaster.* Proc Natl Acad Sci U S A, 2004. **101**(35): p. 12980-5. PMID or DOI: 15328413. PMC516504.
202. Kumar, R., et al., *Withania somnifera root extract extends lifespan of Caenorhabditis elegans.* Ann Neurosci, 2013. **20**(1): p. 13-6. PMID or DOI: 25206003. PMC4117092.
203. Navrotskaya, V.V., et al., *Berberine Prolongs Life Span and Stimulates Locomotor Activity of Drosophila melanogaster.* American journal of plant sciences, 2012. **3**(7A): p. 1037-1040. PMID or DOI: 26167392.

204. Jung, S.-K., et al., *QuantWorm: A Comprehensive Software Package for Caenorhabditis elegans Phenotypic Assays.* PLoS ONE, 2014. **9**(1): p. e84830. PMID or DOI: 10.1371/journal.pone.0084830.
205. Lee, J.-H., et al., *Effects of ginsenosides, active ingredients of Panax ginseng, on development, growth, and life span of Caenorhabditis elegans.* Biological and Pharmaceutical Bulletin, 2007. **30**(11): p. 2126-2134. PMID or DOI:
206. Weimer, S., et al., *D-Glucosamine supplementation extends life span of nematodes and of ageing mice.* Nature communications, 2014. **5**(1): p. 1-12. PMID or DOI:
207. Abbas, S. and M. Wink, *Epigallocatechin gallate from green tea (Camellia sinensis) increases lifespan and stress resistance in Caenorhabditis elegans.* Planta medica, 2009. **75**(3): p. 216. PMID or DOI:
208. Lopez, T., et al., *Green tea polyphenols extend the lifespan of male drosophila melanogaster while impairing reproductive fitness.* Journal of medicinal food, 2014. **17**(12): p. 1314-1321. PMID or DOI:
209. Wagner, A.E., et al., *Epigallocatechin gallate affects glucose metabolism and increases fitness and lifespan in Drosophila melanogaster.* Oncotarget, 2015. **6**(31): p. 30568. PMID or DOI:
210. Strong, R., et al., *Evaluation of resveratrol, green tea extract, curcumin, oxaloacetic acid, and medium-chain triglyceride oil on life span of genetically heterogeneous mice.* The journals of gerontology. Series A, Biological sciences and medical sciences, 2013. **68**(1): p. 6-16. PMID or DOI: 22451473.
211. Sun, K., et al., *Anti-aging effects of hesperidin on Saccharomyces cerevisiae via inhibition of reactive oxygen species and UTH1 gene expression.* Bioscience, biotechnology, and biochemistry, 2012: p. 1202232809-1202232809. PMID or DOI:
212. Reigada, I., et al., *Antioxidant and Antiaging Effects of Licorice on the Caenorhabditis elegans Model.* Journal of Medicinal Food, 2019. **23**(1): p. 72-78. PMID or DOI:
213. Zhang, Z., et al., *Lutein extends the lifespan of Drosophila melanogaster.* Archives of Gerontology and Geriatrics, 2014. **58**(1): p. 153-159. PMID or DOI:
214. Kumar, J., et al., *Silymarin extends lifespan and reduces proteotoxicity in C. elegans Alzheimer's model.* CNS Neurol Disord Drug Targets, 2015. **14**(2): p. 295-302. PMID or DOI: 25613505.
215. Oh, S.-I., J.-K. Park, and S.-K. Park, *Lifespan extension and increased resistance to environmental stressors by N-acetyl-L-cysteine in Caenorhabditis elegans.* Clinics, 2015. **70**(5): p. 380-386. PMID or DOI:
216. Shaposhnikov, M.V., et al., *Effects of N-acetyl-L-cysteine on lifespan, locomotor activity and stress-resistance of 3 Drosophila species with different lifespans.* Aging, 2018. **10**(9): p. 2428-2458. PMID or DOI: 30243020.
217. Brack, C., E. Bechter-Thuring, and M. Labuhn, *N-acetylcysteine slows down ageing and increases the life span of Drosophila melanogaster.* Cell Mol Life Sci, 1997. **53**(11-12): p. 960-6. PMID or DOI: 9447249.
218. Flurkey, K., C.M. Astle, and D.E. Harrison, *Life extension by diet restriction and N-acetyl-L-cysteine in genetically heterogeneous mice.* J Gerontol A Biol Sci Med Sci, 2010. **65**(12): p. 1275-84. PMID or DOI: 20819793. PMC2990268.
219. Kampkötter, A., et al., *Increase of stress resistance and lifespan of Caenorhabditis elegans by quercetin.* Comparative Biochemistry and Physiology Part B: Biochemistry and Molecular Biology, 2008. **149**(2): p. 314-323. PMID or DOI:
220. Pietsch, K., et al., *Quercetin mediated lifespan extension in Caenorhabditis elegans is modulated by age-1, daf-2, sek-1 and unc-43.* Biogerontology, 2009. **10**(5): p. 565-578. PMID or DOI:
221. Chattopadhyay, D., et al., *Hormetic efficacy of rutin to promote longevity in Drosophila melanogaster.* Biogerontology, 2017. **18**(3): p. 397-411. PMID or DOI:
222. Li, S., et al., *Sodium rutin extends lifespan and health span in mice including positive impacts on liver health.* Br J Pharmacol, 2021. PMID or DOI: 33555034.
223. Rawal, S., et al., *Dietary intake of Curcuma longa and Emblica officinalis increases life span in Drosophila melanogaster.* BioMed research international, 2014. **2014**. PMID or DOI:
224. Cañuelo, A., et al., *Tyrosol, a main phenol present in extra virgin olive oil, increases lifespan and stress resistance in Caenorhabditis elegans.* Mech Ageing Dev, 2012. **133**(8): p. 563-74. PMID or DOI: 22824366.
225. Patel, P., J.-P. Julien, and J. Kriz, *Early-Stage Treatment with Withaferin A Reduces Levels of Misfolded Superoxide Dismutase 1 and Extends Lifespan in a Mouse Model of Amyotrophic Lateral Sclerosis.* Neurotherapeutics, 2015. **12**(1): p. 217-233. PMID or DOI:
226. Koval, L., et al., *Evaluation of the geroprotective effects of withaferin A in Drosophila melanogaster.* Aging (Albany NY), 2021. **13**(2): p. 1817-1841. PMID or DOI: 33498013.

227. Kaeberlein, M., *Longevity and aging.* F1000Prime Rep, 2013. **5**: p. 5. PMID or DOI: 23513177. PMC3590784.
228. Kaeberlein, M., C.R. Burtner, and B.K. Kennedy, *Recent developments in yeast aging.* PLoS Genet, 2007. **3**(5): p. e84. PMID or DOI: 17530929. PMC1877880 for the identification of new aging genes. BKK has a minor stock holding in Elixir Pharmaceuticals.
229. Myers, A. and G.J. Lithgow, *Drugs that target aging: how do we discover them?* Expert opinion on drug discovery, 2019: p. 1--8. PMID or DOI: 10.1080/17460441.2019.1597049.
230. Zhou, B.P., et al., *Cytoplasmic localization of p21Cip1/WAF1 by Akt-induced phosphorylation in HER-2/neu-overexpressing cells.* Nature Cell Biology, 2001. **3**(3): p. 245--252. PMID or DOI: 10.1038/35060032.
231. Vasko, V., et al., *Akt activation and localisation correlate with tumour invasion and oncogene expression in thyroid cancer.* Journal of Medical Genetics, 2004. **41**(3): p. 161. PMID or DOI: 10.1136/jmg.2003.015339.
232. Yamamoto, S., et al., *Prognostic Significance of Activated Akt Expression in Pancreatic Ductal Adenocarcinoma.* Clinical Cancer Research, 2004. **10**(8): p. 2846--2850. PMID or DOI: 10.1158/1078-0432.ccr-02-1441.
233. Daido, S., et al., *Inhibition of the DNA-Dependent Protein Kinase Catalytic Subunit Radiosensitizes Malignant Glioma Cells by Inducing Autophagy.* Cancer Research, 2005. **65**(10): p. 4368--4375. PMID or DOI: 10.1158/0008-5472.can-04-4202.
234. Faried, L.S., et al., *Predictive and prognostic role of activated mammalian target of rapamycin in cervical cancer treated with cisplatin-based neoadjuvant chemotherapy.* Oncology reports, 2006. **16**(1): p. 57--63. PMID or DOI: null.
235. Mita, M.M., et al., *Phase I Trial of the Novel Mammalian Target of Rapamycin Inhibitor Deforolimus (AP23573; MK-8669) Administered Intravenously Daily for 5 Days Every 2 Weeks to Patients With Advanced Malignancies.* Journal of Clinical Oncology, 2008. **26**(3): p. 361--367. PMID or DOI: 10.1200/jco.2007.12.0345.
236. Chen, C., et al., *Mammalian target of rapamycin activation underlies HSC defects in autoimmune disease and inflammation in mice.* Journal of Clinical Investigation, 2010. **120**(11): p. 4091--4101. PMID or DOI: 10.1172/jci43873.
237. Zheng, P., et al., *Cytopenia and autoimmune diseases: A vicious cycle fueled by mTOR dysregulation in hematopoietic stem cells.* Journal of Autoimmunity, 2013. **41**: p. 182--187. PMID or DOI: 10.1016/j.jaut.2012.12.011.
238. Choi, J.C., et al., *Dual Specificity Phosphatase 4 Mediates Cardiomyopathy Caused by Lamin A/C (LMNA) Gene Mutation*.* Journal of Biological Chemistry, 2012. **287**(48): p. 40513--40524. PMID or DOI: 10.1074/jbc.m112.404541.
239. Chen, S.N., et al., *Human Molecular Genetic and Functional Studies Identify TRIM63, Encoding Muscle RING Finger Protein 1, as a Novel Gene for Human Hypertrophic Cardiomyopathy.* Circulation Research, 2012. **111**(7): p. 907--919. PMID or DOI: 10.1161/circresaha.112.270207.
240. Marin, T.M., et al., *Rapamycin reverses hypertrophic cardiomyopathy in a mouse model of LEOPARD syndrome–associated PTPN11 mutation.* Journal of Clinical Investigation, 2011. **121**(3): p. 1026--1043. PMID or DOI: 10.1172/jci44972.
241. Li, X., et al., *Levels of mTOR and its downstream targets 4E‐BP1, eEF2, and eEF2 kinase in relationships with tau in Alzheimer's disease brain.* The FEBS Journal, 2005. **272**(16): p. 4211--4220. PMID or DOI: 10.1111/j.1742-4658.2005.04833.x.
242. Caccamo, A., et al., *Molecular Interplay between Mammalian Target of Rapamycin (mTOR), Amyloid-β, and Tau EFFECTS ON COGNITIVE IMPAIRMENTS*.* Journal of Biological Chemistry, 2010. **285**(17): p. 13107--13120. PMID or DOI: 10.1074/jbc.m110.100420.
243. Caccamo, A., et al., *Genetic Reduction of Mammalian Target of Rapamycin Ameliorates Alzheimer's Disease-Like Cognitive and Pathological Deficits by Restoring Hippocampal Gene Expression Signature.* The Journal of Neuroscience, 2014. **34**(23): p. 7988--7998. PMID or DOI: 10.1523/jneurosci.0777-14.2014.
244. Crino, P.B. and E.P. Henske, *New developments in the neurobiology of the tuberous sclerosis complex.* Neurology, 1999. **53**(7): p. 1384--1390. PMID or DOI: 10.1212/wnl.53.7.1384.
245. Stanfel, M.N., et al., *The TOR pathway comes of age.* Biochimica et Biophysica Acta (BBA) - General Subjects, 2009. **1790**(10): p. 1067--1074. PMID or DOI: 10.1016/j.bbagen.2009.06.007.

246. Kaeberlein, M., *mTOR Inhibition: From Aging to Autism and Beyond.* Scientifica, 2013. **2013**: p. 1--17. PMID or DOI: 10.1155/2013/849186.
247. Lee, M.B., et al., *Pterocarpus marsupium extract extends replicative lifespan in budding yeast.* GeroScience, 2021: p. 1-15. PMID or DOI:
248. Ahmad, A., et al., *Biotechnological Advances in Pharmacognosy and In Vitro Manipulation of Pterocarpus marsupium Roxb.* Plants, 2022. **11**(3): p. 247. PMID or DOI: 10.3390/plants11030247.
249. Dar, M.I., et al., *In Silico Analysis of PTP1B Inhibitors and TLC-MS Bioautography-Based Identification of Free Radical Scavenging and α-Amylase Inhibitory Compounds from Heartwood Extract of Pterocarpus marsupium.* ACS Omega, 2022. **7**(50): p. 46156--46173. PMID or DOI: 10.1021/acsomega.2c04283.
250. Dar, M.I., et al., *Heartwood Extract of Pterocarpus marsupium Roxb. Offers Defense against Oxyradicals and Improves Glucose Uptake in HepG2 Cells.* Metabolites, 2022. **12**(10): p. 947. PMID or DOI: 10.3390/metabo12100947.
251. Adinarayana, D., et al., *Structure Elucidation of Pterosupin from Pterocarpus marsupium, the First Naturally Occurring C-Glycosyl-β-hydroxy-dihydrochalcone.* Zeitschrift für Naturforschung C, 1982. **37**(3-4): p. 145--147. PMID or DOI: 10.1515/znc-1982-3-401.
252. Maurya, R., et al., *Constituents of Pterocarpus marsupium.* Journal of Natural Products, 1984. **47**(1): p. 179--181. PMID or DOI: 10.1021/np50031a029.
253. Jahromi, M.A.F., A.B. Ray, and J.P.N. Chansouria, *Antihyperlipidemic Effect of Flavonoids from Pterocarpus marsupium.* Journal of Natural Products, 1993. **56**(7): p. 989--994. PMID or DOI: 10.1021/np50097a001.
254. Chakravarthy, B. and K. Gode, *Isolation of (-)-Epicatechin from Pterocarpus marsupium and its Pharmacological Actions.* Planta Medica, 1985. **51**(01): p. 56--59. PMID or DOI: 10.1055/s-2007-969393.
255. Gosetti, F., et al., *Characterization of the Volatile and Nonvolatile Fractions of Heartwood Aqueous Extract from Pterocarpus marsupium and Evaluation of Its Cytotoxicity against Cancer Cell Lines.* Planta Medica, 2016. **82**(14): p. 1295--1301. PMID or DOI: 10.1055/s-0042-104659.
256. Singh, P., et al., *Identification and quantification of secondary metabolites of Pterocarpus marsupium by LC–MS techniques and its in-vitro lipid lowering activity.* Industrial Crops and Products, 2019. **127**: p. 26--35. PMID or DOI: 10.1016/j.indcrop.2018.10.047.
257. Joshi, K.R., H.P. Devkota, and S. Yahara, *Chemical Analysis of Heartwood of Bijayasal (Pterocarpus marsupium Roxb.).* Nepal Journal of Science and Technology, 2012. **13**(2): p. 219--224. PMID or DOI: 10.3126/njst.v13i2.7740.
258. Lin, W.S., et al., *Occurrence, Bioavailability, Anti-inflammatory, and Anticancer Effects of Pterostilbene.* J Agric Food Chem, 2020. **68**(46): p. 12788-12799. PMID or DOI: 32064876.
259. Navrotskaya, V.V., et al., *Berberine Prolongs Life Span and Stimulates Locomotor Activity of Drosophila melanogaster.* American journal of plant sciences, 2012. **3**(7A): p. 1037--1040. PMID or DOI: 10.4236/ajps.2012.327123.
260. Proshkina, E., et al., *Geroprotective and Radioprotective Activity of Quercetin, (-)-Epicatechin, and Ibuprofen in Drosophila melanogaster.* Frontiers in Pharmacology, 2016. **7**: p. 505. PMID or DOI: 10.3389/fphar.2016.00505.
261. Kampkötter, A., et al., *Increase of stress resistance and lifespan of Caenorhabditis elegans by quercetin.* Comparative Biochemistry and Physiology Part B: Biochemistry and Molecular Biology, 2008. **149**(2): p. 314--323. PMID or DOI: 10.1016/j.cbpb.2007.10.004.
262. Pietsch, K., et al., *Quercetin mediated lifespan extension in Caenorhabditis elegans is modulated by age-1, daf-2, sek-1 and unc-43.* Biogerontology, 2009. **10**(5): p. 565--578. PMID or DOI: 10.1007/s10522-008-9199-6.
263. Si, H., et al., *Dietary Epicatechin Promotes Survival of Obese Diabetic Mice and Drosophila melanogaster.* The Journal of Nutrition, 2011. **141**(6): p. 1095--1100. PMID or DOI: 10.3945/jn.110.134270.
264. Lee, M.B., et al., *Pterocarpus marsupium extract extends replicative lifespan in budding yeast.* Geroscience, 2021. **43**(5): p. 2595-2609. PMID or DOI: 34297314. PMC8599564.
265. Lee, M.B., et al., *A system to identify inhibitors of mTOR signaling using high-resolution growth analysis in Saccharomyces cerevisiae.* GeroScience, 2017. **39**(4): p. 419--428. PMID or DOI: 10.1007/s11357-017-9988-4.

266. Zhang, L., et al., *Pterostilbene, a natural small-molecular compound, promotes cytoprotective macroautophagy in vascular endothelial cells.* The Journal of Nutritional Biochemistry, 2013. **24**(5): p. 903--911. PMID or DOI: 10.1016/j.jnutbio.2012.06.008.
267. Chen, R.J., C.T. Ho, and Y.J. Wang, *Pterostilbene induces autophagy and apoptosis in sensitive and chemoresistant human bladder cancer cells.* Molecular Nutrition \& Food Research, 2010. **54**(12): p. 1819--1832. PMID or DOI: 10.1002/mnfr.201000067.
268. Wakimoto, R., et al., *Differential Anticancer Activity of Pterostilbene Against Three Subtypes of Human Breast Cancer Cells.* Anticancer Research, 2017. **37**(11): p. 6153--6159. PMID or DOI: 10.21873/anticanres.12064.
269. Sirerol, J.A., et al., *Role of Natural Stilbenes in the Prevention of Cancer.* Oxidative Medicine and Cellular Longevity, 2016. **2016**. PMID or DOI: 10.1155/2016/3128951. PMC4698548.
270. Chakraborty, A., et al., *In vitro evaluation of the cytotoxic, anti-proliferative and anti-oxidant properties of pterostilbene isolated from Pterocarpus marsupium.* Toxicology in Vitro, 2010. **24**(4): p. 1215--1228. PMID or DOI: 10.1016/j.tiv.2010.02.007.
271. Billack, B., V. Radkar, and C. Adiabouah, *In Vitro evaluation of the cytotoxic and anti-proliferative properties of resveratrol and several of its analogs.* Cellular and Molecular Biology Letters, 2008. **13**(4): p. 553--569. PMID or DOI: 10.2478/s11658-008-0022-9.
272. Roslie, H., et al., *3,5-Dibenzyloxy-4'-hydroxystilbene induces early caspase-9 activation during apoptosis in human K562 chronic myelogenous leukemia cells.* The Journal of Toxicological Sciences, 2012. **37**(1): p. 13--21. PMID or DOI: 10.2131/jts.37.13.
273. Hasiah, A.H., et al., *Cytotoxic and antioxidant effects of methoxylated stilbene analogues on HepG2 hepatoma and Chang liver cells: Implications for structure activity relationship.* Human \& Experimental Toxicology, 2011. **30**(2): p. 138--144. PMID or DOI: 10.1177/0960327110368739.
274. Lombardi, G., et al., *Effect of polyphenols on enniatins-induced cytotoxic effects in mammalian cells.* Toxicology Mechanisms and Methods, 2012. **22**(9): p. 687--695. PMID or DOI: 10.3109/15376516.2012.717120.
275. Harun, Z. and A.R. Ghazali, *Potential Chemoprevention Activity of Pterostilbene by Enhancing the Detoxifying Enzymes in the HT-29 Cell Line.* Asian Pacific Journal of Cancer Prevention, 2012. **13**(12): p. 6403--6407. PMID or DOI: 10.7314/apjcp.2012.13.12.6403.
276. Wang, Y., et al., *Pterostilbene simultaneously induces apoptosis, cell cycle arrest and cyto-protective autophagy in breast cancer cells.* American journal of translational research, 2011. **4**(1): p. 44--51. PMID or DOI: null.
277. Dias, S.J., et al., *Trimethoxy‐Resveratrol and Piceatannol Administered Orally Suppress and Inhibit Tumor Formation and Growth in Prostate Cancer Xenografts.* The Prostate, 2013. **73**(11): p. 1135--1146. PMID or DOI: 10.1002/pros.22657.
278. Nikhil, K., et al., *Role of isothiocyanate conjugate of pterostilbene on the inhibition of MCF-7 cell proliferation and tumor growth in Ehrlich ascitic cell induced tumor bearing mice.* Experimental Cell Research, 2014. **320**(2): p. 311--328. PMID or DOI: 10.1016/j.yexcr.2013.10.015.
279. Siedlecka-Kroplewska, K., et al., *Pterostilbene induces cell cycle arrest and apoptosis in MOLT4 human leukemia cells.* Folia Histochemica et Cytobiologica, 2012. **50**(4): p. 574--580. PMID or DOI: 10.5603/fhc.2012.0080.
280. Zhang, B., et al., *Involvement of the Nrf2 Pathway in the Regulation of Pterostilbene-Induced Apoptosis in HeLa Cells via ER Stress.* Journal of Pharmacological Sciences, 2014. **126**(3): p. 216--229. PMID or DOI: 10.1254/jphs.14028fp.
281. Medrano-Padial, C., et al., *Toxicological Evaluation of Piceatannol, Pterostilbene, and ε-Viniferin for Their Potential Use in the Food Industry: A Review.* Foods, 2021. **10**(3): p. 592. PMID or DOI: 10.3390/foods10030592.
282. Ruiz, M.J., et al., *Dietary Administration of High Doses of Pterostilbene and Quercetin to Mice Is Not Toxic.* Journal of Agricultural and Food Chemistry, 2009. **57**(8): p. 3180--3186. PMID or DOI: 10.1021/jf803579e.
283. Riche, D.M., et al., *Analysis of Safety from a Human Clinical Trial with Pterostilbene.* Journal of Toxicology, 2013. **2013**: p. 463595. PMID or DOI: 10.1155/2013/463595.

284. Benlloch, M., et al., *Pterostilbene Decreases the Antioxidant Defenses of Aggressive Cancer Cells In Vivo: A Physiological Glucocorticoids- and Nrf2-Dependent Mechanism.* Antioxidants \& Redox Signaling, 2016. **24**(17): p. 974--990. PMID or DOI: 10.1089/ars.2015.6437.
285. McDonnell, A.M. and C.H. Dang, *Basic Review of the Cytochrome P450 System.* Journal of the advanced practitioner in oncology, 2013. **4**(4): p. 263--268. PMID or DOI: 10.6004/jadpro.2013.4.4.7.
286. Detampel, P., et al., *Drug interaction potential of resveratrol.* Drug Metabolism Reviews, 2012. **44**(3): p. 253--265. PMID or DOI: 10.3109/03602532.2012.700715.
287. Tian, D. and Z. Hu, *CYP3A4-mediated Pharmacokinetic Interactions in Cancer Therapy.* Current Drug Metabolism, 2015. **15**(8): p. 808--817. PMID or DOI: 10.2174/1389200216666150223152627.
288. Hyrsova, L., et al., *Trans-resveratrol, but not other natural stilbenes occurring in food, carries the risk of drug-food interaction via inhibition of cytochrome P450 enzymes or interaction with xenosensor receptors.* Toxicology Letters, 2019. **300**: p. 81--91. PMID or DOI: 10.1016/j.toxlet.2018.10.028.
289. Albassam, A.A. and R.F. Frye, *Effect of pterostilbene on in vitro drug metabolizing enzyme activity.* Saudi Pharmaceutical Journal, 2019. **27**(3): p. 406--412. PMID or DOI: 10.1016/j.jsps.2019.01.001.
290. Rosebrock, A.P., *Analysis of the Budding Yeast Cell Cycle by Flow Cytometry.* Cold Spring Harbor Protocols, 2017. **2017**(1): p. pdb.prot088740. PMID or DOI: 10.1101/pdb.prot088740.
291. Wu, T.-J.J., et al., *Identification of a Non-Gatekeeper Hot Spot for Drug-Resistant Mutations in mTOR Kinase.* Cell reports, 2015. **11**(3): p. 446--59. PMID or DOI: 10.1016/j.celrep.2015.03.040.
292. Guarente, L. and F. Picard, *Calorie Restriction— the SIR2 Connection.* Cell, 2005. **120**(4): p. 473--482. PMID or DOI: 10.1016/j.cell.2005.01.029.
293. Baur, J.A. and D.A. Sinclair, *Therapeutic potential of resveratrol: the in vivo evidence.* Nature Reviews Drug Discovery, 2006. **5**(6): p. 493--506. PMID or DOI: 10.1038/nrd2060.
294. Fabrizio, P., et al., *Sir2 Blocks Extreme Life-Span Extension.* Cell, 2005. **123**(4): p. 655--667. PMID or DOI: 10.1016/j.cell.2005.08.042.
295. Bass, T.M., et al., *Effects of resveratrol on lifespan in Drosophila melanogaster and Caenorhabditis elegans.* Mechanisms of Ageing and Development, 2007. **128**(10): p. 546--552. PMID or DOI: 10.1016/j.mad.2007.07.007.